

ANALYSIS OF WOOD CHIP COMBUSTION SYSTEM FOR HOT AIR GENERATION IN THE INDUSTRIAL DRYING PROCESS

A thesis
submitted in partial fulfilment
of the requirements for the Degree
of
Master of Science
by
J.K.A.T.Rajika



University of Moratuwa, Sri Lanka.
Electronic Theses & Dissertations
www.lib.mrt.ac.lk



University of Moratuwa
2015

Declaration

I declare that this is my own work and this thesis/dissertation1 does not incorporate without acknowledgement any material previously submitted for a Degree or Diploma in any other University or institute of higher learning and to the best of my knowledge and belief it does not contain any material previously published or written by another person except where the acknowledgement is made in the text. Also, I hereby grant to University of Moratuwa the non-exclusive right to reproduce and distribute my thesis/dissertation, in whole or in part in print, electronic or other medium. I retain the right to use this content in whole or part in future works (such as articles or books).

Signature:

Date:

The above candidate has carried out research for the Masters thesis/Dissertation under my supervision.



University of Moratuwa, Sri Lanka
Electronic Theses & Dissertations
www.lib.mrt.ac.lk

Signature of the supervisor:

Date



To my parents Charlotte Gamage and late Siripala Jayawickrama
University of Moratuwa, Sri Lanka.
Electronic Theses & Dissertations
www.lib.mrt.ac.lk

Abstract

A two-dimensional steady state packed bed CFD model is developed for the combustion of wood chip in a moving grate. The model is validated using an industrial moving bed hot air generator used in Tea industry. Various empirical models have used for thermophysical property modeling. For this purpose free-board region of the hot air generator is also simulated including volatile reactions and turbulent combustion. Modeling and simulation carried out using open source CFD software OpenFOAM. Radiation heat incident on the packed bed is unknown and it is assumed in the first packed bed simulation. Therefore, CFD simulation involves number of iterative runs of the packed bed model and free board model to obtain the radiation temperature incident on packed bed due to free board heat. According to the validation results the developed packed bed model can be used to predict temperature of the packed bed wood chip combustion of thermally thin wood particles. The gas compositions could not be validated using the model. Further improvements to the model have suggested.



University of Moratuwa, Sri Lanka.
Electronic Theses & Dissertations
www.lib.mrt.ac.lk

Acknowledgments

This work is supported by SRC Research Grant numbered:SRC/LT/2012/19 by University of Moratuwa, Faculty of Engineering. The dissertation would not have been possible without my Supervisor Dr.M.Narayana who introduced me new fields of Engineering, guidance and great patience on me. You opened doors in CFD modeling and simulation of biomass combustion field for me. A special thank should go to Eng.N.K.Edirisinghe, Eng.Bharatha Udaya and all other members of NERD centre for providing me facilities for validation purposes and other relevant data. I am very much grateful to the head of the Chemical and Process Engineering Department Dr.P.G.Rathnasiri, Technical officers and Lab attendants Mr.C.L.Gunarathna, Mr.Dananjaya Epa, Mr.M.T.A.J.Kumara, Mr.Sunil Dayananda and other academic and non-academic staff for facilitating me the flexible working and computational environment. I should be thankful to my friends K.D.Nishanthi, Sureshini Warnasooriya and M.A.M Jinasena for persuading me for an MSc. A very special thank should go to other PG mates including K.G.Nirajan, Uditha, Bhagya Herath, Sachini Thilakarathna, Gayani Jayatunga and Imesha Samarathunga for the fruitful discussions we had on many matters came across during research period. Finally, I am deeply indebted to my mother Charlotte Gamage, sisters Hiranthi Nadeeka Jayawickrama, Madhuri Jayawickrama, Chandima Jayawickrama and Brother in-laws Pramod Weerasinghe, Manjula jayaweera and L.U.Edirisinghe for helping me in every occasions.

Table of Contents

| | |
|---|------------|
| Declaration | i |
| Abstract | iii |
| Acknowledgments | v |
| List of Figures | v |
| List of Tables | vii |
| CHAPTER 1: INTRODUCTION | 1 |
| 1.1 Background and Motivation | 1 |
| 1.1.1 Biomass as renewable energy source | 2 |
| 1.1.2 Use of CFD for design and optimizing furnaces | 2 |
| 1.1.3 Problem Statement | 4 |
| 1.2 Objective | 4 |
| 1.3 General Approach | 5 |
| CHAPTER 2: LITERATURE REVIEW | 8 |
| 2.1 Biomass Combustion and modeling | 8 |
| 2.1.1 Drying models | 9 |
| 2.1.2 Devolatilization models | 10 |
| 2.1.3 Char combustion models | 10 |
| 2.1.4 Volatile combustion | 11 |
| 2.2 Modeling packed bed combustion of biomass | 11 |
| 2.2.1 Packed bed combustion models | 13 |
| 2.2.1.1 According to dimensional variations | 13 |
| 2.2.1.2 According to the treatment for the biomass | 14 |
| 2.3 Chemical kinetics | 17 |
| 2.4 Turbulence modeling | 18 |



University of Moratuwa, Sri Lanka.
 Electronic Theses & Dissertations
www.lib.mrt.ac.lk

| | | |
|-------|---|----|
| 2.4.1 | Favre-averaged equations | 18 |
| 2.4.2 | standard $k - \varepsilon$ model | 19 |
| 2.4.3 | Wall Functions | 20 |
| 2.4.4 | Low-Reynolds number $k - \varepsilon$ model | 21 |
| 2.5 | Turbulence/combustion interaction models | 22 |
| 2.6 | Radiation modeling | 25 |

CHAPTER 3: MATHEMATICAL MODEL FOR THE PACKED-BED COMBUSTION OF WOOD-CHIP 27

| | | |
|---------|---|----|
| 3.1 | Model Assumptions | 27 |
| 3.2 | Governing equations | 29 |
| 3.2.0.1 | Gas phase | 29 |
| 3.2.0.2 | solid phase | 31 |
| 3.3 | Boundary conditions | 32 |
| 3.4 | Chemical and physical properties modeling | 33 |
| 3.4.1 | Combustion properties of biomass | 33 |
| 3.4.1.1 | Composition | 33 |
| 3.4.1.2 | Moisture content | 33 |
| 3.4.1.3 | Volatiles | 34 |
| 3.4.1.4 | Density | 34 |
| 3.4.1.5 | Heating value | 35 |
| 3.4.2 | Thermal conductivity of the bed | 35 |
| 3.4.3 | Mass diffusivity of the bed | 37 |
| 3.4.4 | Specific heat capacity of the bed | 37 |
| 3.4.5 | Pressure drop | 38 |
| 3.4.6 | Particle shrinkage | 38 |
| 3.4.7 | Particle size and shape | 39 |

CHAPTER 4: CFD SIMULATION METHOD 40

| | | |
|-------|----------------------------------|----|
| 4.1 | Finite volume approach | 40 |
| 4.2 | Pressure correction | 41 |
| 4.2.1 | Rhie-Chow method | 42 |
| 4.3 | SIMPLE algorithm | 43 |

| | |
|--|-----------|
| CHAPTER 5: INTRODUCTION TO OPENFOAM | 45 |
| 5.1 Introduction to OpenFOAM | 45 |
| 5.2 History of OpenFOAM | 45 |
| 5.3 OpenFOAM C++ library | 46 |
| 5.3.0.1 OpenFOAM lists and fields | 47 |
| 5.3.0.2 Mesh generation | 48 |
| 5.3.0.3 Defining a <i>geometricField</i> in OpenFOAM | 50 |
| 5.3.0.4 Boundary Conditions | 52 |
| 5.3.0.5 Equation discretization | 53 |
| 5.4 Running a case | 54 |
| 5.4.1 “system” sub directory | 54 |
| 5.4.2 “constant” sub directory | 56 |
| 5.4.3 Time directories (0, . . .) | 56 |
| 5.4.4 other directories or files | 57 |
| 5.4.5 Community developed additional OpenFOAM tools | 57 |
| CHAPTER 6: DEVELOPING A NEW SOLVER IN OPENFOAM | 59 |
| 6.1 Compiling applications and libraries | 59 |
| 6.1.0.1 Compiling with <i>wmake</i> | 60 |
| 6.2 Rhie-Chow method in OpenFOAM | 63 |
| 6.3 Steps of developing a new solver | 65 |
| CHAPTER 7: CFD MODELING OF HOT AIR GENERATOR SYSTEM | 71 |
| 7.1 Hot air generator simulation | 71 |
| 7.1.1 Packed bed modeling and simulation | 75 |
| 7.1.1.1 Thermo-physical properties modeling | 75 |
| 7.1.1.2 Chemical kinetics modeling | 75 |
| 7.1.1.3 Biomass properties for simulation | 77 |
| 7.1.1.4 Boundary conditions | 77 |
| 7.2 Free board simulation | 81 |
| 7.2.1 Turbulence simulation | 81 |
| 7.2.2 Radiation | 81 |
| 7.2.3 Transport properties | 83 |
| 7.2.4 Thermo-physical properties | 83 |

| | | |
|--|---|------------|
| 7.2.5 | Combustion properties | 84 |
| 7.2.6 | Chemistry properties | 84 |
| CHAPTER 8: RESULTS AND DISCUSSION | | 85 |
| 8.1 | Simulation results of packed bed-free board | 85 |
| 8.1.1 | Mesh Refinement | 85 |
| 8.1.2 | Evaluation of simulation results | 92 |
| 8.1.3 | Validation of Results | 93 |
| 8.2 | Comments on the model | 95 |
| 8.2.1 | Ash density | 95 |
| 8.2.2 | Interface between packed bed-free board | 95 |
| 8.2.3 | Radiation heat flux | 95 |
| 8.2.4 | Simulation time | 96 |
| 8.3 | Drawbacks of the model | 96 |
| 8.4 | Optimization of packed bed combustion | 97 |
| CHAPTER 9: CONCLUSION AND FURTHER STUDIES | | 99 |
| References | | 100 |



University of Moratuwa, Sri Lanka.
 Electronic Theses & Dissertations
www.lib.mrt.ac.lk

List of Figures

| | | |
|-----|--|----|
| 1.1 | Typical hot air generator system | 6 |
| 1.2 | Integral approach of the model | 7 |
| 2.1 | macro model mesh | 15 |
| 2.2 | Single particle modeling | 16 |
| 2.3 | Particle resolved macro scale models | 16 |
| 2.4 | Conceptual diagram of PaSR Reactor | 23 |
| 2.5 | Two steps occurring in a cell with turbulence and chemistry | 24 |
| 3.1 | heat and mass transfer between solid and gas | 28 |
| 3.2 | combustion process in the packed bed (model) | 29 |
| 3.3 | Modeling gas phase and solid phase separate using porosity(ϵ) | 30 |
| 3.4 | packed bed boundary conditions | 32 |
| 4.1 | one-dimensional grid having checker board pressure field | 41 |
| 4.2 | SIMPLE algorithm | 44 |
| 5.1 | hexahedral cells in a mesh with part of polyMesh data | 49 |
| 5.2 | <i>A geometricField<Type></i> and its operators | 54 |
| 5.3 | Typical case file structure in OpenFOAM | 55 |
| 6.1 | Header files,source files,compilation and linking | 60 |
| 6.2 | Directory structure of an application | 61 |
| 7.1 | Conventional hot air generator system in Tea factories | 72 |
| 7.2 | Hot air generator after retrofitting | 73 |
| 7.3 | Schematic diagram of simulation case structure | 74 |
| 7.4 | Packed bed with dimensions and boundaries | 79 |
| 7.5 | Free board with dimensions and boundaries | 81 |
| 8.1 | Packed bed gas outlet(interface) temperature with iterations | 86 |
| 8.2 | Radiation temperature incident on packed bed | 86 |

| | | |
|------|---|----|
| 8.3 | Mesh refinement results(Temperature at packed bed outlet | 87 |
| 8.4 | Residual mapping of packed bed simulation with 300*300 mesh | 87 |
| 8.5 | Velocity at packed bed outlet along the grate | 88 |
| 8.6 | Mass fractions of CO , CO_2 , H_2O and O_2 at packed bed outlet | 88 |
| 8.7 | Gas phase and solid phase temperature of packed bed at steady state | 89 |
| 8.8 | Packed bed porosity at steady state | 89 |
| 8.9 | Gas component mass fraction at steady state | 90 |
| 8.10 | Moisture,volatile,char and ash mass fractions in solid phase at steady state | 91 |
| 8.11 | Temperature of the gas at inlet to the heat exchangers with the height from the packed bed | 94 |
| 8.12 | Temperature along a vertical line starting from edge of the flame at packed bed -free board interface | 94 |
| 8.13 | Temperature at packed bed outlet with different input conditions | 98 |



University of Moratuwa, Sri Lanka.
 Electronic Theses & Dissertations
www.lib.mrt.ac.lk

List of Tables

| | | |
|-----|---|----|
| 1.1 | Energy Consumption of Sri Lanka (thousand toe) | 3 |
| 1.2 | Industrial Energy consumption of Sri Lanka (thousand toe) | 3 |
| 2.1 | volatile combustion reaction models in literature | 12 |
| 2.2 | Westbrook-Dryer mechanism (WD) | 18 |
| 5.1 | defining mesh of the geometry | 48 |
| 5.2 | fvMesh stored data | 50 |
| 5.3 | S.I. base units of measurement | 51 |
| 6.1 | Optional compilation arguments to wmake | 62 |
| 7.1 | solvers and basic boundary conditions of each case | 75 |
| 7.2 | Empirical models used for thermo-physical properties and their values | 76 |
| 7.3 | Chemical kinetic models for reactions of combustion | 77 |
| 7.4 | Properties of biomass, for simulation | 78 |
| 7.5 | Ultimate and Proximate analysis of biomass | 79 |
| 7.6 | packed bed boundary conditions | 80 |
| 7.7 | Free board boundary conditions | 82 |

Nomenclature

Abbreviations

| | |
|----------|---|
| Bi | Thermal Biot number |
| CFD | Computational Fluid Dynamics |
| FV | Finite Volume |
| NERDC | National Engineering Research and Development Centre |
| OpenFOAM | Open Source Field Operation and Manipulation CFD tool box |
| Pa | Pascal |
| PaSR | Partially Stirred Reactor |
| PDEs | Partial Differential Equations |
| Pr | Prandlt number |
| PSR | Perfectly Stirred Reactor |
| Re | Reynolds number |
| toe | tonnes of oil equivalent |

Subscripts

| | |
|---|--|
| 0 | initial,reference (temperature in degrees Rankine) |
| a | Activation |
| b | bed |
| c | convective |

| | |
|------|--------------------------|
| char | char combustion |
| dry | drying reaction |
| G | grate |
| g | gas phase |
| i | i-th component |
| mix | mixing due to turbulence |
| p | particle |
| pyr | pyrolysing |
| s | solid phase |
| surf | surface |
| vol | volatile |

| | |
|---|--------------------------|
| x | x-direction (horizontal) |
| y | y-direction (vertical) |



University of Moratuwa, Sri Lanka.
 Electronic Theses & Dissertations
www.moratuwa.ac.lk

Symbols

| | |
|-----------------|---|
| l | length scale (m) |
| λ | thermal conductivity (W/mK) |
| $\lambda_{e,0}$ | effective thermal conductivity of a quiescent bed (without fluid flow) (W/mK) |
| λ_e | effective thermal conductivity of bed (W/mK) |
| μ | dynamic viscosity (kg/ms) |
| μ_0 | reference viscosity in centipoise at reference temperature T_0 (kg/mms) |

| | |
|---------------|---|
| μ_t | eddy viscosity (kg/ms) |
| ν | kinematic viscosity (m ² /s) |
| ω | reaction rate (kg/m ³ s) |
| Ω_D | Diffusion collision integral |
| ρ | density (kg/m ³) |
| ξ_{ij} | rate of deformation (m ² /s) |
| σ_{AB} | Binary pair characteristic length(dimensionless) |
| τ | integration time step (s) |
| \tilde{u}_i | density weighted mean velocity (m/s) |
| ε | rate of dissipation of turbulent kinetic energy per unit mass (m ² /s ³) |
| ϑ | velocity scale (m/s) |
| ξ | mixture fraction |
| c_p | specific heat capacity (J/kgK) |
| ϵ | porosity of the bed |
| A | pre-exponential factor(1/s) |
| A | volumetric particle surface (m ² /m ³) |
| c | concentration (kg/m ³) or (mol/m ³) |
| D | mass diffusion coefficient (m ² /s) |
| d | particle diameter (m) |
| E | Energy (J/mol) |
| H | evaporation heat (J/kg) |



| | |
|-----|---|
| h | specific sensible enthalpy/heat transfer coefficient (J/kg,W/m ² K) |
| J | Joule |
| K | Kelvin/Equilibrium constant |
| k | Thermal conductivity (W/mK), turbulent kinetic energy (m ² /s ²) |
| kg | kilogram |
| M | moisture content(wet basis) |
| M | molecular weight (g/mol) |
| P | pressure (kg/m/s ²) |
| Q | heat transferred to the solid phase by convection and radiation (W/m ³) |
| R | universal gas constant (J/molK) |
| r | reaction-rate (kg/m ³ s) |
| T | temperature (K) |
| t | temperature (K) |
| U,V | velocity vector (m/s) |
| V | volume (m ³) |
| v | velocity component (m/s) |
| Y | mass fraction |



CHAPTER I

INTRODUCTION

1.1 Background and Motivation

Attention on climate changes are being increasing day by day with its effects to all living beings. It is a fact that the industrial activities which emit Green House Gases (GHGs) are the major source to the climate change. Whoever or whichever factors contributed; each and every living species have to face extreme weather conditions and catastrophic consequences. Some examples are high frequency of heavy precipitation, longer and more severe droughts, an increase of intense tropical cyclone activities, increasing number of heat waves and decreasing snow cover. An important greenhouse gas is CO_2 , emitted as a consequence of combustion of fossil fuel such as coal and oil. The CO_2 emissions have grown from 1970 to 2004 by about 80% [1]. To change the trend of an increasing average global temperature, drastic actions need to be undertaken concerning emissions in general and of CO_2 in particular.

One global approach to mitigate greenhouse emissions is “Kyoto Protocol” came in to practise in 1993; although it has now become weak as some powerful countries have been opted out to sign for second commitment period though most of the countries have local plans to reduce GHG emissions.

Apart from climate change effects, depletion and sky rocketed prices of fossil fuels are the other problem which third world countries are highly prone.

Damage to the environment and the uncertainty of fossil fuels has forced the world to think about non-fossil fuels; specially renewable energy options, energy efficiency and more energy savings.

As a country without having any fossil fuel resources so far and as a developing country Sri Lanka has been keen on developing renewable energy to cut the foreign exchange for importing fossil fuels and to be more environment friendly. National energy management plan of Sri Lanka (2012-2016) is targeting to achieve a 20% energy

saving equivalent total energy consumption of 2010, by 2020[2]. According to the national energy policy of Sri Lanka; government will endeavour to reach a minimum level of 10% of electrical energy supplied to the grid to be from Non conventional renewable energy[3].

1.1.1 Biomass as renewable energy source

Replace fossil fuel by biomass is one step to achieve reduction of CO_2 emissions to the atmosphere. Biomass is considered to be CO_2 neutral since it is fast growing and thereby consuming an equal amount of CO_2 as produced during combustion, provided that biomass is sustainably grown. Biomass is a very heterogeneous group of fuel. It consists of wood, bark, branches, twigs, various kinds of crops, straw, rape-oil, ethanol and many other things. Biomass supplies some 50 EJ energy in globally, which represents 10% of global annual primary energy consumption[4]. However, this number also includes primitive combustion methods, without any process control or emission reductions.

Biomass is an important renewable energy source of primary energy supply in Sri Lanka, supplying more than 57% of primary energy and more than 75% of industrial energy supply of Sri Lanka[5] (See Table 1.1 and Table 1.2). Therefore, biomass based energy generation and its technologies are very vital to Sri Lanka.

The challenges of industries are primitive and inefficient methods for converting biomass into useful energy and lack of dense availability of biomass in a particular place. Biomass resources are highly scattered throughout the country. Therefore the supply chain should be very well organized. Demand for renewable energy sources are escalating and it is essential for introducing efficient biomass conversion methods. Even though biomass is the oldest type of fuel for small scale, domestic energy production, modern, large scale biomass combustion is still a fairly new technology. The fuel properties of biomass differ from those of traditional fuels like coal and oil and to achieve an effective combustion with a minimum of emissions, modifications of existing technologies are necessary.

1.1.2 Use of CFD for design and optimizing furnaces

When designing grates and furnaces the applied technology is based on experience and not much on theoretical studies. By developing numerical methods of the process in

| Source | 2008 | 2009 | 2010 | 2011 | 2012 |
|--------------------|----------|----------|----------|---------|---------|
| Biomass | 4,654.70 | 4,771.15 | 5,054.40 | 4923.01 | 4845.44 |
| Petroleum | 2,581.38 | 2,667.93 | 2,947.18 | 3358.04 | 3424.04 |
| Electricity | 719.45 | 721.43 | 791.93 | 859.13 | 895.15 |
| Total | 7,955.53 | 8,160.51 | 8,793.5 | 9140.18 | 9164.63 |

Table 1.1: Energy Consumption of Sri Lanka (thousand toe)

| Industry | 2008 | 2009 | 2010 | 2011 | 2012 |
|--------------------|---------|---------|---------|---------|---------|
| Biomass | 1359.41 | 1393.5 | 1619.39 | 1582.54 | 1630.51 |
| Petroleum | 283.51 | 261.01 | 243.74 | 228.73 | 251.99 |
| Electricity | 254.30 | 238.43 | 270.73 | 290.62 | 303.41 |
| Total | 1897.22 | 1892.94 | 2133.86 | 2101.89 | 2185.91 |

Table 1.2: Industrial Energy consumption of Sri Lanka (thousand toe)

the furnace a detailed knowledge can be achieved and valuable insights can be drawn. By simulating the combustion behavior; different parameters can be studied such as fuel type, fuel properties, air distribution and their effect on the emission levels and furnace efficiency, without having to make expensive and time consuming real scale measurements.

Computational Fluid Dynamics (CFD) has become an increasingly used tool for this type of calculations. Lots of research work is carried out in developing CFD models of the free board area¹ in a furnace to investigate the optimal air distribution and identify re-circulation zones.

A frequent problem with the CFD codes is that there is a lack of accurate inlet conditions from the fuel bed. The process in the fuel bed is of great significance and it would be extremely valuable to be able to predict the right distribution and amount of particles and volatiles leaving the bed to use as inlet conditions to a CFD model.

The purpose of bed models is not alone to provide inlet conditions to CFD models, it is also of great importance to study the combustion process inside the bed and understanding the underlying mechanisms. Bed models have been developed for different types of grates, such as fixed beds and traveling grates, and many kinds of biomass fuels, e.g. wood, wood chips, waste and saw dust.

¹ region just above the fuel bed with gas combustion products

1.1.3 Problem Statement

With its reputation for quality sustained and reinforced, and with serious new attention being paid to sustainability and care for the environment, the future of Ceylon Tea looks bright.

Sri Lanka Tea Board²

Tea industry is the second largest export of Sri Lanka ;currently exporting more than 300,000 metric tons. A major drawback facing by the tea industry is high energy intensity. Actions have to be taken to overcome the problem. As a result,when moving in to efficient technologies in biomass based energy generation systems;controlling, densification, shape, size are key factors. National Engineering Research and Development Center (NERDC) has played an important role on development of biomass technologies in Sri Lanka for past few decades. One major improvement is retrofitting old wood log fed boilers with wood chip in Tea factories. Unlike old technology;wood chip feeding rate can be controlled. There are large number of reasons that determine the wood feeding rates for a furnace at different stages of combustion;biomass source,initial properties,furnace conditions,fuel size and shape,etc. Therefore still controlling has been a difficult task with such varieties.



University of Moratuwa, Sri Lanka.
Electronic Theses & Dissertations
www.lib.mrt.ac.lk

1.2 Objective

This research work is aiming to develop a numerical model for the hot air generator system in tea factories by wood chip combustion. That model will be used to generate a CFD model using a software. For the modeling purpose open source CFD software OpenFOAM will be used for promoting open source as well as for introducing OpenFOAM to Sri Lanka. A good CFD model will assist in understanding combustion process inside the furnace which is necessary for further development and to develop a control system for combustion of the furnace.

In this study, the developed CFD model was compared with experimental data for validation. The CFD model provides suggestions for the optimization of combustion process by means of wood chip inlet conditions, furnace dimensions, air inlet flow rates, secondary air requirements.

² http://www.pureceylontea.com/index.php?option=com_content&view=article&id=114&Itemid=226&lang=en

Research work is a collaborative action with NERDC which is providing the boiler facility and necessary data for validation purposes.

1.3 General Approach

A typical air heating system consists of a grate, fuel feeding system, primary air inlet, a free board region with/without secondary air. This model is developed to analyze the combustion of the furnace and therefore the heat exchanger unit is not considered. A schematic of an air heating system is shown in Figure 1.1; recent research have been more concerned on fuel bed as a stand alone model which have more advantages in modeling.

1. A comprehensive bed model can be developed which provide more detail about combustion process
2. Some CFD software will not provide necessary features to develop the bed model
3. Developed bed model may use for more applications with simplification or adding necessary functionalities (packed bed, fixed bed in drying applications, adsorption, etc)

Creating a model for packed bed combustion is very complex which involve heat, mass and momentum transfer and highly anisotropic nature of biomass. OpenFOAM is still not popular in Sri Lanka for research purposes and then lack of available knowledge. Therefore, this study need to be elaborated to learn including developing necessary codes which require a thorough knowledge on C⁺⁺.

Biomass combustion of a furnace can be clearly distinguished to two systems; free board region and packed bed region (See Figure 1.2). The free board model and packed bed model will be coupled using inter-facial boundary conditions which is very sensitive for the accuracy of the whole model and it is complex to be modeled radiation heat transfer from free board and heat, mass and momentum transfer from bed to the free board region. Another important aspect of the stand alone approach is placement of interface between fuel bed and free board [6]. In this work as discussing in the chapter and the chapter bed shrinkage is neglected and interface is placed just above the packed bed.

Collective modeling approach is depicted in the Figure 1.2.

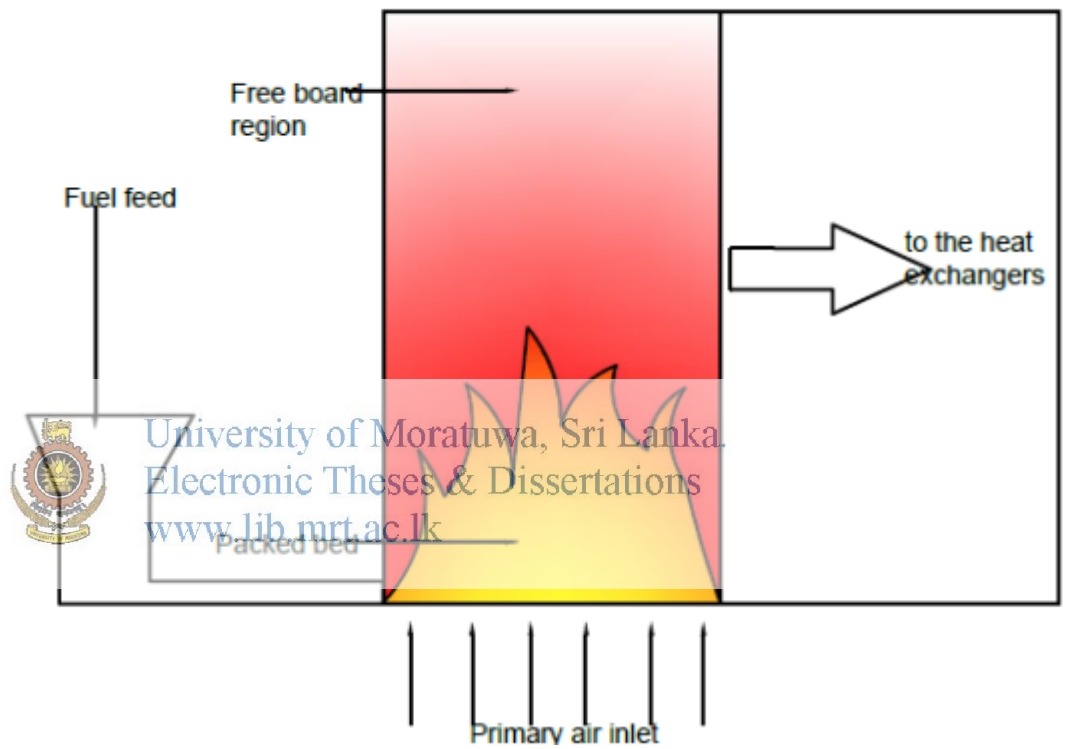


Figure 1.1: Typical hot air generator system

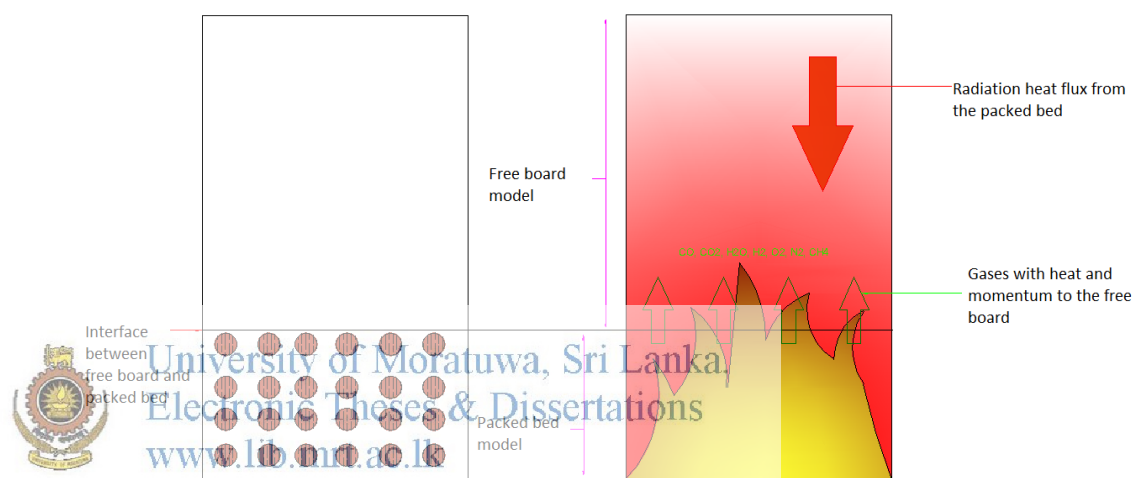


Figure 1.2: Integral approach of the model

CHAPTER II

LITERATURE REVIEW

2.1 Biomass Combustion and modeling

Biomass combustion is known by humans since thousands years ago. Biomass energy is used for energy generation purposes in a wide range of applications from households to large scale industries. Availability, low cost, renewable energy, etc uplifts the biomass as a source of energy while low energy density, supply management, etc limits the usage.

Biomass fuels are primarily wood, agricultural residues and refuse [7]. Owing to the variety of biomass fuel types, chemical and physical properties also significantly vary. Generally all biomass types consist moisture, volatile matter and fixed carbon.

Moisture exists in 3 forms; water vapour in pores, free water in the pores and bound water adsorbed in to wood [8]. Typically biomass contain moisture in the range of 50%-10% on wet basis. Volatiles release as gases when biomass heated. It is mainly consist of carbon monoxide, carbon dioxide, hydrogen, water vapour and various other hydro carbons. Volatile contain large part of wood which is about 60-90% of weight in range. Char is the minor component in the biomass but most important in combustion, typically less than 15% of wood. Ash is the inorganic remaining of biomass combustion which is typically less than 5% of weight.

Biomass combustion involves 3 sub processes drying, devolatilization and char combustion. Following sections describe the 3 phenomena in detail as this research work focus on biomass combustion modeling.

Thermal Biot number relates the internal and external heat transfer rates as in Equation 2.1.

$$Bi = \frac{r_{car} h_{c,eff}}{k} \quad (2.1)$$

Where r_{car} -a characteristic length(m), $h_{c,eff}$ -effective heat transfer(W/m^2K) and k -thermal conductivity of the particle(W/mK).

Depending on the thermal biot number, a wood particle combustion may be in one of the following regimes;

- Thermally thin regime ($Bi < 0.2$)-there is no temperature gradient within a particle;drying,pyrolysis and char combustion occur in series
- Thermally thick regime ($0.2 < Bi < 10$) -there is a temperature gradient within a particle,but since reaction rates are low compared to heat transfer rates; drying, pyrolysis and char combustion still occur in series.
- Thermal wave regimes ($Bi > 10$)-drying, pyrolysis and char combustion travel through a particle like a wave

Very often in modeling, for simplification of complex processes; particles considered as thermally thin.

2.1.1 Drying models

Following drying models are available in literature. These can be divided in to 3 categories [9]



University of Moratuwa, Sri Lanka
Electronic Theses & Dissertations
www.lib.mrt.ac.lk

- Heat sink model

This model assumes that drying occurs at a fixed boiling temperature and drying zone is infinitely thin. There is no resistance to mass transfer and reaction rate is completely controlled by heat transfer.[10]

$$r_{dry} = \frac{Q}{H_{dry}} \quad [kg/m^3s] \quad (2.2)$$

- First-order kinetic rate model

Drying rate depend on the temperature of the particle and moisture content. Where E_a —activation energy(J/mol), ρ_s —solid density(kg/m^3), t_s —solid phase temperature(K), A -pre-exponential factor(1/s) and $Y_{H_2O,s}$ —mass fraction of moisture in solid phase.

$$r_{dry} = A \exp\left(-\frac{E_a}{Rt_s}\right) \rho_s Y_{H_2O,s} \quad [kg/m^3s] \quad (2.3)$$

- Equilibrium model

Model assumes that the water vapour in gas phase surrounded by particle is in equilibrium with water in solid phase. Partial pressure of water vapour fixed to the saturation pressure. Reaction rate depend on both heat and mass transfer. Where k_d – mass transfer coefficient (m/s), A_p – volumetric surface area of solid particle, C – concentration

$$r_{dry} = k_d A_p (C_{H_2O,surf} - C_{H_2O,g}) \quad [kg/m^3s] \quad (2.4)$$

2.1.2 Devolatilization models

Devolatilization rate depend on the temperature and the type of fuel [11]. Devolatilization releases volatile gases while char remains in the biomass. Devolatilization also refer as pyrolysis since the volatiles released in reaction precludes penetration of oxygen to the fuel [7].

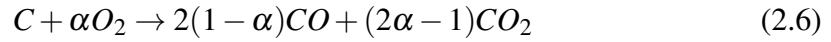
Devolatilization models used for packed bed combustion is the concern here, although different models used for different applications such as fluidized beds. Devolatilization of most fuels can be represented as a one-step global reaction [12]. The first order kinetic rate model of reaction can be represented as,

$$r_{pyr,i} = A \exp\left(-\frac{E_a}{Rt_s}\right) \rho_s Y_{vol,s} \quad [kg/m^3s] \quad (2.5)$$

Effect of the parameters of one-step reaction models on the biomass combustion have evaluated. Range of very slow devolatilization rates to very fast rates have suggested a weak influence on burning rate [11]. However, reaction rate parameters has effect on ignition rate and reaction zone thickness. Overall devolatilization reaction can be considered thermally neutral [9].

2.1.3 Char combustion models

Char combustion/gasification is the dominant reaction in biomass combustion [13]. When pyrolysis is finish, gas can penetrate in to the surface of char and ash remain in the biomass particles. The char combustion rate is controlled by both diffusion and kinetics [14, 15, 13]. Char may be fully or partially oxidized as follows;



α -determined by ratio which depends on temperature of particle[16];

$$\frac{CO}{CO_2} = 2500 \exp\left(-\frac{6420}{T_s}\right).$$

Rate of char combustion can be expressed as;

$$r_{char} = A_p C_{O_2} \left(\frac{1}{k_r} + \frac{1}{k_d} \right) \quad [kg/m^3 s] \quad (2.7)$$

where k_r —kinetic rate constant(m/s) and k_d —mass transfer coefficient(m/s)

2.1.4 Volatile combustion

Devolatilization generates volatile gases enter in to gas phase of the bed;which might be reacted within the packed bed depending on the mixing rate and air to fuel ratio.Almost all volatile combustion models have simplified large number of volatile gases to represent by a single component in common;while there are deviations of other volatile reactions assumed.Some have used carbon monoxide(CO) reaction only[10, 17] with volatile combustion reaction,but some have further added hydrogen(H_2) combustion as well as methane(CH_4)combustion.Very often the reaction rates have calculated by minimum of mixing rate and kinetic reaction rate[16, 18],although there are exceptions of using directly the kinetic reaction rate[19, 17].The reactions and their reaction rates used in different research works have integrated, which is shown in Table 2.1.

The released volatile gases will react in the free board region,if sufficient air is available for reactions.Free board region reaction rates will be calculated on the turbulence mixing rates and kinetic reaction rates using turbulence/combustion interaction models.

2.2 Modeling packed bed combustion of biomass

A packed bed may be a fixed bed in small scale industrial applications or for testing purposes in a pilot plant.Generally in large scale or medium scale applications they are moving grate/bed or vibrating grate type.Modeling packed bed combustion is complex owing to many reasons;anisotropy of biomass particles and then biomass properties, wide variation of type,size and shapes of biomass used,large number of particles in

| Research | Reactions | Reaction rates |
|-------------------------|---|---|
| Yang et al.[10] | $C_xH_y + (\frac{x}{2} + \frac{y}{4})O_2 \rightarrow xCO + \frac{y}{2}H_2O$ $CO + \frac{1}{2}O_2 \rightarrow CO_2$ | $R_{CO} = 1.3 * 10^{11} C_{CO} C_{H_2O}^{0.5} C_{O_2}^{0.5}$ $R_{C_xH_y} = 59.8 t_g P^{0.3} C_{C_xH_y}^{0.5} C_{O_2} \exp(\frac{-12200}{t_g})$ $R = \text{Min}[R_{kin}, R_{mix}]$ |
| Yang et al.[14] | $C_mH_n + \frac{m}{2}O_2 \rightarrow$ $mCO + \frac{n}{2}H_2CO + \frac{1}{2}O_2 \rightarrow CO_2$ $H_2 + \frac{1}{2}O_2 \rightarrow H_2O$ | $R_{CO} = 1.3 * 10^{11} C_{CO} C_{H_2O}^{0.5} C_{O_2}^{0.5}$ $R_{C_xH_y} = 59.8 t_g P^{0.3} C_{C_xH_y}^{0.5} C_{O_2} \exp(\frac{-12200}{t_g})$ $R_{H_2} = 3.9 * 10^{17} \exp(\frac{-20500}{t_g}) C_{H_2}^{0.85} C_{O_2}^{1.42}$ $R = \text{Min}[R_{kin}, R_{mix}]$ |
| Shin and Choi[17] | $C_xH_y + (\frac{x}{2} + \frac{y}{4})O_2 \rightarrow xCO + \frac{y}{2}H_2O$ $CO + \frac{1}{2}O_2 \rightarrow CO_2$ | $R_{CO} = 1.3 * 10^{11} C_{CO} C_{H_2O}^{0.5} C_{O_2}^{0.5} \exp(\frac{-15105}{t_g})$ $R_{C_xH_y} = 59.8 t_g P^{0.3} C_{C_xH_y}^{0.5} C_{O_2} \exp(\frac{-12200}{t_g})$ |
| Wurzenberger et al.[19] | $CO + \frac{1}{2}O_2 \rightarrow CO_2$ $H_2 + \frac{1}{2}O_2 \rightarrow H_2O$ $CH_4 + O_2 \rightarrow CO_2 + 2H_2O$ $CO + H_2O \rightarrow CO_2 + H_2$ | $R_{CO,1} = 2.78 * 10^{-3} \exp(\frac{-1510}{t_g}) (y_{CO} y_{H_2O} - \frac{y_{CO_2} y_{H_2}}{K}) \cdot c^2$ $R_{H_2} = 3.98 * 10^{14} \exp(\frac{-20119}{t_g}) y_{CO} y_{O_2}^{0.25} y_{H_2O}^{0.5} \cdot c^{1.75}$ $R_{CH_4} = 2.19 * 10^{12} \exp(\frac{-13127}{t_g}) y_{H_2} y_{O_2} \cdot c^2$ $R_{CO,2} = 1.58 * 10^{13} \exp(\frac{-24343}{t_g}) y_{CH_4}^{0.7} y_{O_2}^{0.8} \cdot c^{1.5}$ |

Table 2.1: volatile combustion reaction models in literature

a packed bed, combustion reactions, complexities due to moving bed/grate conditions, turbulence in the gas phase, etc. Therefore, for modeling packed bed combustion, simplifications are inevitable.

Packed bed combustion modeling has been stemmed for different areas with the researcher's interests;

- single particle modeling
- chemical and thermo physical properties modeling
- packed bed modeling
- modeling for further development on equipments-pollution control, deposit formation

2.2.1 Packed bed combustion models

Models available can be primarily categorized in two different approaches;

1. According to the dimensional variations considered

2. According to the treatment for the bed particles

Both models are discussed in next two sections.

2.2.1.1 According to dimensional variations

1. Zero-dimensional model

The biomass conversion is uniform along the grate length and width like a continuous stirred tank reactor (CSTR). Heat release and the released species are assumed by integral assumption [20].

2. One-dimensional

Model heat release and species concentration profiles are calculated over the length of the grate. The conversion across the grate is assumed to be uniform. To get the profile at the top of the bed, overall mass and energy balances are solved [20].

3. One-dimensional transient model

In addition to the model described above, the burnout progress in the vertical direction is also included. 1-D transient model has been the most popular method for combustion modeling so far. It has been able to validate macro scale combustion properties like burning rate but not the gas compositions [17, 10].

4. Two-dimensional model

The conversion process is modeled both across and along the grate. A homogeneous two dimensional mathematical model has been developed by [21] for the combustion of straw in a grate furnace. Considering the relatively small horizontal gradients in the grate bed, they also used fixed bed model to approximate the moving bed combustion. However this model only accounted for the reactions of char with O₂, because of the unavailability of the data on the products' kinetic models. Another steady state 2-D method for predicting straw combustion in a moving grate furnace is used by [9].

5. Three-dimensional model

A fully three-dimensional model solves the conversion process in all three directions. An innovative 3D-CFD packed bed model consisting Euler-Granular model for hydro-dynamics of gas particle multiphase flow and a thermally thin particle model for combustion of biomass has been introduced by [22]. The model have successfully applied for a small scale under-feed stoker furnace. Further it has been developed for thermally-thick biomass applying a layer model for thermally thick biomass. In both cases good qualitative agreements for temperature and gas compositions have been obtained [15].

2.2.1.2 According to the treatment for the biomass

These models are classified according to the level of approximation for particles in the fuel bed. Simple approximations would not be valid due to non-negligible situations of intra-particle gradients of fuel in large particles.

1. Macro scale models

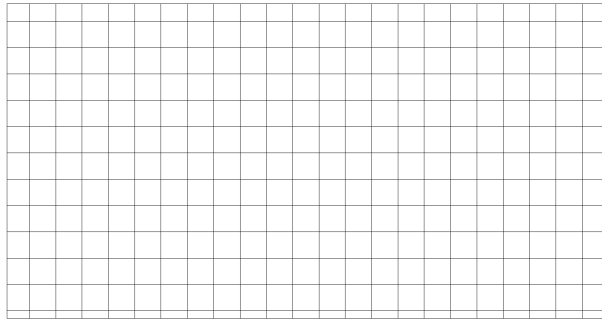



Figure 2.1: macro model mesh

Fuel bed considers as a continuous porous medium with gas and solid phases which is treated as two fluid mediums. This model can be applied to thermally thin particle beds only since intra-particle gradients are negligible [10, 20, 9, 17, 23]. Macro model mesh is shown in the Figure 2.1

2.  Micro scale models
University of Moratuwa, Sri Lanka.
Electronic Theses & Dissertations
www.lib.mru.ac.lk
Combustion in a single particle is considered in the model and it is important in further development of combustion models by understanding micro level in detail (refer). Water in the wood particles also can be modeled by adding another phase [24] (See the Figure 2.2).

3. Particle-resolved macro-scale models

A fuel bed consists of finite number of particles in the porous structure of the bed. The particles have modeled separate using micro scale models and gas phase and particles connected through boundary conditions (refer the Figure 2.3). Gas phase is modeled same as the macro scale models. This model has been developed to avoid implications in macro scale models due to non-negligible intra-particle gradients of thermally-thick particles [14, 25, 15] (See the Figure 2.3).

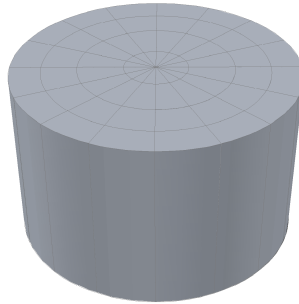


Figure 2.2: Single particle modeling

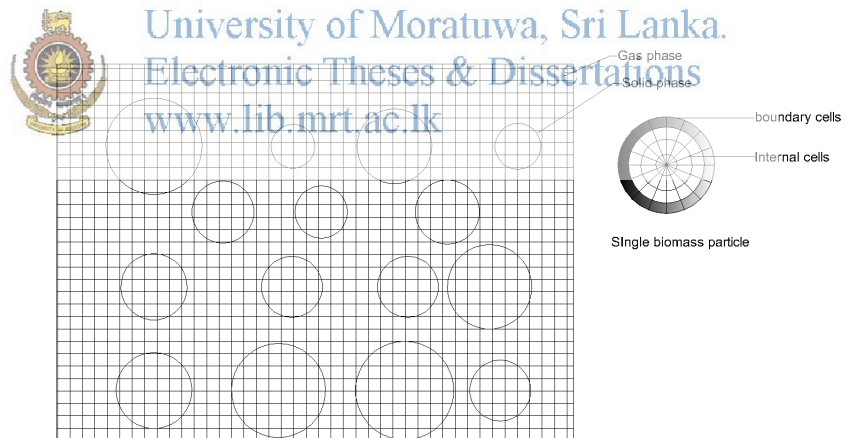
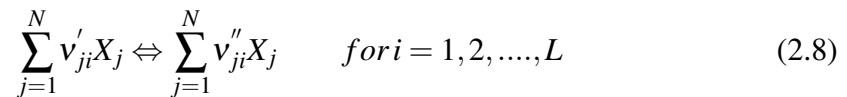


Figure 2.3: Particle resolved macro scale models

2.3 Chemical kinetics

Chemical kinetics presents the elementary reactions and their rates[26]. Reactions involve large number of gas components, reactions and different reaction rates (as the case for combustion too). Therefore, a compact notation has been developed for reactions and reaction rates.

For a certain reacting environment; we can write a reaction as follows;



where v'_{ji}, v''_{ji} - stoichiometric coefficients on the reactants and products of j^{th} specie in i^{th} reaction.

Similarly production rate of each specie in a multi-step mechanism;

$$\dot{\omega}_j = \sum_{i=1}^L v_{ji} q_i \quad \text{for } j = 1, 2, \dots, N \quad (2.9)$$

where $v_{ji} = (v''_{ji} - v'_{ji})$

and

$$q_i = k_{fi} \prod_{j=1}^N [X_j]^{v'_{ji}} - k_{ri} \prod_{j=1}^N [X_j]^{v''_{ji}}$$

where q_i - rate of progress variable, k_{fi} and k_{ri} are the Arrhenius reaction rates for the forward and reverse reaction.

The reaction rates are modeled using Arrhenius form;

$$k_{f(r)i} = AT^b \exp(-E_A/R_u T) \quad (2.10)$$

where A- pre-exponential factor, b-temperature exponent, E_A -activation energy.

Arrhenius reaction rates should modeled carefully in OpenFOAM since units used for reaction rates in OpenFOAM($kmol, m^3, s, K$) are different from CHEMKIN($mol, cm^3, s, K, cal, Joule$).

In CFD modeling; adoption of detailed chemistry have been computationally complex and there are simplified mechanisms for oxy-fuel combustion such as[27]; Westbrook-Dryer mechanism (WD) and Jones-Lindstedt mechanism (JL). WD method reaction and reaction rates are depicted that is shown in the Table 2.2.

| Reaction | Reaction rate(<i>cal, mol, l, s</i>) |
|--|--|
| $CH_4 + \frac{3}{2}O_2 \rightarrow CO + 2H_2O$ | $5.10^{11} e^{-\frac{47800}{RT}} C_{CH_4}^{0.7} C_{O_2}^{0.8}$ |
| $CO + O_2 \rightarrow CO_2$ | $2.24.10^{12} e^{-\frac{40700}{RT}} C_{CO} C_{H_2O}$ |
| $CO_2 \rightarrow CO + O_2$ | $5.10^8 e^{-\frac{40700}{RT}} C_{CO_2}$ |

Table 2.2: Westbrook-Dryer mechanism (WD)

2.4 Turbulence modeling

Turbulence appears when inertia forces exceeds a certain limit compared to viscous forces in a fluid flow. It is visual with the rotational flow structures created; called “eddies”. Eddy motions help effective mixing in practical applications with high mass, momentum and energy transfer rates. Therefore turbulence is important in almost all engineering applications.

Turbulence flow properties can be decomposed into a steady mean value and a fluctuating component; which is called “Reynolds decomposition” [28]. In most engineering applications Engineers interested in mean flow properties rather than instantaneous values. Therefore, Reynolds Averaged Navier-Stokes equations have been sufficient for CFD modeling. Compressible flow modeling is preferred with Favre-averaged (mass average) equations instead of time-averaged equations.

2.4.1 Favre-averaged equations

According to Favre decomposition, a property can be represented as;

$$\varphi = \tilde{\varphi} + \varphi'' \quad (2.11)$$

where $\tilde{\varphi}$ -mass averaged quantity (mean value) and φ'' -fluctuating value

$$\tilde{\varphi} = \frac{1}{\bar{\rho}} T \lim_{\alpha} \int_t^{t+T} \rho(x, \tau) \varphi(x, \tau) d\tau \quad (2.12)$$

Favre-averaged conservation equations can be obtained after some algebraic manipulations as follows;

continuity equation

$$\frac{\partial \rho}{\partial t} + \frac{\partial (\bar{\rho} \tilde{u}_i)}{\partial x_i} = 0 \quad \text{kg/m}^3 \text{s} \quad (2.13)$$

Momentum equations

$$\frac{\partial (\bar{\rho} \tilde{u}_i)}{\partial t} + \frac{\partial (\bar{\rho} \tilde{u}_i \tilde{u}_j)}{\partial x_j} + \frac{\partial P}{\partial x_j} = \left[\mu \left(\frac{\partial \tilde{u}_i}{\partial x_j} + \frac{\partial \tilde{u}_j}{\partial x_i} \right) - \frac{2}{3} \mu \frac{\partial \tilde{u}_k}{\partial x_k} \delta_{ij} - \overline{\rho u_i'' u_j''} \right] + \bar{\rho} g_i \quad \text{kg/m}^2 \text{s}^2 \quad (2.14)$$

Enthalpy equation

$$\frac{\partial (\bar{\rho} \tilde{h}_s)}{\partial t} + \frac{\partial (\bar{\rho} \tilde{u}_i \tilde{h}_s)}{\partial x_i} = \frac{\partial}{\partial x_i} \left[\bar{\rho} \alpha \frac{\partial \tilde{h}_s}{\partial x_i} - \overline{\rho u_i'' h_s''} \right] + \bar{q}_R''' \quad (2.15)$$

Species conservation equation

$$\frac{\partial (\bar{\rho} \tilde{Y}_k)}{\partial t} + \frac{\partial (\bar{\rho} \tilde{u}_j \tilde{Y}_k)}{\partial x_j} = \frac{\partial}{\partial x_i} \left(\bar{\rho} D_k^M \frac{\partial \tilde{Y}_k}{\partial x_i} - \overline{\rho u_i'' Y_k''} \right) + \tilde{\omega}_k \quad (2.16)$$

These equations create a closure problem with unknowns; Reynolds stress term in momentum equation; $\overline{\rho u_i'' u_j''}$ and turbulent convective fluxes in enthalpy; $\overline{\rho u_i'' h_s''}$ and specie equations; $\overline{\rho u_i'' Y_k''}$. To solve those terms standard $k - \epsilon$ model is used in the model.

2.4.2 *standard* $k - \epsilon$ model

According to Boussinesq hypothesis Reynolds stress tensor is proportional to the stress-rate-of-strain of a Newtonian fluid;

$$\overline{\rho u_i'' u_j''} = \frac{2}{3} \bar{\rho} k \delta_{ij} - \mu_t \left(\frac{\partial \tilde{u}_i}{\partial x_j} + \frac{\partial \tilde{u}_j}{\partial x_i} - \frac{2}{3} \mu \frac{\partial \tilde{u}_k}{\partial x_k} \delta_{ij} \right) \quad (2.17)$$

where k -kinetic energy defined as $\frac{1}{2} \overline{u_i'' u_i''}$, δ_{ij} -Kronecker delta ($\delta_{ij} = 1$ if $i = j$ and $\delta_{ij} = 0$ if $i \neq j$) and μ_t -eddy viscosity

According to the gradient-diffusion hypothesis, turbulent transport of a scalar is taken to be proportional to the gradient of the mean value of the transported quantity;

$$\overline{\rho u_i'' h_s''} = -\Gamma_s \frac{\partial \tilde{h}_s}{\partial x_i} \quad (2.18)$$

$$\overline{\rho u_i'' Y_k''} = -\Gamma_k \frac{\partial \tilde{Y}_k}{\partial x_i} \quad (2.19)$$

where Γ_s -turbulent heat diffusivity and mass diffusivity

$$\Gamma_{s,k} = \frac{\mu_t}{\sigma_t} \quad (2.20)$$

where σ_t -turbulent prandlt or schmidt number

therefore equations 2.18 and 2.19 can be re-write as;

$$\overline{\rho u_i'' h_s''} = - \frac{\mu_t}{Pr_t} \frac{\partial \tilde{h}_s}{\partial x_i} \quad (2.21)$$

$$\overline{\rho u_i'' Y_k''} = - \frac{\mu_t}{Sc_t} \frac{\partial \tilde{Y}_k}{\partial x_i} \quad (2.22)$$

Still there is an unknown term μ_t calculated by $k - \varepsilon$ model which is calculated using an equation for kinematic viscosity derived from turbulent kinetic energy and turbulent kinetic energy dissipation rate.

$$\vartheta = k^{1/2}, \ell = \frac{k^{3/2}}{\varepsilon}$$

$$\mu_t = C_\mu \rho \vartheta \ell = \rho C_\mu \frac{k^2}{\varepsilon} \quad (2.23)$$

The standard k- ε model uses the following transport equations for k and ε :

$$\frac{\partial (\rho k)}{\partial t} + \nabla \cdot (\rho k U) = \nabla \cdot \left[\left(\frac{\mu_t}{\sigma_k} \right) \nabla k \right] + 2\mu_t S_{ij} \cdot S_{ij} - \rho \varepsilon \quad (2.24)$$

$$\frac{\partial (\rho \varepsilon)}{\partial t} + \nabla \cdot (\rho \varepsilon U) = \nabla \cdot \left[\left(\frac{\mu_t}{\sigma_\varepsilon} \right) \nabla \varepsilon \right] + C_{1\varepsilon} \frac{\varepsilon}{k} 2\mu_t S_{ij} \cdot S_{ij} - C_{2\varepsilon} \rho \frac{\varepsilon^2}{k} \quad (2.25)$$

The equations contain five adjustable constants: C_μ , σ_k , σ_ε , $C_{1\varepsilon}$ and $C_{2\varepsilon}$. The standard k- ε model uses values for the constants arrived at by comprehensive data fitting for a wide range of turbulent flows. $C_\mu = 0.09$, $\sigma_k = 1.00$, $\sigma_\varepsilon = 1.30$, $C_{1\varepsilon} = 1.44$, $C_{2\varepsilon} = 1.92$.

2.4.3 Wall Functions

The velocity profile of a turbulent flow near a flat plate can be clearly distinguished with four regions[29];

- viscous sub layer -which exists very much near the wall,viscosity effects are more important ($0 < y^+ < 5$)
- buffer layer -transition from viscous to inertial sub layer occurs ($5 < y^+ < 30$)
- inertial sub-layer -main turbulent stream starting,viscous effects becoming negligible ($30 < y^+ < 100$)
- main turbulent stream -viscosity is not important

Viscous sub-layer and buffer layer thickness are very small compared to inertial sub layer region;therefore instead of making very smaller grids in the computational domain wall functions are used to calculate the values at inertial sub layer(log-law region).This will make computations less time consuming.In the log-law region epsilon(ϵ) and $k(k)$ values can be calculated using Equation 2.26and Equation 2.27. [29, 30]

$$k_P = c_\mu^{-\frac{1}{2}} u_*^2 \quad (2.26)$$

where $u_* = \sqrt{\frac{\tau_0}{\rho}}$ and u_* -friction velocity(m/s), τ_0 -wall shear stress(kg/ms^{-2}) and P-first interior node adjacent to the wall.



University of Moratuwa, Sri Lanka.
Electronic Theses & Dissertations
www.lib.mrt.ac.lk

$$\epsilon_P = \frac{u_*^3}{k y} \quad (2.27)$$

There are instances that flow near the boundary is important such as for external flows (flow around an airplane, car, house, etc), low Reynolds number flows which viscous effects non-negligible and where heat transfer involves through walls.In these situations, Low-Re number turbulence models used for modeling purposes.There are large number of low Reynolds number models and in the section 2.4.4 Low-Re number $k - \epsilon$ models are briefly described.

2.4.4 Low-Reynolds number $k - \epsilon$ model

In the Low-Re number $k - \epsilon$ models, model equations for k , ϵ and μ_t have been corrected to calculate values at the walls using “damping terms” which are really augmenting the functions near the walls and becoming equal to one(1) at log-law region[30].Where Equation 2.23, 2.24 and 2.25 becoming as 2.28, 2.29 and 2.30;

$$\mu_t = C\rho\vartheta\ell = \rho C_\mu f_\mu \frac{k^2}{\varepsilon} \quad (2.28)$$

$$\frac{\partial(\rho k)}{\partial t} + \nabla \cdot (\rho k U) = \nabla \cdot \left[\left(\frac{\mu_t}{\sigma_k} \right) \nabla k \right] + 2\mu_t S_{ij} \cdot S_{ij} - \rho \varepsilon \quad (2.29)$$

$$\frac{\partial(\rho \varepsilon)}{\partial t} + \nabla \cdot (\rho \varepsilon U) = \nabla \cdot \left[\left(\frac{\mu_t}{\sigma_\varepsilon} \right) \nabla \varepsilon \right] + C_{1\varepsilon} f_1 \frac{\varepsilon}{k} 2\mu_t S_{ij} \cdot S_{ij} - C_{2\varepsilon} f_2 \rho \frac{\varepsilon^2}{k} \quad (2.30)$$

According to popular Lam and Bremhost Low-Re $k - \varepsilon$ model, f_μ , f_1 and f_2 are calculated from Equation 2.31, 2.32 and 2.33.

$$f_\mu = [1 - \exp(-0.0165 Re_y)]^2 [1 + \frac{20.5}{Re_t}] \quad (2.31)$$

$$f_1 = [1 + \frac{0.05}{f_\mu}]^3 \quad (2.32)$$

$$f_2 = 1 - \exp(-Re_t^2) \quad (2.33)$$

Where $Re_t = \vartheta\ell/\nu = k/\varepsilon\nu$ and $Re_y = k\vartheta_y/\nu$.

This models can be used for high Reynolds numbers as well and it produces more accurate results unless the computational resources and time spending. The results of the model may be grid dependent. Therefore, it is important to look at the results at different mesh refinements to check the deviations[28].

2.5 Turbulence/combustion interaction models

There is a remaining un-closed term $\tilde{\omega}_k$ in the equation 2.16. It is closed by using the Partially Stirred Reactor (PaSR) model developed by Chalmers university[31, 32].

PaSR model has been developed for modeling Diesel spray combustion to overcome the difficulties in available combustion models due to number of reasons[33][31];

1. difficulties in application of detailed chemistry to Eddy Break Up model
2. considering slow chemistry in Diesel spray combustion compared to laminar flamelet model which considers as chemical time scale is much smaller than

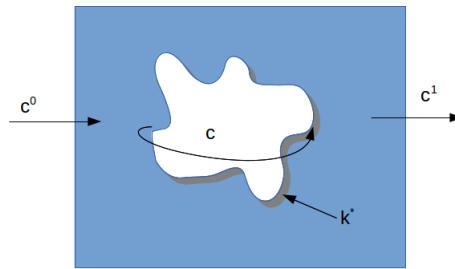



Figure 2.4: Conceptual diagram of PaSR Reactor

turbulent time scale

3. complexity of Probability Density Function approach due number of correlations
4. This model has developed under the following assumptions;
 - (a) A computational cell is consisting of two parts;
 - i. one is non-reacting fraction
 - ii. reacting fraction
5. Reacting fraction is considered as a Perfectly Stirred Reactor (PSR-homogeneously mixed)
 

University of Moratuwa Sri Lanka
Electronic Theses & Dissertations
www.lib.mrt.ac.lk
6. Three average concentrations present in the mixture;
 - (a) mean average inlet concentration to the cell (c^0)
 - (b) concentration in the reacting zone of the cell (c)
 - (c) mean average concentration at the outlet of the cell (c^1)
7. whole combustion process is consisting two steps;
 - (a) converting concentration from c^0 to c
 - (b) converting from c to c^1 after mixing with non-reacting zone

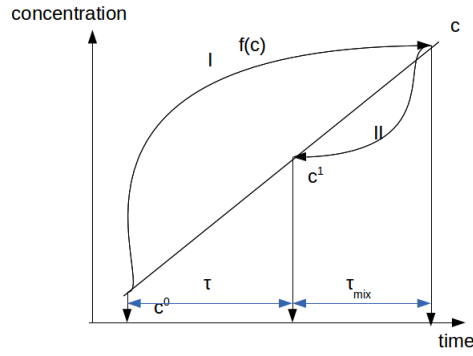


Figure 2.5: Two steps occurring in a cell with turbulence and chemistry

Considering the mass conservation of a certain specie, within the cell following equation can be derived;

$$c^1 = c^0(1 - k^*) + k^* c \quad (2.34)$$

where k^* -is mass fraction of mixture, reacting.

c^1 can be obtained using a linear interpolation between c^0 and c . Within a computational cell; part of mixture reacts resulting concentration of c and then c and c_0 of unreacted part mix together to produce the resulting concentration flow out of the cell c^1 . Time between c^0 and c must be integration time step (τ). c^0 and c mixes due to turbulent mixing and produce c^1 . This time period can be considered as turbulent mixing time scale (τ_{mix}). According to the figure 2.5;

$$\frac{c^1 - c^0}{\tau} = \frac{c - c^1}{\tau_{mix}} = f(c) \quad (2.35)$$

and also it can be represented as;

$$c^1 = \frac{\tau}{\tau + \tau_{mix}} c + \frac{\tau_{mix}}{\tau + \tau_{mix}} c^0 = k^* c + (1 - k^*) c^0 \quad (2.36)$$

where, $k^* = \frac{\tau}{\tau + \tau_{mix}}$

c is a sub-grid level information, which cannot directly find out without grid level information, therefore it has to be replaced with some known values. To represent reaction rate instead of c , c^1 is used with Taylor series expansion as follows;

$$f(c) = f(c^1) - \frac{\partial f}{\partial c}(c - c^1) + \frac{1}{2} \frac{\partial^2 f}{\partial c^2}(c - c^1)^2 \quad (2.37)$$

Diagonal elements are zero and neglecting off-diagonal elements and assuming that the dominating term of the Jacobian matrix is the derivative with respect to the reference specie ($\frac{\partial f(c)}{\partial c_r}$), and chemical time (τ_c) can be defined using jacobian element as follows;

$$\frac{\partial f(c)}{\partial c_r} = \frac{1}{\tau_c} \quad (2.38)$$

By neglecting higher order terms, the equation (19) will be;

$$f(c) = f(c^1) - \frac{1}{\tau_c}(c - c^1) \quad (2.39)$$

substituting c from equation 2.35 to 2.39;

$$\frac{c^1 - c^0}{\tau} = f(c) = f(c^1) - \frac{1}{\tau_c} \left(\frac{c^1 - (1 - K^*)c^0}{K^*} - c^1 \right) \quad (2.40)$$

which is leading to;

$$\left(\frac{1}{\tau} + \frac{1 - K^*}{\tau_c K^*} \right) (c^1 - c^0) = f(c^1) \quad \text{finally;} \quad (2.41)$$



University of Moratuwa, Sri Lanka.
Electronic Theses & Dissertations
www.lib.mrt.ac.lk

where

$$k = \frac{\tau_c}{\tau_c + \tau_{mix}} \quad (2.42)$$

If τ_{mix} equals to zero, the whole cell is perfectly stirred. The combustion model reduced to the quasi-laminar combustion. If τ_{mix} dominates, the reaction rate is equivalent to the eddy break-up rate.

2.6 Radiation modeling

The general Radiation Transfer Equation (RTE) for the radiation intensity $I(r, s)$; traveling through a non-scattering participating medium in the direction s at a given location r , can be represented by following equation 2.43 [34, 28].

$$\frac{dI(r, s)}{ds} = KI_b(r) - KI(r, s) \quad (2.43)$$

Where I_b —black body radiation intensity, K -absorption coefficient of the medium
 Boundary conditions for diffuse surfaces are taken from the relation giving the intensity leaving the wall I_w as a function of the black-body intensity of the wall $I_{b,w}$ and of the incident radiative intensity:

$$I_w(s) = \epsilon_w I_{b,w} + \frac{\rho_w}{\pi} \int_{n \cdot s' < 0} I_w(s') |n \cdot s'| d\Omega' \quad (2.44)$$

Where ϵ_w -wall emissivity, ρ_w -wall reflectivity, n -unit vector normal to the wall and s' -direction of propagation of the incident radiation confined within a solid angle $d\Omega'$.

According to Discrete Ordinates Method(DOM);the solid angles are discretized in to finite number(N) of directions $s_j(\mu_i, \eta_i, \xi_i)$, associated to the corresponding weights w_j , contained in the solid angle 4π , and where (μ_i, η_i, ξ_i) are directional cosines.

$$\frac{dI^n}{ds} = K(I^n - I_b) \quad (2.45)$$

$$I_w^n = \epsilon_w I_{b,w} + \frac{\rho_w}{\pi} \sum_j I_j |n \cdot s_j| w_j \quad n \cdot s_j > 0 \quad (2.46)$$

Where n is the direction index.

The radiative heat transfer source term in the enthalpy equation 2.15 will be calculated as;



University of Moratuwa, Sri Lanka
 Electronic Theses & Dissertations
www.lib.mrt.ac.lk

$$\overline{q_R'''} = K(4\sigma T^4 + G) \quad (2.47)$$

Where T -medium temperature, σ -Stefan-Boltzmann constant and G -incident irradiation.

$$G = \int_{4\pi} I d\Omega \approx \sum_{j=1}^N w_j I_j^n \quad (2.48)$$

The medium of radiation transfer in a combustion environment composing mixture of gases at different temperature and pressure. Therefore, to calculate the medium radiation properties a suitable approach has to be used. Most widely used method for radiative property calculation is Weighted-Sum-of-Grey-Gases-Model(WSGG)[28].

CHAPTER III

MATHEMATICAL MODEL FOR THE PACKED-BED COMBUSTION OF WOOD-CHIP

3.1 *Model Assumptions*

As mentioned in the section 2.2, packed bed combustion involves many serial and parallel reactions involving more than one phase with mass, momentum and energy transfer in a transient manner. Therefore, assumptions are inescapable even for a three-dimensional model.

The packed bed combustion model, which was developed in this study, basically assumes that the packed bed can be considered as two-dimensional and the model is developed for steady state; i.e. variations of the properties through the grate are negligible.

Model assumptions are,

1. The fuel bed can be considered as a continuous porous layer consisting of gas and solid phases.
2. Fuel particles are thermally thin, i.e. intra-particle temperature gradients are negligible.
3. Fuel consists of four major species - moisture, volatile matter, char and ash.
4. Combustion can be divided into four sub-processes;
 - (a) moisture evaporation
 - (b) volatile release/char formation
 - (c) combustion of volatiles

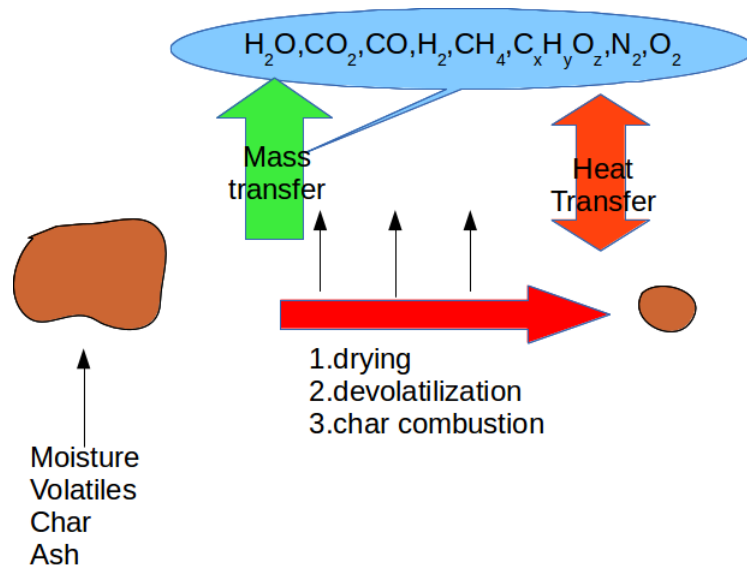


Figure 3.1: heat and mass transfer between solid and gas

(d) combustion of char

5. Heat of devolatilization reaction is negligible.

6. No heat is transferred through the walls of the packed bed (adiabatic process).

7. Packed bed volume does not change with proceeding of combustion but porosity will (no shrinkage of the bed see Figure 3.2).

8. Gas flow is in-compressible.

9. Pressure drop due to fuel bed resistance to gas flow is included in source terms f_x, f_y and can be approximated by e.g. the ERGUN'S equation

10. The combustion gas is a mixture of species $H_2O, O_2, CO_2, CO, H_2, N_2$, light hydrocarbons and tar represented by $CH_4, C_xH_yO_z$, respectively.

11. The radiative heat transfer inside the bed can be modeled by effective thermal conductivity.

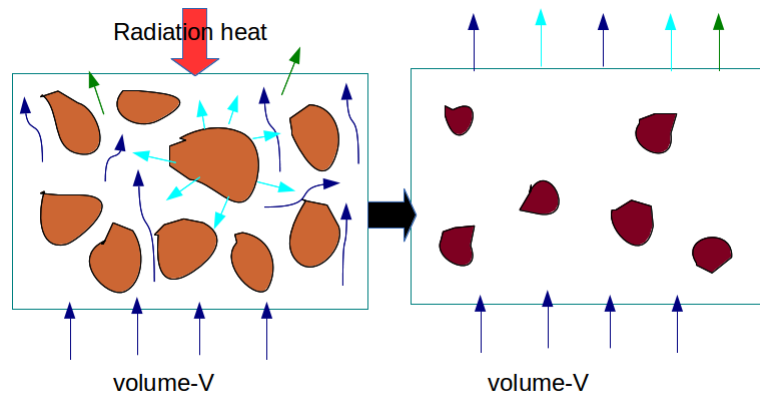


Figure 3.2: combustion process in the packed bed (model)

12. The effects of moving grates can be modeled by the diffusion coefficient $D_{s,i}$ and its considered as constant[35].

Neither packed bed combustion of biomass nor packed bed properties have well established models or theories. Therefore except major assumptions listed above; various other assumptions adopted in modeling thermo-physical or chemical properties of gas/solid phase and packed bed properties are discussed in the section 3.4.1.

3.2 Governing equations



University of Moratuwa, Sri Lanka.
Electronic Theses & Dissertations
www.lib.mrt.ac.lk

3.2.0.1 Gas phase

Gas phase model is two-dimensional and is presumed behave incompressibly. During combustion the gaseous products are released from biomass from drying, pyrolysis and char combustion. Resistance on the gas phase due to solid particles of packed bed is considered. Separate gas specie conservation equations used to predict gas phase mass fractions. Specie mass diffusion coefficients have been calculated as discussed in section 3.4.3. Specific heat capacity and effective thermal conductivity models used are being discussed in section 3.4.4 and section 3.4.2 respectively.

Continuity equation

$$\nabla \cdot (\epsilon_b \rho_g V_g) = r_{dry} + r_{pyr} + r_{char} \quad (3.1)$$

Gas phase mass always increasing due to heterogeneous reactions which occurs in

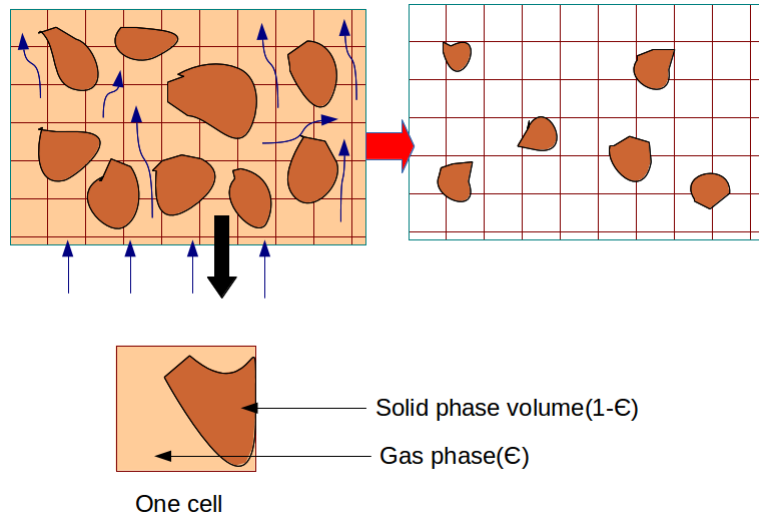


Figure 3.3: Modeling gas phase and solid phase separate using porosity(ϵ)

solid phase.

Momentum equation

$$\nabla \cdot (\epsilon_b \rho_g V_g v_{g,x}) = -\frac{\partial P}{\partial x} + \nabla \cdot (\epsilon_b \mu \nabla v_{g,x}) - f_x \quad (3.2)$$

$$\nabla \cdot (\epsilon_b \rho_g V_g v_{g,y}) = -\frac{\partial P}{\partial y} + \nabla \cdot (\epsilon_b \mu \nabla v_{g,y}) - f_y \quad (3.3)$$

Ergun's equation is used to calculate pressure drop due to resistance for a gas flow in a packed-bed(f_x and f_y)[14].

$$f_x = \frac{\Delta P}{L} = 150 \frac{\mu \nabla v_{g,x} (1 - \epsilon_b)^2}{d_p^2 \epsilon_b^3} + 1.75 \frac{\rho_g |v_{g,x}| v_{g,x} (1 - \epsilon_b)}{d_p \epsilon_b^3} \quad (3.4)$$

$$f_y = \frac{\Delta P}{L} = 150 \frac{\mu \nabla v_{g,y} (1 - \epsilon_b)^2}{d_p^2 \epsilon_b^3} + 1.75 \frac{\rho_g |v_{g,y}| v_{g,y} (1 - \epsilon_b)}{d_p \epsilon_b^3} \quad (3.5)$$

Specie conservation equation

$$\nabla \cdot (\epsilon_b \rho_g V_g Y_{g,i}) = \nabla \cdot (\epsilon_b D_{g,i} \nabla Y_{g,i}) + r_i + \epsilon_b \sum_j r_{i,j} \quad (3.6)$$

species can be generated due to heterogeneous reactions and generated/destroyed

due to homogeneous reactions.

enthalpy equation.

$$\nabla \cdot (\varepsilon_b \rho_g V_g h_g) = \nabla \cdot \left(\frac{\varepsilon_b \lambda_g}{c_{p,g}} \nabla h_g \right) + h_c A_p (t_s - t_g) + (r_{dry} + r_{pyr} + r_{char}) h_s - \varepsilon_b \sum_j [\varepsilon G] \sum \Delta h_j r_j \quad (3.7)$$

where,

r_i -specie generation due to the heterogeneous reactions

$r_{i,j}$ - i^{th} gas component generated due to the j -th homogeneous reaction

$\Delta h_j r_j$ -heat of reaction due to the j -th homogeneous reaction

$(r_{dry} + r_{pyr} + r_{char}) h_s$ -heat transferred from solid phase reactions due to the gaseous products generated

$h_c A_p (T_s - T_g)$ -convective heat transfer from solid phase to gaseous phase.

Gases generated from heterogeneous reactions will add heat to the gas phase, which is having the enthalpy of solid phase. Further heat adds to the gas phase due to exothermic homogeneous reactions as well. Heat will add/remove to/from gas phase due to convection and diffusion (radiation is lumped in to the effective thermal conductivity).

3.2.0.2  www.lib.mrt.ac.lk
 University of Moratuwa, Sri Lanka.
 Electronic Theses & Dissertations

Although the gas phase is treated as two-dimensional in the model, solid phase is treated as one-dimensional neglecting vertical motion of the bed due to bed volume shrinkage. It is assumed that the fuel moves on the grate only due to moving grate/fuel supply velocity (V_G).

Continuity equation

$$\frac{\partial((1 - \varepsilon_b) \rho_s V_G)}{\partial x} = -r_{dry} - r_{pyr} - r_{char} \quad (3.8)$$

Velocity changes in the vertical direction of the bed is neglected for the solid phase and horizontal velocity is constant which is the moving bed/grate velocity. Therefore, momentum equation can be omitted.

Specie conservation equation

$$\frac{\partial((1 - \varepsilon_b) \rho_s V_G Y_{s,i})}{\partial x} = \nabla \cdot ((1 - \varepsilon_b) D_{s,i} \nabla Y_{s,i}) - r_i \quad (3.9)$$

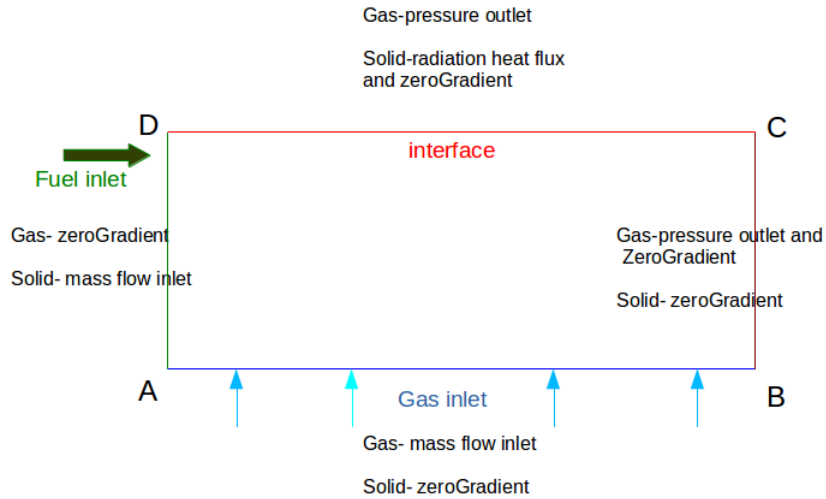


Figure 3.4: packed bed boundary conditions

Solid phase species mass fractions are reducing due to the removal of mass from heterogeneous reactions.

enthalpy equation

$$\frac{\partial((1 - \epsilon_b)\rho_s M G h_s)}{\partial t} = \nabla \cdot \left(\frac{(1 - \epsilon_b)\lambda_s}{c_{p,s}} \nabla h_s \right) + h_c A_p (t_s - t_g) - (r_{dry} + r_{pyr} + r_{char})h_s - r_c \Delta h_c - r_{dry} \Delta h_{dry} \quad (3.10)$$

Solid phase enthalpy is increasing due to char combustion reaction and decreases due to drying reaction. Heat of devolatilization reaction is neglected[36].

3.3 Boundary conditions

In this study, a packed bed biomass combustion is occurring in a horizontal moving bed/grate furnace. Fuel is fed from the left hand side of the furnace and air is supplied from under the grate. Boundary conditions are depicted in the section 3.4.

At the DC boundary, which is shown in figure 3.4; radiation heat is considered as a diffusion heat source at boundary where the radiation heat flux is the heat flux through the boundary surface for the energy equation 3.10;

$$\frac{(1 - \epsilon_b)\lambda_s}{c_{p,s}} \nabla h_s = \epsilon_{rad} \sigma (T_{env}^4 - T_{top}^4) \quad (3.11)$$

$$(\nabla T_s)_{boundary} = \left(\frac{\epsilon_{rad} \sigma (T_{env}^4 - T_{top}^4)}{(1 - \epsilon_b) \lambda_s} \right)_{boundary} \quad (3.12)$$

3.4 Chemical and physical properties modeling

A packed bed requires large number of properties for modeling. Most of the packed bed properties cannot be considered as constants throughout the combustion process, unless to simplify the mathematical model. Gas phase and solid phase conditions are highly an-isotropic in the ignition region, where the reaction rates are very high. Properties of packed bed at combustion are still at the research stage which makes selection of proper empirical models a challenge. Therefore total model, which in terms of physical and chemical properties modelling is not available for packed bed combustion in the literature. However, there are various other properties such as biomass compositions, heating values, enthalpies, bulk density, etc which are well documented.

3.4.1 Combustion properties of biomass

3.4.1.1 Composition

Biomass composition is defined as proximate analysis or ultimate analysis. Ultimate analysis is chemical composition of biomass in elements. Major components of biomass are Carbon (C-45%-55%), Oxygen (O-38%-45%) and Hydrogen (H-5.5%-7.5%)¹ respectively. Trace amounts of Nitrogen (N), Potassium (K), Sulfur (S) and Chlorine (Cl) may also available. All the mentioned trace amounts have negative effects in combustion more or less depending on the quantities [37]. Those effects are out of scope of this study. According to the proximate analysis there are four pseudo components in biomass, i.e-moisture, volatiles, char and ash.

3.4.1.2 Moisture content

Moisture content is highly varying with the biomass source which is an additional burden for combustion. Moisture content is defined in two methods; wet basis (M_{wb}) and dry basis (M_{db}). Moisture content of wood chips may vary from about 40%-60% in biomass on wet basis. For the biomass of beyond 90% moisture, the energy needed

¹ weight on dry basis

to vaporize water exceeds the heating value of the feed-stock. Auto-thermal limit which the fire is self-sustaining is typically in the range of 70–80% of moisture in wet basis. Therefore, flame stability becomes poor in most combustion systems above 50–55% moisture on wet basis[38].

$$M_{wb} = \frac{\text{moisture content}}{\text{Total weight}} \quad (3.13)$$

$$M_{db} = \frac{\text{moisture content}}{\text{dry weight}} \quad (3.14)$$

Dry weight of biomass is the weight at oven-dry state which is achieved by heating up to $102^{\circ}\text{C} \pm 3^{\circ}\text{C}$, assuming that no bound water is remaining and no volatile is released during drying. It is important to mention the form of measurement of moisture content to avoid consequences of wrong calculations.

3.4.1.3 Volatiles

The major component of biomass proximate analysis is volatile which may range from 60-85% of weight[39]. The volatile gases starting to release when biomass is heated up to a certain temperature (about 200°C). The volatile yield contains CO , CO_2 , H_2 , H_2O , tar and light hydrocarbons. Average composition of tar can be considered as $\text{C}_6\text{H}_{6.2}\text{O}_{0.2}$ [13]. Light hydrocarbons are mainly methane (CH_4). Considering heat of devolatilization is neutral, heating value of tar can be calculated.

In spite of moisture content and volatiles, biomass contain fixed carbon(char) and ash. Typically char contains about 11%-16% while ash is containing about 1.5%-3%[38] (agricultural bio-fuels like Rice straw have high ash contents; around 18%[37]).

3.4.1.4 Density

The density of biomass is two folded; Density of wood particles and bulk density of stockpile of wood. Both have wide variations depending on the type of biomass and type of fuel (saw dust, wood chips, wood logs, pellets, etc). Bulk density is stock weight divided by total volume while density is particle weight divided by particle volume. Bulk density of biomass fuels may vary from $120\text{kg}/\text{m}^3 - 400\text{kg}/\text{m}^3$ and density may vary from $100\text{kg}/\text{m}^3 - 600\text{kg}/\text{m}^3$.

3.4.1.5 Heating value

The lower heating value(also known as netv calorific value) of a fuel is defined as “the amount of heat released by combusting a specified quantity (initially at 25°C) and returning the temperature of the combustion products to 150°C, which assumes the latent heat of vaporization of water in the reaction products is not recovered”[40].Higher heating value(also known gross calorific value or gross energy) of a fuel is defined as “the amount of heat released by a specified quantity (initially at 25°C) once it is combusted and the products have returned to a temperature of 25°C, which takes into account the latent heat of vaporization of water in the combustion products”[40].

Following formulas can be used to estimate HHV and LHV of a biomass fuel using ultimate analysis and proximate analysis[39, 9].

$$HHV = 0.3491Y_c + 1.1783Y_H + 0.1005Y_s - 0.0151Y_N - 0.1034Y_O - 0.0211Y_{ash} [MJ/kg] \quad (3.15)$$

$$LHV = HHV(1 - Y_{H_2O}) - h_{vap}(Y_{H_2O} + Y_H \frac{M_{H_2O}}{M_{H_2}}(1 - Y_{H_2O})) [MJ/kg] \quad (3.16)$$

where HHV is expressed on dry basis and LHV on wet basis. $Y_C, Y_H, Y_S, Y_O, Y_N,$ and Y_{ash} are the weight percent (dry basis) of carbon, hydrogen, sulfur, oxygen, nitrogen, and ash in the feed-stock. Y_{H_2O} is moisture content on wet basis. $h_{vap} [MJ/kg]$ is enthalpy of vaporization and $M_{H_2O}, M_{H_2} [kg/kmol]$ is molecular weight of water and hydrogen respectively.

3.4.2 Thermal conductivity of the bed

There are packed bed models that considers thermal conductivity and radiation either as separate aspects of heat transfer or single aspect by defining effective thermal conductivity.

In the first method generally radiation effect has been modeled using flux model. Effective thermal conductivity of solid phase have assumed as a combination of mixing due to grate movement in grate furnaces and weighted sum of solid constituents (moisture, volatile, char, ash).

$$\lambda_s = \lambda_{s0} + \lambda_{sm} \quad [W/mK] \quad (3.17)$$

assuming

$$Pr_s = Sc_s = 1$$

$$\mu_s = \rho_{sb}D_s \text{ and } \lambda_{sm} = \mu_s C_{ps} = \rho_{sb}C_{ps}D_s$$

where, λ_s -solid conductivity[W/mK], λ_{s0} -solid material conductivity[W/mK], λ_{sm} -thermal transport caused by particle random movements[W/mK], Pr_s -Particle Prandlt Number, Sc_s -Particle Schmidt Number and D_s -particle diffusion coefficient[m²/s][10].

Gas phase thermal conductivity as a combination of laminar and turbulent effects.

$$\lambda_{rg} = \lambda_0 + 0.1d_p |V_g| \rho_g C_{pg} \quad [W/mK] \quad (3.18)$$

$$\lambda_{axg} = \lambda_0 + 0.5d_p |V_g| \rho_g C_{pg} C_{pg} \quad [W/mK] \quad (3.19)$$

where, λ_{rg} -thermal conductivity along the grate length direction(radial)[W/mK] and λ_{axg} -thermal conductivity along bed height direction(axial)[W/mK].

Second method can be seen in two approaches; one mostly used for homogeneous beds where a single energy equation is applied for both phases. Model consists of effective thermal conductivity for a quiescent bed(no fluid flow) and a correction for fluid flow;



University of Moratuwa, Sri Lanka
Electronic Theses & Dissertations
www.lib.mrt.ac.lk

$$\lambda_{e,b} = \lambda_{e,0} + aPrRe\lambda_g C_{pg} \quad [W/mK] \quad (3.20)$$

$$\lambda_g = 4.8 \times 10^{-4} t_g^{0.717} C_{pg} \quad [W/mK] \quad (3.21)$$

$$\text{and } \lambda_{e,0} = 0.8\lambda_g$$

where, $\lambda_{e,b}$ -effective thermal conductivity of the bed[W/mK], $\lambda_{e,0}$ -effective thermal conductivity of the bed without fluid flow[W/mK], λ_g -thermal conductivity of gas[W/mK].

The other method of effective thermal conductivity is assumed that effective thermal conductivity of solid is containing thermal conductivity of solid constituents, mixing effects due to grate movement and radiation. Gas phase thermal conductivity is expressed same as in equation 3.18,3.19 and 3.21.

$$\lambda_s = \eta \lambda_{VF} + (1 - \eta) \lambda_c + \lambda_{rad} + \lambda_{mix} C_{pg} \quad [W/mK] \quad (3.22)$$

$$\lambda_{rad} = 4\sigma \varepsilon_{rad,p} d_p \frac{\varepsilon_b}{(1 - \varepsilon_b)} t_s^3 C_{pg} \quad [W/mK] \quad (3.23)$$

$$\lambda_{mix} = \rho_s c_{p,s} D_s C_{pg} \quad [W/mK] \quad (3.24)$$

where, η -degree of mass loss, λ_{VF} -thermal conductivity of virgin fuel[W/mK], λ_c -thermal conductivity of carbon[W/mK], t_s [K] is solid phase temperature, d_p [m] is solid particle diameter, $\varepsilon_{rad,p}$ is solid particle emissivity, σ [W/m²K⁴] is Stefan-Boltzman constant and D_s [m²/s] is the particle diffusion coefficient.

Data related to particle diffusion coefficient(D_s) is difficult to find out in literature and it has to be experimentally determined. Therefore, in this study; although gas phase and solid phase energy equations separately considered; first method of effective thermal conductivity approach is used for modeling (equation 3.20, 3.21).

3.4.3 Mass diffusivity of the bed

Mass diffusivity of gas phase is also considered as a combination of diffusional and turbulent effects like thermal conductivity.

$$D_{i,e} = D_{i,0} + a d_p |v_g| C_{pg} \quad [m^2/s] \quad (3.25)$$

where, $D_{i,e}$ -effective mass diffusion coefficient of gas specie i, $D_{i,0}$ [m²/s] is the coefficient of diffusion of gas species i.

$D_{i,0}$; at different conditions is estimated through Wilke-Lee equation [9, 41].

3.4.4 Specific heat capacity of the bed

Specific heat capacity is heat required for a unit mass to increase the temperature for a unit degree of temperature. Heat capacity can be generally expressed as a combination of constituents's heat capacities. As biomass containing large number of constituents (volatile matter), it is difficult to evaluate overall heat capacity. Heat capacity will also be significantly affected by moisture content. Therefore, this modeling work uses an empirical model of heat capacity, which suggest heat capacity of biomass as a

variable of moisture content and temperature as shown below[13].

$$c_{P,wet} = \frac{c_{P,dry} + 4.19M}{1 + M} + A \quad [kJ/kgK] \quad (3.26)$$

where, $A = (0.02355T - 1.32M - 6.191)M$ and $c_{p,dry} = 0.1031 + 0.003867T$ and M-moisture content on wet basis

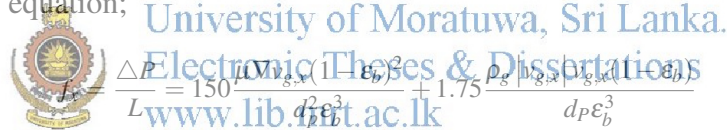
Gas phase heat capacity values are well established and expressed as follows;

$$c_{p,g} = 990 + 0.122t_g - 5680 \cdot 103t_g^{-2} \quad [J/kgK] \quad (3.27)$$

3.4.5 Pressure drop

Packed bed biomass combustion models developed so far have been hardly considered about pressure drop through packed beds. The reason is most popular one-dimensional transient model which considers bed as a plug flow reactor does not account the pressure drop and also calculations of packed bed maximum pressure drops have shown that this assumption is reasonable[21]. However, in a two-dimensional model this cannot be neglected.

Gas phase pressure drop due to resistance in the packed bed is calculated from Erguns's equation;



$$f_x = \frac{\Delta P}{L} = 150 \frac{\mu \nabla v_{g,y} (1 - \epsilon_b)^2}{d_p^2 \epsilon_b^3} + 1.75 \frac{\rho_g |v_{g,y}| v_{g,y} (1 - \epsilon_b)}{d_p \epsilon_b^3} \quad \left[\frac{N}{m^3} \right] \quad (3.28)$$

$$f_y = \frac{\Delta P}{L} = 150 \frac{\mu \nabla v_{g,x} (1 - \epsilon_b)^2}{d_p^2 \epsilon_b^3} + 1.75 \frac{\rho_g |v_{g,x}| v_{g,x} (1 - \epsilon_b)}{d_p \epsilon_b^3} \quad \left[\frac{N}{m^3} \right] \quad (3.29)$$

where, $f_{x(y)}$ -pressure drop in x-direction(y-direction), μ -dynamic viscosity[kg/ms], $v_{g,x(y)}$ -velocity of gas phase in x (y-direction)[m/s], d_p -particle diameter[m], ϵ_b -porosity of the bed.

3.4.6 Particle shrinkage

Succession of combustion shrinks biomass particles and therefore fuel bed will shrink too. This will make bed volume reduction and porosity changes as well. Shrinkage does not affect much on pyrolysis of thermally thin or thermally thick regime but on thermal wave regime and char yield have shown very little effect from shrinkage[42].

In early stages of biomass combustion models;particle shrinkage have been neglected to simplify the models.Later on research work have been carried out on numerical calculation on shrinking of a stationary bed in macro scale models and shrinkage of bed have been considered in modeling[17, 43, 44].

This model assumes that the bed volume is constant and only porosity will change with combustion.Porosity change due to drying is neglected and pyrolysis and char combustion affect according to 3.30.

$$\varepsilon_b = \varepsilon_{0,b} + (1-\varepsilon_{0,b}) \sum f_i(X_{i,0}-X_i) \quad (3.30)$$

where ε_b (porosity of bed) = $\frac{V_g}{V}$, $\varepsilon_{0,b}$ -initial porosity of the bed, $X_{i,0}$ -initial mass fraction of i^{th} solid component, X_i -mass fraction of i-th solid component, i-volatile and char, $f_i = \frac{\rho_s}{\rho_i}$, ρ_i -density of i-th component, ρ_s -density of solid.

Porosity within the biomass particles are not considered in this model and initial porosity assumed as 0.5[16].

3.4.7 Particle size and shape

In most practical situations biomass does not have regular shapes and sizes. Therefore for modeling purposes particles have often considered as spherical by means of keeping surface area to volume ratio same as in non-spherical particle. In a spherical particle surface area to volume ratio is equal to:

$$A = \frac{4\pi r^2}{\frac{4}{3}\pi r^3} = \frac{6}{d} \quad [1/m] \quad (3.31)$$

But when the particles in a packed bed;depending on the porosity surface area will be different.

Therefore;

$$A = \frac{6(1-\varepsilon_b)}{d} \quad [1/m] \quad (3.32)$$

where A-volumetric surface area[1/m], r-radius of spherical particle, d-diameter of spherical particle.

For wood chips used in this model;calculated A=240 and considered it as constant for all particles.

CHAPTER IV

CFD SIMULATION METHOD

There are three numerical solution techniques for partial differential equations created for CFD applications; finite difference, finite element and spectral methods [28]. Finite volume method; a special finite difference method uses in CFD software used for this modeling work; OpenFOAM and therefore, discussing more detail in this chapter.

4.1 Finite volume approach

Finite volume approach is consisting four major steps of solution process.

1. Divide the physical system of interest in to a finite number of non-overlapping control volumes
2. Integration of governing equations over all control volumes in the geometry
3. “Discretization”-conversion of integral equations in to a set of algebraic equations
4. Solution of algebraic equations by an iterative method.

Integration of governing equations employ Gauss divergence theorem to convert volume integrals in to surface integrals. The general transport equation for a dynamic system of a property ϕ can be represented as ;

$$\underbrace{\int_{cv} \frac{\partial(\rho\phi)}{\partial t} dV}_{unsteady\ term} + \underbrace{\int_{cv} div.(\rho u\phi) dV}_{convective\ term} = \underbrace{\int_{cv} div(\Gamma grad\phi) dV}_{diffusive\ term} + \underbrace{\int_{cv} S_\phi dV}_{source\ term} \quad (4.1)$$

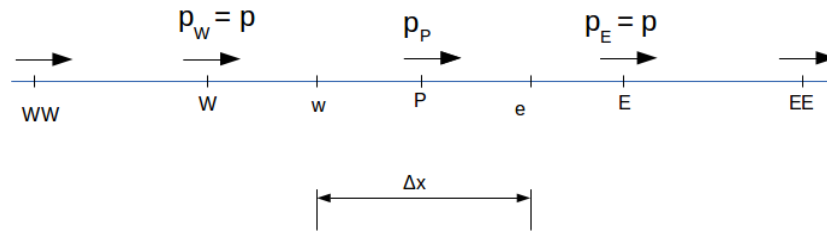


Figure 4.1: one-dimensional grid having checker board pressure field

Using the Gauss theorem which states that for a vector a ;

$$\int_{cv} \text{div.}(a) dV = \int_A n \cdot a dA \quad (4.2)$$

$n \cdot a$ is the component of vector a in the direction of the vector n normal to surface element dA . Simply the physical meaning of this theorem is that divergence a over control volume will be equal to the sum of a – component values normal to the surfaces which bounds the control volume. This can be applied to the convective term and diffusive term of equation 4.1.

Discretization techniques should be selected carefully depending on the transport method of terms in Equation 4.1: Convection term, Diffusion term, source terms and rate of change. There are various approximation techniques available like, central differencing, upwind differencing, QUICK, FVD, etc. Discretized equations will create a set of linear algebraic equations of each property going to be solved. Usually iterative methods are preferred to solve them such as Jacobi, Gauss-siedel point iteration methods, TDMA, etc. An algorithm will be used to approach overall solution combining all property equations of the system with pressure-velocity correction. There are algorithms like SIMPLE, PISO, SIMPLEC, etc to iteratively solve the overall system of equations.

4.2 Pressure correction

There are situations; a certain domain of interest having a checker board type pressure field as shown in the Figure 4.1.

Discretized momentum equation can be written at point P;

$$a_P u_P = \sum a_{nb} u_{nb} + (p_w - p_e) A_P + b_P \quad (4.3)$$

$$p_w - p_e = \frac{p_P + p_W}{2} - \frac{p_P + p_E}{2} = \frac{p_W + p_E}{2} = 0 \quad (4.4)$$

This zero pressure difference affects to point E as well as W which lead to non physical situations in velocity equations and further affected in pressure correction, which requires velocities at cell faces (u_e and u_w). This have been resulted in erroneous oscillatory velocity fields in the past.

In structured grid systems checker board effects are avoided by staggered grid systems, which velocity is defined at surface of the control volumes, while pressure is defined at grid centroids. However, in unstructured grids, this will make complexities in discretized equations. Therefore, unstructured grid systems often use Rhie-Chow method as a solution.

4.2.1 Rhie-Chow method

In the Rhie-Chow method; first an intermediate velocity field is calculated from momentum equation by neglecting pressure differences. This velocity is interpolated to the face including pressure gradient for pressure correction, which is presented in Equation 4.5 [45]. These interpolated velocities will be applied to continuity equation to obtain the correct velocities.

In Rhie-Chow method, instead of linear interpolation; velocity at cell faces presented as;

$$u_e = \frac{u_P + u_E}{2} + \underbrace{\frac{d_P + d_E}{2} (p_P - p_E) - \frac{d_P}{4} (p_W - p_E) - \frac{d_E}{4} (p_P - p_{EE})}_{\text{pressure correction}} \quad (4.5)$$

Assuming $d_P = d_E$ Parenthesized term in equation 4.5 is equal to $\frac{d}{4} (p_{EE} - 3p_E + 3p_P - p_W)$.

$$\left(\frac{\partial^3 p}{\partial x^3} \right)_e = \frac{1}{\Delta x^3} (p_{EE} - 3p_E + 3p_P - p_W) \quad (4.6)$$

and substituting equation 4.6 to 4.5;

$$u_e = \frac{u_P + u_E}{2} + \frac{d}{4} \left(\frac{\partial^3 p}{\partial x^3} \right)_e \Delta x^3 \quad (4.7)$$

$\frac{d}{4} \left(\frac{\partial^3 p}{\partial x^3} \right)_e \Delta x^3$, is called pressure smoothing term or added dissipation term and it will remove the oscillation of velocities in co-located grid arrangement due to checker board pressure fields. The Rhie and Chow procedure has been extremely successful in co-located unstructured grids[28].

4.3 SIMPLE algorithm

In CFD equations for mass, momentum, energy can be generated using conservation of those properties. As pressure is involved in momentum equation there should be a method to solve it. In a compressible flow equation of state $p = p(\rho, T)$ can be used. However, in an in-compressible situation it would not be satisfied equation of state and some other procedure would have to be used. When the correct pressure field is applied to momentum equation, the resulting velocity field should be satisfied in the continuity equation. Since the correct pressure field is not known in advance an iterative method has to be followed.

SIMPLE algorithm is such a method which is developed for pressure-velocity linking flows to obtain correct pressure and velocity fields and solution for other property equations by using an iterative method. SIMPLE stands for Semi Implicit Method for Pressure Linked Equations which is developed by Patankar and Spalding in 1972[28].

SIMPLE algorithm is generally used to solve steady state flows although it can be adjusted to transient conditions as well. Initially all the properties will be assumed including pressure field which will be used to obtain a velocity field from momentum equation. Then that velocity will be applied to obtain a pressure correction from continuity equation which will be used back in momentum equation to attain new velocity field. These velocity fields will be used to generate fluxes in other transport equations (energy and species) and solve them. This procedure will follow until all the convergence criteria are satisfied. The solution procedure of SIMPLE algorithm for a CFD simulation is shown in Figure 4.2.

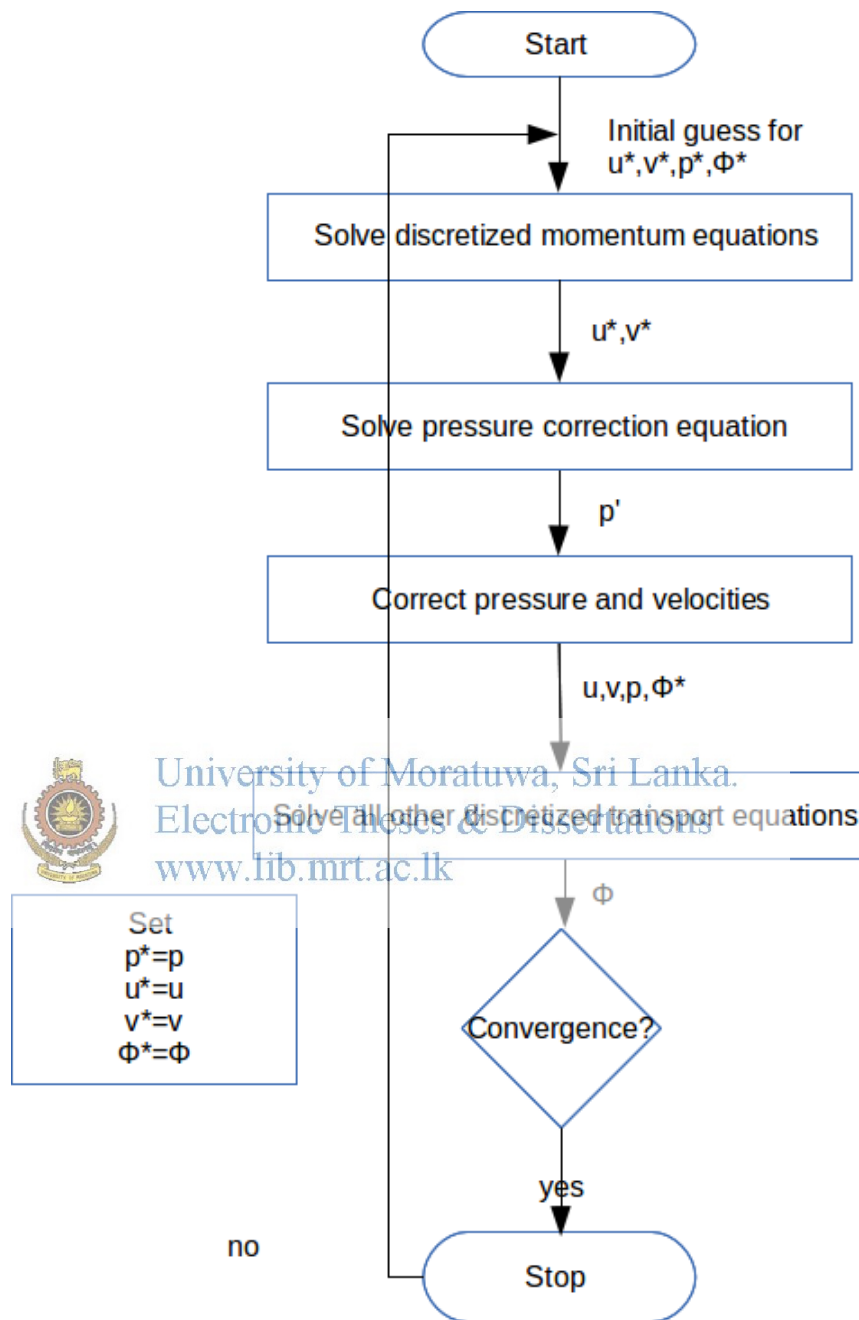


Figure 4.2: SIMPLE algorithm

CHAPTER V

INTRODUCTION TO OPENFOAM

5.1 Introduction to OpenFOAM

OpenFOAM stands for “Open Source Field Operation and Manipulation”. OpenFOAM is a very popular CFD software specially among research communities owing to special features of an open source software. OpenFOAM uses finite volume method for solving CFD problems which is capable of handling unstructured mesh and employing a co-located grid arrangement.

OpenFOAM codes written in C++; which is an intermediate language comprises both high level and low level language features including object oriented programming paradigm as well. An understanding about object oriented programming is important to work with OpenFOAM. Object-oriented programming (OOP) is a programming paradigm that represents concepts as “objects” that have data fields (attributes that describe the object) and associated procedures known as methods (member functions). “Objects”, which are usually instances of classes, are used to interact with one another to design applications and computer programs [46, 47]. OOP reduces the gap between speaking languages vs computer languages as “Object” of a class correspond to the objects of real world.

The web site <http://www.openfoam.org>, main sources of information about OpenFOAM are the user guide, programmer’s guide, OpenFOAM message board and OpenFOAM Wiki. Theses related to OpenFOAM can be found out in these.

5.2 History of OpenFOAM

Working on software have begun with Prof. David Gosman and Dr. Raad Issa from Imperial college, London around 1990 [45]. The motivation to develop CFD software have been mainly dissatisfaction with legacy codes in Fortran and the goal to create some-

thing reusable by others[48]. OpenFOAM started as FOAM around 1993 as a collaboration of Henry Weller and Hrvoje Jasak then became OpenFOAM after releasing as an open source software in December 2004. Since then, 11 major releases have been launched; the latest version is OpenFOAM 2.3.0, released in February 2014.

Dr. Jasak maintains a fork of OpenFOAM called the Extend-Project (also known as OpenFOAM-extend) which includes additional modeling capability not found in the official version and is centered on community-driven development[45].

5.3 OpenFOAM C++ library

OpenFOAM C++ library can be divided into three main categories; solvers, libraries and utilities. Running a case in a CFD software has three major steps; pre-processing, solving, post-processing. Rather than describe about OpenFOAM C++ libraries and CFD solution steps, it can be understood in an integrated manner. Therefore, each step and involvement of C++ library is briefly discussed below.

- Pre-processing

1. Definition of the geometry of the region of interest (computational domain) and grid generation, division of the domain into a number of smaller, non-overlapping sub-domains. The utilities necessary to create mesh (*cfxToFoam*, *ansysToFoam*, *blockMesh*, *checkMesh*, *mapFields*).
2. Selection of the physical and chemical phenomena that need to be modeled-thermophysical model libraries, combustion model libraries, chemistry libraries, Fields library, radiation model library, etc.
3. Definition of fluid properties (empirical models)-libraries for defining physical and chemical properties (*janafThermo*, *specific enthalpy*, *perfect gas*, *sutherland transport* libraries, etc).
4. Specification of appropriate boundary conditions and initial conditions-*patch* type libraries.

- Solving

1. Integration of the governing equations of fluid flow over all the (finite) control volumes of the domain-finite volume library

2. Discretization – conversion of the resulting integral equations into a system of algebraic equations using numerical methods-finite volume schemes library
 - (a) divergence terms
 - (b) gradient terms
 - (c) laplacian terms
 - (d) time
 - (e) interpolation
 3. Solution of the algebraic equations by an iterative method-finite volume solution libraries
 - (a) SIMPLE
 - (b) PISO
 - (c) PIMPLE
- Post-processing-paraView and other utilities of OpenFOAM(*sample, probeLocations, foamCalc, etc*)

1. Domain geometry and grid display
2. Vector plots-line and shaded contour plots
3. 2D and 3D surface plots
4. Particle tracking
5. View manipulation (translation, rotation, scaling etc.)
6. Colour PostScript output

comes with more than 80 precompiled application solvers which are designed to simulate specific problems in Engineering Mechanics and large set of utilities for Pre and Post processing.

5.3.0.1 *OpenFOAM lists and fields*

Tensors may be scalar,vector or higher order tensors which happen frequently in mathematics, physics, as well as CFD(velocity vector, density scalar, pressure scalar, temperature scalar, etc).In finite volume, each cell in a mesh have unique values for these

| | points | faces | cells | boundary |
|------------|--|---|---|---|
| definition | -vector in units of metre (m) -compiled in to a <i>pointList</i> -point label starts from zero. | -ordered list of points -direction of face normal defined by right-hand rule -for boundary faces;ordering of the point labels is such that the face normal points outside of the computational domain. | -list of faces in arbitrary order | -list of patches,each associated with a boundary condition |
| conditions | cannot contain either 2 points for the same location or a point which is not part of at least one face | expected to be: -convex ¹ -allowed to be warped ² | must be: -contiguous ³ -convex ⁴ -closed ⁵ and orthogonality constraint must be satisfied ⁶ | -contain only boundary faces and no internal faces ⁷ -must be closed ⁷ |

Table 5.1: defining mesh of the geometry

tensors. Therefore, a list of tensors have to be represented. In OpenFOAM there is an array template class called `Field<Type>`, which is renamed as `FieldType` (`scalarField`, `vectorField`, `symmTensorField`, etc). Same operations can be performed between `Field-Types` of same number of elements which carry with single tensor. OpenFOAM also supports operations between a field and single tensor, e.g. all values of a **Field U** can be multiplied by the **scalar 2** with the operation $U = 2.0 * U$ [49].

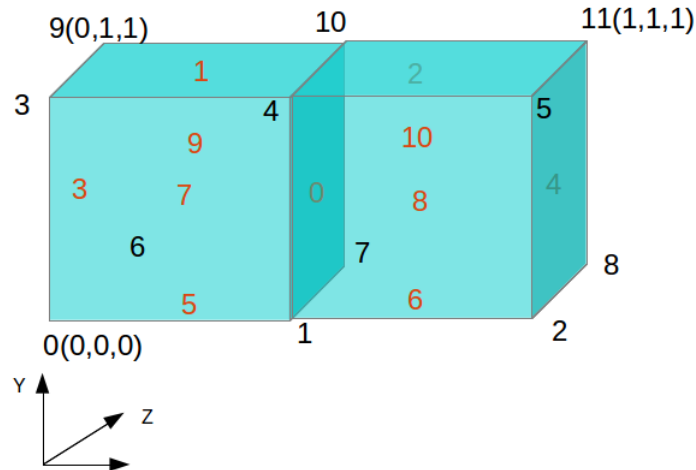
5.3.0.2 Mesh generation

In OpenFOAM, a single cell of a mesh can have an unlimited number of faces where, for each face, there is no limit on the number of edges nor any restriction on its alignment. A mesh with this general structure is known in OpenFOAM as a **polyMesh**[50].

A mesh is constructed from points, faces, cells and boundary patches.

The components and conditions that a mesh must satisfy are:

polyMesh sub-dictionary in a case file has the full set of data which identifies the mesh structure of the geometry. *blockMeshDict* is prepared according to the defined geometry. Running “*blockMesh*” utility within the case file create the files containing the list of faces, neighbour, owner, points and also the boundary face data.



| pointList | pointLabel | faceList | faceLabel |
|-----------|------------|-------------|-----------|
| (0 0 0) | 0 | (1 7 10 4) | 0 |
| (1 0 0) | 1 | (3 4 10 9) | 1 |
| (2 0 0) | 2 | (4 5 11 10) | 2 |
| (0 1 0) | 3 | (0 6 9 3) | 3 |
| (1 1 0) | 4 | (2 8 11 5) | 4 |
| (2 1 0) | 5 | (0 1 7 6) | 5 |
| (0 0 1) | 6 | (1 2 8 7) | 6 |
| (1 0 1) | 7 | (0 1 4 3) | 7 |
| (0 1 1) | 8 | (4 2 5 4) | 8 |
| (1 1 1) | 9 | (6 7 10 9) | 9 |
| (2 1 1) | 10 | (7 8 11 10) | 10 |
| | 11 | | |



University of Moratuwa, Sri Lanka.
 Electronic Theses & Dissertations
 www.lib.mrt.ac.lk

Figure 5.1: hexahedral cells in a mesh with part of polyMesh data

OpenFOAM has the ability to create cells in different shapes, creating automatic meshes for complex geometries using *snappyHexMesh* utility and creating *polyMesh* using third party meshes.

Figure 5.1 shows a mesh with two hexahedral cells with point and face labels and lists.

FV discretization uses specific data that is derived from the mesh geometry stored in *polyMesh*. OpenFOAM therefore extends the *polyMesh* class to *fvMesh* which stores the additional data needed for FV discretisation. *fvMesh* is constructed from *polyMesh* and stores the data shown in the Table 5.2 which can be updated during run

| class | description | symbol | access function |
|---------------------------|----------------------|----------|-----------------|
| <i>volScalarField</i> | Cell volumes | V | $V()$ |
| <i>surfaceScalarField</i> | Face area magnitudes | S_f | $magSf()$ |
| <i>suraceVectorField</i> | Face area vectors | S_f | $Sf()$ |
| <i>volVectorField</i> | Cell centres | C | $C()$ |
| <i>surfaceScalarField</i> | Face motion fluxes | ϕ_g | $phi()$ |
| <i>suraceVectorField</i> | Face centres | C_f | $Cf()$ |

Table 5.2: fvMesh stored data

time in cases where the mesh moves, refined etc..

5.3.0.3 Defining a *geometricField* in *OpenFOAM*

The term tensor describes an entity that belongs to a particular space and obeys certain mathematical rules[49].

A property of an interested system can be expressed as a tensor. But in CFD these properties must have list of tensors with a value in each finite volume (refer Section 5.3.0.1), the relevant discrete point at geometry, units, boundary conditions at boundaries, values at each iterations, values with time, etc. Therefore, just a tensor or Field Type would not satisfy the requirements to represent properties in real cases of CFD. The relevant requirements can be combined to define a class relating to discrete points in a geometry, specified in *OpenFOAM* by the template class *geometric Field<Type>*. The Field values are separated into those defined within the internal region of the domain, e.g. at the cell centres, and those defined on the domain boundary, e.g. on the boundary faces.

The *geometric Field<Type>* stores the following information[49]:

- ***Internal field***

- This is simply a list of the specific tensor.

- ***Boundary Field***

- This is a *GeometricBoundaryField*, in which a Field is defined for the faces of each patch and a Field is defined for the patches of the boundary. This

| No. | Property | SI unit |
|-----|--------------------|----------------------|
| 1 | Mass | kilogram(kg) |
| 2 | Length | metre(m) |
| 3 | Time | second(s) |
| 4 | Temperature | Kelvin(K) |
| 5 | Quantity | kilogram-mole(kgmol) |
| 6 | Current | Ampere(A) |
| 7 | Luminous intensity | candela(cd) |

Table 5.3: S.I. base units of measurement

is then a field of fields, stored within an object of the *Field Field<Type>* class. A reference to the *fvBoundaryMesh* is also stored.

- **Mesh**

- A reference to an *famish*, with some additional detail as to the whether the field is defined at cell cent res, faces, etc.

- **Dimensions**

- Dimensions of the relevant property represented by *geometric Filed<Type>*.
- The input/output format for a dimension Set is 7 scalars delimited by square brackets for basic units, e.g. for m^2/s [0 2 -1 0 0 0 0]. The 5.3 provides the order of units presenting inside the square bracket.

- **Old values**

- Discretisation of time derivatives requires field data from previous time steps. The *geometricField<Type>* will store references to stored fields from the previous, or old, time step and its previous, or old-old, time step where necessary.

- **Previous iteration values**

- The iterative solution procedures can use under-relaxation which requires access to data from the previous iteration. Again, if required, *geometric-Field<Type>* stores a reference to the data from the previous iteration.

5.3.0.4 Boundary Conditions

Implementation of most appropriate boundary condition is a necessity for avoiding errors in numerical simulations. OpenFOAM divides a boundary into patches for the purpose of applying boundary conditions. One patch may include one or more enclosed areas of the boundary surface which do not necessarily need to be physically connected. The hierarchy of patch conditions available in OpenFOAM can be basically described as follows[50];

- Base type -The type of patch described purely in terms of geometry or a data 'communication link'(the base type is specific in the *blockMeshDict* file)
 - patch
 - wall
 - symmetryPlane
 - wedge
 - cyclic
 - empty
 - processor
- Primitive type -The base numerical patch condition assigned to a field variable on the patch
 - fixedValue
 - fixedGradient
 - mixed
 - zeroGradient
 - calculated
 - directionMixed
- Derived type -A complex patch condition, derived from the primitive type, assigned to a field variable on the patch. There is a large number of derived patch types in OpenFOAM which can be found on following locations



- `$FOAM SRC/finiteVolume/fields/fvPatchFields/derived { \textstyle { \scriptstyle fvVectorMatrixUEqn (fvm::ddt(U)+fvm::div(phi,U) - fvm::laplacian(nu, U))}};`
 - within certain model libraries, that can be located by typing the following command in a terminal window `find $FOAM SRC -name "*derivedFvPatch*"`
 - within certain solvers, that can be located by typing the following command in a terminal window `find $FOAM SOLVERS -name "*fvPatch*"`
- There are other boundary conditions which can be applied using other OpenFOAM based software developed by community.(eg:groovyBC, user developed boundary conditions.)

5.3.0.5 Equation discretization

Equation discretization is a vital part of finite volume approach on solving CFD problems, which generates algebraic equations from PDEs. Algebraic equations are in the form of matrix:



University of Moratuwa, Sri Lanka.
Electronic Theses & Dissertations
www.lib.mrt.ac.lk

$$[A] \cdot [x] = [b] \quad (5.1)$$

where $[A]$ is a square matrix, $[x]$ is the column vector of dependent variable and $[b]$ is the source vector. Matrix presents i.e. a ***geometricField<Type>***, or more specifically a ***volField<Type>*** (values defined at centroid of the grid) when using FV discretisation[49].

$[A]$ is a list of coefficients of a set of algebraic equations, and cannot be described as a ***geometricField<Type>***. It is therefore given a class of its own: ***fvMatrix***. ***fvMatrix<Type>*** is created through discretization of a ***geometric<Type>Field*** and therefore inherits the $\langle Type \rangle$. It supports many of the standard algebraic matrix operations of addition "+", subtraction "-" and multiplication "*".

Each term in a PDE is represented individually in OpenFOAM code using functions of *finiteVolumeMethod* or *finiteVolumeCalculus*, abbreviated to *fvm* and *fvc* respectively. *fvm* and *fvc* contain static functions, devoted for differential operators, e.g.

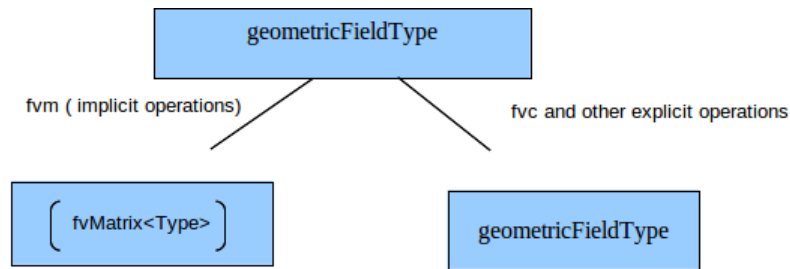


Figure 5.2: A *geometricField<Type>* and its operators

∇^2 , $\nabla \cdot$ and $\partial/\partial t$, that discretize *geometricField<Type>*s. The purpose of defining these functions within two classes, *fvn* and *fvc*, rather than one, is to distinguish:

- functions of *fvn* that calculate implicit derivatives of and return an *fvMatrix<Type>*
- some functions of *fvc* that calculate explicit derivatives and other explicit calculations, returning a *geometricField<Type>*

5.4 Running a case

Each OpenFOAM case has a similar structure with slight differences according to the particular choice of solver and methods of pre-processing and post-processing.

The major directories of an OpenFOAM case file are;

- constant
- system
- “0”(initial conditions)
- time directories

5.4.1 “system” sub directory

system directory contains input data required for discretization, discretised equation solving and controls of used algorithm and time controls related to the case.

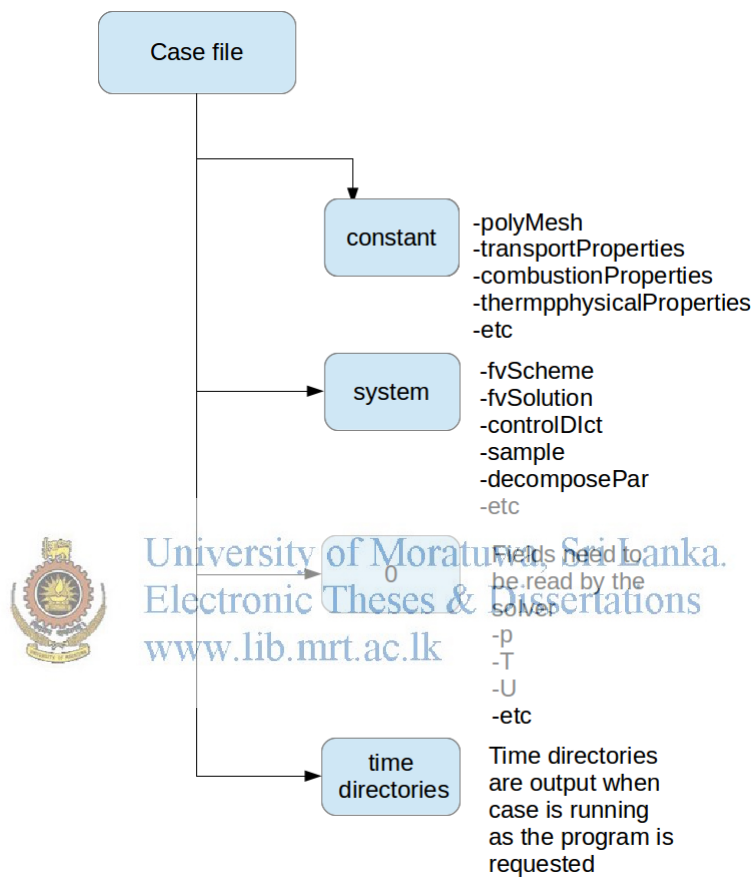


Figure 5.3: Typical case file structure in OpenFOAM

fvSchemes file is to provide the discretization methods for each and every term in transport equations which is used by the case. There is a variety of selections available for each terms and it can be referred in openFOAM user guide.

fvSolution file is to input all data necessary for solving discretized equations. It should have all the properties going to be solved by the application solver and solvers required by each property which is necessary to solve set of linear algebraic equations generated by discretization, convergence criteria and some more data. Apart from that *fvSolution* file contains data required by the algorithm such as number of correctors, relaxation factors for equations or fields, pressure reference value, etc.

controlDict have the time controls like time step (for transient problems), time period of run, period at which the time is written to case file, start time, etc. In spite of that the name of the using solver is mentioned in the file and also maximum courant number which is important for accuracy of the results. There are more data can be added in *controlDict* file but not discussing here further.

In a parallel running; *decomposeParDict* has to be created in the system directory.

5.4.2 “constant” sub directory

The *polyMesh* sub-dictionary is having *blockMeshDict* file which contains all the necessary data to create the geometry and mesh with boundary names and its basic types. There may be more files in the constant directory depending on the requirement of the solver. If the case involves combustion; *combustionProperties* file and then necessary thermo-physical properties have to be calculated which is mentioned in *thermo-physicalProperties* file. Very often *transportProperties* file is used to provide details on properties like viscosity. If radiation is involved there will be *radiationProperties* file. Further lot more files may be appear in a case file like, *turbulenceProperties*, *reactions*, *LESProperties*, etc.

5.4.3 Time directories (0, . . .)

“0” directory contains initial and boundary conditions of input parameters. Putting more accurate initial and boundary condition is essential to get results close to real conditions. Other “time” directories will create when model is running according to the conditions given in the *controlDict*. Sometimes “o” directory is not necessary, since initial and boundary conditions are provided through other methods like “senk.inp”,

”senk.out” sub-directories in *CHEMKIN* directory (eg:\$FOAM_RUN/ tutorials/ combustion/ chemFoam).

5.4.4 other directories or files

For any additional requirements like validation data,files from software such as *swak4Foam*, *gnuplot* may be included in the case directory.And also “log” file will automatically creates when a case is running as a background process.Any other “postProcessing” files will be created when resulting data post processing is requested (eg:*sample*).

5.4.5 Community developed additional OpenFOAM tools

- **OpenFOAM Extend** -A community-driven initiative on the extension of OpenFOAM in the spirit of the Open Source development model. OpenFOAM-extend is maintained by Wiki Ltd OpenFOAM-extend.This fork has a large repository of community-generated contributions, much of which can be installed into the official version of OpenFOAM with minimal effort.It is developed in parallel to the official version of OpenFOAM, incorporating its latest versions, although these are released one or two years later.

-  **swak4Foam** (“Swiss Army Knife 4 Foam”)
 University of Moratuwa, Sri Lanka.
 Electronic Theses & Dissertations
 www.lib.mrt.ac.lk

Like that knife it rarely is the best tool for any given task, but sometimes it is more convenient to get it out of your pocket than going to the tool-shed to get the chain-saw *swak4Foam*.

- A library that combines the functionality of *groovyBC* and *funkySetFields*: it offers the user the possibility to specify expressions involving the fields and evaluates them. This library offers a number of utilities (for instance *funkySetFields* to set fields using expression), boundary conditions (*groovyBC* to specify arbitrary boundary conditions based on expressions) and function objects that allow doing many things that would otherwise require programming[51, 52].
- **groovyBC** This boundary condition is basically a mixed-boundary condition where value, gradient and valueFraction are specified as expressions

instead as fields. It can be used to **set non-uniform boundary-conditions without programming**[53].

- **funkySetFields** This utility sets the value of a scalar or a vector field depending on an expression that can be entered via the command line or a dictionary. It can also be used to set the value of fields on selected patches. It can be used to **set non-uniform initial-conditions without programming**.
- **pyFoam** A python library to control OpenFOAM-runs and manipulate OpenFOAM-data. Comes with a number of utilities that should make easier for people who like to work in command lines. This Python-library can be used to[54];
 - analyze the logs produced by OpenFoam-solvers
 - execute OpenFoam-solvers and utilities and analyze their output simultaneously
 - manipulate the parameter files and the initial-conditions of a run in a non-destructive manner
 - plots the residuals of OpenFOAM solvers



University of Moratuwa, Sri Lanka.
Electronic Theses & Dissertations
www.lib.mrt.ac.lk

CHAPTER VI

DEVELOPING A NEW SOLVER IN OPENFOAM

Developing a new solver in OpenFOAM cannot be fulfilled alone by user guide and programmer's guide although they provide an insight in to OpenFOAM; still lot of matters will remain to be solved. An interesting thing about CFD code development in open source software is that there is a community having issues with their codes who is anticipating for help and also veterans of the field are always give their helping hand to amateurs. Therefore, in this study assistance obtained from the community when developing new applications, libraries, boundary conditions, etc in OpenFOAM.

The first thing of creating a new application solver is to write the codes. This requires the knowledge on C++, OpenFOAM class structure which essentially include; representing finite volume method, pressure correction using Rhie-Chow method, writing transport equations, linearization of source terms, introducing new fields, solution algorithms, etc. Then to compile the code and make a binary program requires the knowledge on compilation of programs and debugging options which is most time consuming part in whole process. After that a real case has to be prepared and run as a case file in OpenFOAM; when errors were appeared, the code was refined again. Latter part includes creating the mesh, boundary conditions, more CFD theories, chemical and thermophysical properties, residual mapping, etc. All in all this chapter is discussing about compiling applications and libraries in OpenFOAM, Rhie-Chow method since it has been modified for this solver and procedure of creating a solver in OpenFOAM.

6.1 Compiling applications and libraries

OpenFOAM, is supplied with the *wmake* utility to compile programs; based on *make* but more versatile and easier to use. As mentioned in 5.1 knowing about OOP is important when work with C++ and classes and their objects have a very important role in programming using C++. Definition of a class, its compilation and calling the class

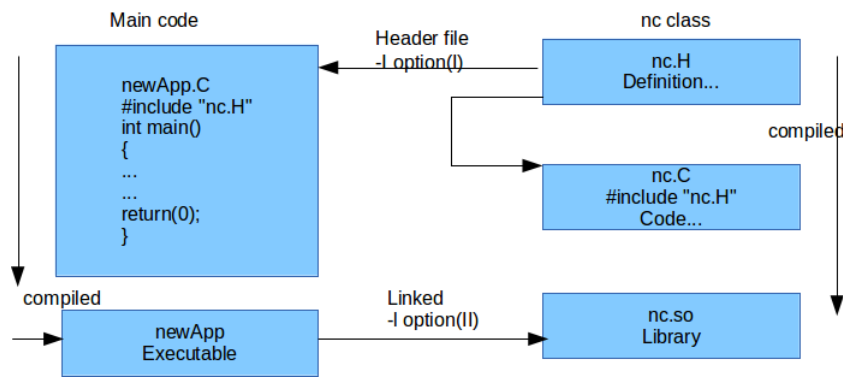


Figure 6.1: Header files,source files,compilation and linking

from another program is schematically shown in the Section 6.1.

A class is defined through a set of instructions such as object construction, data storage and class member functions. The file containing the class definition takes a **.C** extension, e.g. a new class would be written in the file **nc.C**. This file can be compiled independently of other code into a binary executable library file known as a shared object library with the **.so** file extension, **i.e.nc.so**. When compiling a piece of code, say **newApp.C**, that uses the **nc** class, **nc.C** need not be recompiled, rather **newApp.C** calls **nc.so** at run time. This is known as **dynamic linking**(see right hand side of 6.1)[50].



University of Moratuwa, Sri Lanka.
Electronic Theses & Dissertations
www.lib.mrt.ac.lk

6.1.0.1 Compiling with wmake

OpenFOAM applications are organized using a standard convention that the source code of each application is placed in a directory whose name is that of the application. Directory structure for an application is shown in an example below 6.2.

Including Headers

A header file is a declaration file of a class with “.H” extension.

The **Make/options** file contains the full directory paths to **locate header files** using the syntax:

```

EXE INC = \
-I<directoryPath1> \
-I<directoryPath2> \
... \
  
```

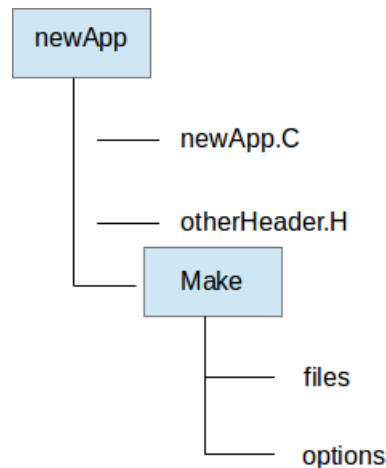


Figure 6.2: Directory structure of an application

–I<directoryPathN >

Linking to object libraries

The compiler links to shared object library paths with the “-L” option in wmake. The actual library files to be linked must be specified using the “-l” option and removing the “lib” prefix and “.so” extension from the library file name, e.g. **libnew.so** is included with the flag `-lnew`.

The Make/options file contains the full directory paths and library names using the syntax:

```

EXE LIBS = \
-L<libraryPath1 > \
-L<libraryPath2 > \
... \
-L<libraryPathN > \
-l<libraryName1 > \
-l<libraryName2 > \
... \
-l<libraryNameN >
  
```

Source files to be compiled

The compiler requires a list of “.C” source files that must be compiled. The list must contain the main “.C” file but also any other source files that are created for

| Argument | Type of compilation |
|----------|---|
| lib | Build a statically-linked library |
| libso | Build a dynamically-linked library |
| libo | Build a statically-linked object file library |
| jar | Build a JAVA archive |
| exe | Build an application independent of the specified project |

Table 6.1: Optional compilation arguments to wmake

the specific application but are not included in a class library. The **Make/files** file includes a full path and name of the compiled executable, specified by the “EXE =” syntax. The OpenFOAM release offers two useful choices for path: standard release applications are stored in \$FOAM_APPBIN; applications developed by the user are stored in \$FOAM_USER_APPBIN (These paths are introduced in etc/bashrc file or etc/cshrc file in OpenFOAM main directory).

Running wmake

The wmake script is executed by typing:

```
wmake <optional Arguments> <optionalDirectory>
```

For an application executable, no <optional Arguments> are required. However “<optional Arguments>” may be specified for building libraries, etc as described in 6.1.

Linking new user-defined libraries to existing applications

Shared object libraries can link at run-time (not at compilation stage) by simply adding the optional keyword entry *libs* to the *controlDict* file for a case and enter the full names of the libraries within a list (as quoted string entries). For example, if a user wished to link the libraries new1 and new2 at run-time, they would simply need to add the following to the case controlDict file:

```
libs (
"libnew1.so"
"libnew2.so" );
```

6.2 Rhie-Chow method in OpenFOAM

OpenFOAM does not apply Rhie-Chow method as an explicit term in the equations, which makes it difficult to see how the Rhie-Chow correction is applied[32]. The method used in OpenFOAM would rather say '**in the spirit of RHIE and CHOW**'.

In a simple incompressible flow example, vector form equations would be:

$$\frac{\partial U}{\partial t} + \nabla \cdot (UU) - \nabla \cdot (\nu \nabla U) = -\frac{1}{\rho} \nabla p \quad (6.1)$$

Lets consider Equation 6.1 in OpenFOAM format:

$$fvVectorMatrixUEqn(fvm::ddt(U) + fvm::div(phi,U) - fvm::laplacian(nu,U)); \quad (6.2)$$

Before defining the terms of the above equation looking at the Gauss theorem, which is used in OpenFOAM to convert volume integrals to surface integrals;

$$\int_V \nabla \cdot (U\Upsilon) dV = \int_S (U\Upsilon)_f \cdot \hat{n} dS = \sum_i U_{f,i} \Upsilon_{f,i} S_{f,i} = \sum_i U_{f,i} \cdot \phi_i \quad (6.3)$$

where



University of Moratuwa, Sri Lanka.
Electronic Theses & Dissertations
www.lib.mrt.ac.lk

(6.4)

subscript f indicates that the term should be evaluated at the cell face. ϕ , is scalar product of cell face velocity and cell face normal (magnitude is surface area of the face).

Now it is easy to look at the Equation 6.2 terms,

$$\int_V \nabla \cdot (U\Upsilon) dV \implies fvm::div(phi,U) \quad (6.5)$$

It is important to note which part of the left hand side is turned into phi and which is solved for. In this case we solve for U , and Υ is related to phi via Equation 6.4. **There is also a difference in that Υ is a field evaluated in the cell centres, while phi is defined on the surfaces.**

Referring to the fvMatrix class of OpenFOAM (which is the class defines a matrix generated in finite volume method discretization), the momentum equation would be in the matrix form as following.

$$\mathcal{A}[U] = \mathcal{H} - \nabla p \quad (6.6)$$

$$[U] = \frac{\mathcal{H}}{\mathcal{A}} - \frac{\nabla p}{\mathcal{A}} \quad (6.7)$$

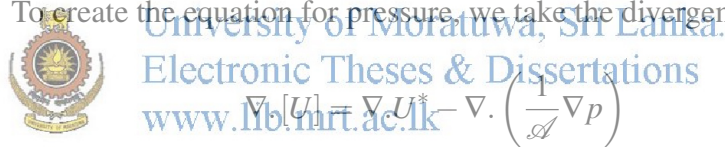
Equation 6.7 cannot be solved at this stage, since pressure is not added to the equation yet. If the problem of interest includes transport of a scalar property, such as enthalpy or the mass fraction of a chemical compound, we need a predictor for U, which is the predictor is calculated from the old pressure:

$$\text{solve}(UEqn == -fvc :: \text{grad}(p)) \quad (6.8)$$

This is called a momentum predictor of U. So far only the momentum equation has been used, but we also have the continuity equation, which is used to create an equation for pressure.

$$U^* = \frac{\mathcal{H}}{\mathcal{A}} \quad (6.9)$$

The velocity from Equation 6.8 does not satisfy continuity, and is lacking influence of pressure. To create the equation for pressure, we take the divergence of Equation 6.7:



$$\nabla \cdot [U] = \nabla \cdot U^* - \nabla \cdot \left(\frac{1}{\mathcal{A}} \nabla p \right) \quad (6.10)$$

The left hand side is zero for in-compressible flows, since it represents the correct velocity. 6.10 is then:

$$\nabla \cdot U^* = \nabla \cdot \left(\frac{1}{\mathcal{A}} \nabla p \right) \quad (6.11)$$

The left hand side will be treated explicitly, since we now need to find the pressure, and thus keep the velocity constant. In OpenFOAM, this is done by utilizing *fvc* instead of *fvm*. The velocity U^* is replaced by the velocity flux ϕ , since the face velocities will be used to evaluate the term. The resulting equation is then:

$$\text{surfaceScalarField } \phi = fvc :: \text{interpolate}(U) \ \& \ \text{mesh.Sf}() \quad (6.12)$$

$$volScalarField rUA = 1.0/UEqn.A() \quad (6.13)$$

$$fvScalarMatrix pEqn(fvm::laplacian(rUA, p) == fvc::div(phi)) \quad (6.14)$$

What cannot be seen in this formulation is that OpenFOAM again uses the Gauss theorem. Thus, it is not necessary to calculate a second derivative of p , but only a first derivative. This derivative is needed on the cell faces, and it is evaluated by using the cell centre values of the pressure. When the PISO/SIMPLE loop is finished, the velocity is corrected with the correct pressure gradient¹.

$$U- = rUA * fvc::grad(p) \quad (6.15)$$

The gradient in 6.15 is again evaluated using the Gauss theorem, and therefore no gradient calculation is necessary. Instead, only the pressure on the cell face is needed.

Rhie-Chow method used for the packed bed solver is bit different; although gas is in-compressible; $\nabla \cdot [U] \neq 0$ and momentum equation involve one more term; resistance due to particles for the gas flow. All the other things are same.

6.3 Steps of developing a new solver



University of Moratuwa, Sri Lanka.
Electronic Theses & Dissertations
www.lib.mrt.ac.lk

Assuming all requirements mentioned below have been fulfilled;

1. Examining on the fluid dynamics (including developing transport equations) of the physical system
2. Models for chemical and thermo-physical properties
3. Geometry of the system

A new solver can be developed in OpenFOAM following the steps below:

1. Selection of a most suitable available solver in OpenFOAM, which is practically most related to the modeling physical system.

¹The code used as example here is icoFoam, but the method is the same in most of the other codes available in OpenFOAM. This is somewhat changing in this research work and it is discussed in

2. Copy the solver to the User's project directory as a new solver.
3. Identify the major differences between two solvers.
4. Editing, addition or deletion of equations and addition of new files in the model or removing unnecessary files²

- Changing "Make" directory according to the libraries, header files used and files need to be compiled

- files my_fireFoam.C

```
EXE = $(FOAM_USER_APPBIN)/my_fireFoam
```

- options EXE_INC = \

```
-I$(LIB_SRC)/finiteVolume/lnInclude \
```

```
-I$(LIB_SRC)/finiteVolume/finiteVolume/laplacianSchemes \
```

```
-I$(LIB_SRC)/fvOptions/lnInclude \
```

```
-I${LIB_SRC}/meshTools/lnInclude \
```

```
-I$(LIB_SRC)/ODE/lnInclude
```

```
EXE_LIBS = \
```

```
-lfiniteVolume \
```

```
-lfvOptions \
```

```
-lmeshTools \
```



University of Moratuwa, Sri Lanka.

Electronics Theses & Dissertations

www.mrt.ac.lk

- change *createFields.H* according to;

- necessary input/output fields

- to introduce new dimensioned constants

- to introduce pressure referencing details(reference cell,value,etc)

- to initialize a variable from an existing class

- UEqn.H

- momentum equation is introduced

- all other chemical and thermo-physical properties have introduced in this file(which depend on packed bed environment and therefore has to be updated with latest values from iterations.i.e.those properties have to be introduced inside the loop)

² all the directories of the solver are attached in Appendix I-directories of the solver.

- pEqn.H
 - pressure correction equation
 - addition of modified Rhie-Chow method for the case refer.
- rhosEqn.H (for solid phase)
 - solid phase continuity equation(gas phase considered in-compressible)
- YshsEqn.H & YghgEqn.H
 - YshsEqn.H-enthalpy equation for solid phase and species equations for moisture,char,volatiles(each volatile specie having a separate equation) and ash.
 - YghgEqn.H-enthalpy equation for gas phase and species equations for $H_2O, N_2, O_2, CH_4, CO_2, CO, C_xH_yO_z$ and H_2 .
- my_fireFoam.C
 - this is the main file which is going to be compiled.
 - all other “.H” files required in the application will call in the main file.
 - this file contains the SIMPLE loop which gives the overall solution of



the system as discussed in Section 4.3.
 University of Moratuwa, Sri Lanka.
 Electronic Theses & Dissertations
 www.lib.mru.ac.lk

5. Compile the solver by running **wmake** inside the my_fireFoam directory and **debug**. There are debugging methods which can be chosen by trial and error method to correct all compile errors.

- (a) running *wmake* will show any compilation errors from built-in feedback from OpenFOAM.
- (b) OpenFOAM also has the facility to provide more debug output on-demand. Global location to turn-on debug switches is “etc/controlDict”, located in the main OpenFOAM folder. A code snippet of “controlDict” debug switches are shown below.

```
DebugSwitches
{
  Analytical          0;
  APIdiffCoefFunc    0;
```

```

Ar                0;
BICCG             0;
BirdCarreau      0;
-
polyMesh          0;
-
}

```

- Those switches can be turn-on using one of following methods
 - within the global controlDict file
 - copy global file to user’s own directory and can be located by running “echo/controlDict”
 - instead of copying whole controlDict file only a part can be copied to personal file,like below

```

DebugSwitches
{
polyMesh          1;
}

```



University of Moratuwa, Sri Lanka.

Electronic Theses & Dissertations

www.lib.mrt.ac.lk

– turn-on inside the case file’s “system/controlDict” file <http://www.openfoam.org/version2.2.0/runtime-control.php>

- (c) looking at the debug messages and referring those errors back in the files will help to find out the place of error.
- (d) in this project lot of community help is attained through <http://cfd-online.com/> directly or indirectly to overcome with number of compile errors.
- (e) running OpenFOAM in “Debug” mode is advised by OpenFOAM experts as it provides more detail to the user about the error(to install “Debug” mode “Source Pack” or “Git Repository” versions of OpenFOAM should be installed-for more detail)
- (f) there are other methods which can be used for debugging,but not used in this project such as by enabling thorough level of debugging, top level debugging, using commercial debuggers, etc.

6. When the code is bug free;it is ready to run for a practical application.

7. Make a new case file to run a case using the solver

- make the geometry according to the real case in case/constant/polyMesh sub directory
- identify the initial parameters to be added and their units
- put the boundary conditions accurately
- add the thermo-physical, chemistry, turbulence, etc properties in constant/properties sub directory.
- “fvSchemes” dictionary according to the dominance of transport methods(convective,diffusive) and controls(default vanLeer01;)
- “fvSolution” dictionary on the accuracy required(high tolerances for sensitive parameters), linear solvers, correctors for non-orthogonality, controls for algorithm, etc.

8. Run **blockMesh** and **checkMesh**

9. Running **my_fireFoam** and **debugging**. Even though there is no compilation errors; still a number of errors may appear in the case. These files can be identified using following methods;

- Applying correct boundary conditions and initial conditions is very important when running a case file. Therefore, it is a precautionary thing to do prior to running the case.
- Running in debug version will provide more detail on the error.
- Applying filters(to make mass fractions between 0-1, temperature higher than ex:298K) to point out the error
- Errors can be located conveniently,(ex: Floating point exception) by looking at “Info<< >>” codes added or error can be approximated by adding more “Info<< >>” codes around that place, if it will not work.
 - “Floating point Exception” errors can be identified observing “time” directory of case files at the time of error and immediately before the error. ex: if error occurs at time=8s, look at the values in time=7s and 8s, if this would not work;

- * use **run** function for suspecting **geometricFields** in each time step and look at them by running case file again and again.
- residual mapping to check the convergence
 - can use **foamLog <logFile>** script to extract residuals, iteration, courant no., etc in the “log” file within the case file. It can be used to plot residual of each I/O parameter.
 - There are other community developed code snippets to plot residuals (ex: gnuplot used in this project)
- runtime changes and running again to attain the convergence for better results

10. run **paraFoam**

- **sampling** resulted parameters which are necessary for free-board region modeling as inlet conditions.



University of Moratuwa, Sri Lanka.
Electronic Theses & Dissertations
www.lib.mrt.ac.lk

CHAPTER VII

CFD MODELING OF HOT AIR GENERATOR SYSTEM

The CFD model generated for wood chip combustion in packed bed is a steady state model. However, it is hard to find any property remain constant throughout the computational domain owing to combustion reactions and their effects; except the incompressible condition which is assumed for gas phase. It is apparent that combustion of biomass involves large number of thermo-physical and chemical properties. One of the main objective of this chapter is to listing of those properties, empirical models and values used for this CFD modeling and simulation work. Further details on modeling important properties can be found in 3.4.1.

This chapter also includes empirical models used for modeling each property in packed bed. A steady state model does not require accurate initial conditions; but both initial and boundary conditions used for the model, are stated.



University of Moratuwa, Sri Lanka.
Electronic Theses & Dissertations
www.lib.mrt.ac.lk

7.1 Hot air generator simulation

A picture of the conventional hot air generator used for Tea factories in Sri Lanka is shown in the Figure 7.1. The Figure 7.2 is an image after retrofitting the same by the National Engineering Research and Development Centre (NERDC) for wood chips combustion with continuous feeding. That hot air generator have been used for the simulation work (refer Sections 7.4 and 7.5) and there were few assumptions made considering the difficulties of measurements in parameters like pressure, machine performances and specifications of ID fan which may consequently affect for the validation part due to non-fitting of real conditions with simulation data. Those assumptions were;

- Secondary air supplied is negligible.
- Pressure at gas inlet to packed bed due to ID fan is 76000Pa.



University of Moratuwa, Sri Lanka.
 Electronic Theses & Dissertations
www.lib.mrt.ac.lk

Figure 7.1: Conventional hot air generator system in Tea factories

- Pressure at packed bed outlet is varying from 76000-75000Pa(Refer Section7.3).
- Pressure at free board outlet is 75000Pa(Refer Section 7.3).
- Velocity at gas inlet is 0.25ms^{-1} to the upward direction.

According to the modeling approach, which is discussed in chapter 1; radiation temperature incident on the packed bed has to be provided to the model for simulation which is not known initially. Therefore, a reasonable value has to guess to run the packed bed model as first iteration. Then a sequence of steps followed to find out the radiation temperature and 'interface' conditions from the packed bed. Finally obtained the outlet conditions of the combustion chamber. Overall simulation approach can be described as follows;

1. Assume radiation temperature incident on packed bed(in this model -1125K).



Figure 7.2: Hot air generator after retrofitting

2. Run the packed bed solver on packed bed geometry(*my_fireFoam*).
3. Use the results from packed bed run as input conditions to the free board region($t_{p,1}, Y_{p,1}, U_{p,1}$).
4. Run the free board case till approaching steady state(*rhoReactingFoam*-a transient solver).
5. Use the resulting temperature of nearest wall as new radiation temperature to the packed bed(t_{f1}).
6. Follow steps 2-5 until temperature from packed bed to the free board($t_{p,n}$) and temperature in the closest wall to the interface in free board($t_{f,n}$) each converging with iterations.



University of Moratuwa, Sri Lanka.
Electronic Theses & Dissertations.
www.lib.mrt.ac.lk

After the results of both models are converging; those were used to predict the inlet conditions to the heat exchangers. The total case structure is presented in Figure 7.3. Practically there are two cases in this simulation which are for packed bed model and free board model. Basic boundary conditions and the solvers of OpenFOAM used are depicted in Table 7.1.

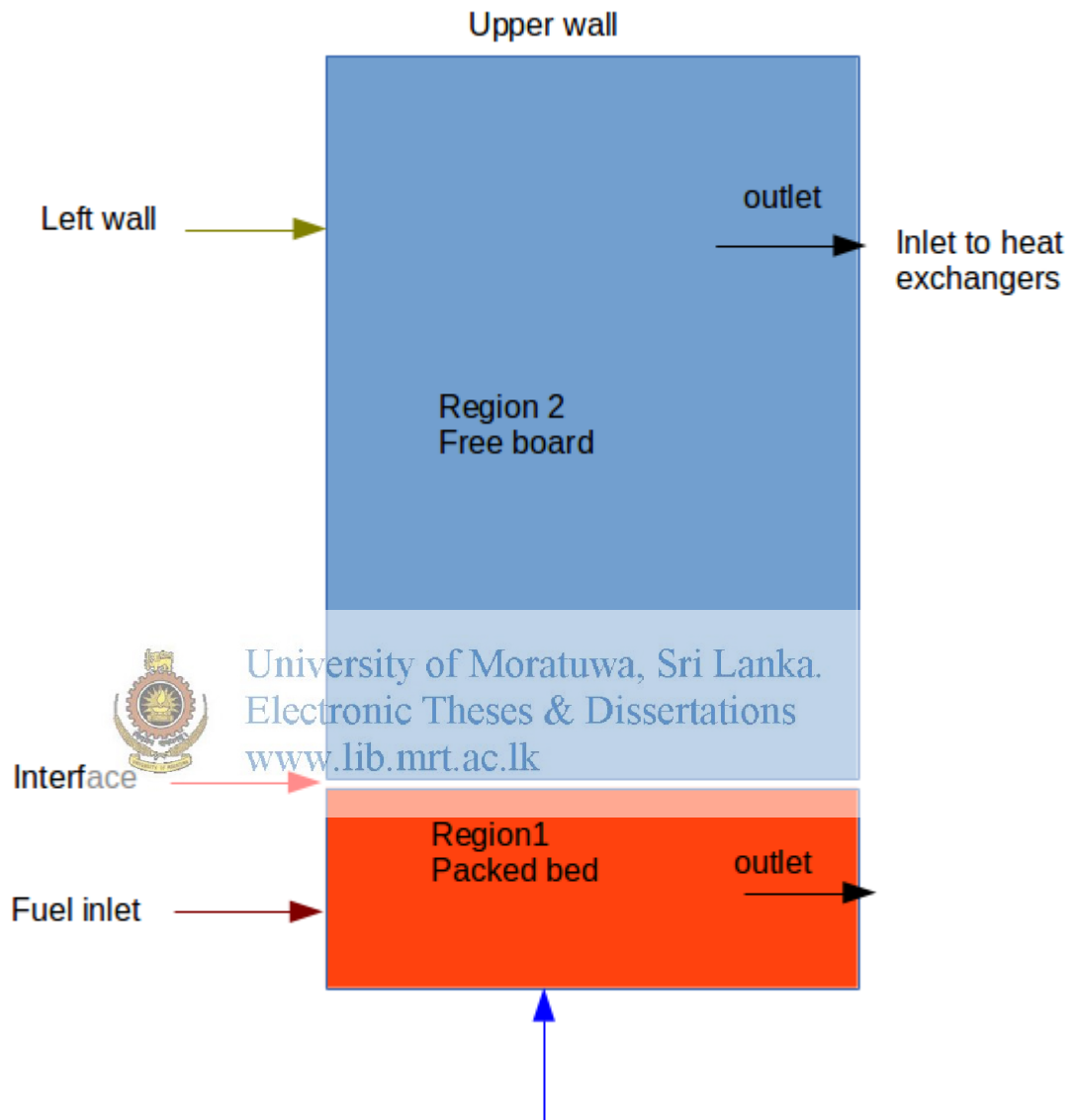


Figure 7.3: Schematic diagram of simulation case structure

| | packed bed | | free board | |
|---------------------|-------------|--------------------|-----------------|--------------------|
| solver | my_fireFoam | | rhoReactingFoam | |
| boundary conditions | boundary | boundary condition | boundary | boundary condition |
| | gasInlet | patch | inlet | patch |
| | fuelInlet | patch | leftWall | wall |
| | interFace | patch | upperWall | wall |
| | outlet | patch | outlet | patch |
| | | | | |

Table 7.1: solvers and basic boundary conditions of each case

7.1.1 Packed bed modeling and simulation

Chapter 2 of this dissertation have discussed about the models for thermo-physical, chemical and turbulence properties for biomass combustion in packed beds. Purpose of this section is to list all the models together and values for all the relevant properties of packed bed modeling and simulation. Further information of the model are described in the Section 3.1. www.lib.mrt.ac.lk

7.1.1.1 Thermo-physical properties modeling

The models used for thermo-physical properties are listed in the Table 7.2. Heat capacity with the temperature of each phase, porosity change of the bed with combustion reactions, initial density of biomass and gas phase(constant), kinematic viscosity variation with temperature, effective thermal conductivity of the packed bed, mass diffusion and other properties required for heat and mass transfer calculations and particle properties have shown in the Table 7.2.

7.1.1.2 Chemical kinetics modeling

Chemical kinetics data have been extracted from the literature out of different models available for combustion reactions. Except for the char combustion reaction; all other

| Property | Model | |
|--|---|---------------------------|
| Heat capacity | | |
| Gas phase [9] | $c_{p,g}(T_g) = 990 + 0.122T_g - 5680 \cdot 10^3 T_g [J/kgK]$ | |
| Solid phase[13] | $c_{p,wet} = \frac{c_{p,dry} + 4.19M}{1+M} + A[kJ/kgK] A = (0.02355T - 1.32M - 6.191)M$ $c_{p,dry} = 0.1031 + 0.003867T$ | |
| Porosity | $\epsilon_0 = \frac{V_g}{V}$ where $\epsilon = \epsilon_0 + (1 - \epsilon_0) \sum_i f_i (Y_{i,0} - Y_i)$, $\epsilon_0 = 0.5$ <i>i - char, volatile</i> | |
| Density [kg/m^3] | | |
| Gas phase | 1.3 | |
| Solid phase(initial) | 700 | |
| Kinematic viscosity(ν) | $\nu = 1.523e^{-05} \frac{t_g}{300}^{0.667} [kg/ms]$ | |
| Effective thermal conductivity of the bed[10] [9][55] | $\lambda_e = \lambda_{e,0} + aPrRe\lambda_g$, $[W/mK]$ $a = 0.1$ along bed length 0.5 along bed height | |
| Pressure gradient [9] | $f_x = \frac{\Delta p}{L} = 150 \frac{\mu v_{g,x}(1-\epsilon_b)^2}{d_p^3 \epsilon_b^3} + 1.75 \frac{\rho_g v_{g,x} v_{g,x} (1-\epsilon_b)}{d_p \epsilon_b^3} \left[\frac{N}{m^3} \right]$ $f_y = \frac{\Delta p}{L} = 150 \frac{\mu v_{g,y}(1-\epsilon_b)^2}{d_p^3 \epsilon_b^3} + 1.75 \frac{\rho_g v_{g,y} v_{g,y} (1-\epsilon_b)}{d_p \epsilon_b^3} \left[\frac{N}{m^3} \right]$ | |
| Emissivity | 0.9 | |
| Diffusion coefficient(m^2/s) | | |
| Gas phase[41][9][10][55] | $D_{i,e} = D_{i,0} + ad_p v_g $ for Temperature <1000K and $P_{max} = 70atm$ (Wilke-Lee Equation) $D_{AB} = \frac{(0.0027 - 0.0005M_{AB})T^{3/2}M_{AB}^{1/2}}{P\sigma_{AB}^2\Omega_D}$ $\sigma_{AB} = \frac{\sigma_A + \sigma_B}{2} (0A)$ $\Omega_D = (44.54T^{0-4.909} + 1.911T^{0-1.575})^{0.1}$, $T^0 = \frac{kT}{\epsilon_{AB}}$ $\epsilon_{AB} = (\epsilon_A \epsilon_B)^{1/2}$, $M_{AB} = [(1/M_A) + (1/M_B)]^{-1}$ | |
| Solid phase[35] | 1.4833×10^{-6} | |
| Fuel particle properties | | |
| Diameter of particle | assuming $\frac{Surface\ area}{Volume} = 240$ constant $d_p = \frac{6(1-\epsilon_b)}{240} = 0.025(1 - \epsilon_b) [m]$ | |
| Shrinkage factors(intra particle porosity change is not considered here) | reaction | shrinkage factor(f_i) |
| | drying | 0 |
| | devolatilization | 1 |
| | char combustion | 1 |

Table 7.2: Empirical models used for thermo-physical properties and their values

| Reaction | Rate of reaction(kg/m^3s) |
|-----------------------------------|---|
| drying | $r_{dry} = 2.822 \cdot 10^{-4} \exp\left(\frac{-10584}{T_s}\right) (1 - \epsilon_b) \rho_s Y_{H_2O,s} T_s - 475 ^7$ |
| devolatilization | $r_{pyr,i} = 7 \cdot 10^4 \exp\left(\frac{-9977}{T_s}\right) (1 - \epsilon_b) \rho_s Y_{i,s}$ |
| char combustion | $r_{char} = A_p \left(\frac{C_{O_2}}{\frac{1}{k_r} + \frac{1}{k_d}} \right) k_r = 2.3 t_s \exp\left(\frac{-11100}{T_s}\right) \frac{CO}{CO_2} = 2500 \exp\left(\frac{-6420}{T_s}\right)$ |
| volatile combustion(mol/m^3s) | |
| carbon monoxide combustion | $R_{CO} = 1.3 \cdot 10^{11} \exp\left(\frac{-62700}{T_g}\right) C_{CO} C_{H_2O}^{0.5} C_{O_2}^{0.5}$ |
| hydrogen combustion | $R_{H_2} = 3.9 \cdot 10^{17} \exp\left(\frac{-20500}{T_g}\right) C_{H_2}^{0.85} C_{O_2}^{1.42}$ |
| methane combustion | $R_{CH_4} = 1.6 \cdot 10^{10} \exp\left(\frac{-24157}{T_g}\right) C_{CH_4}^{0.7} C_{O_2}^{0.8}$ |
| $C_xH_yO_z$ reaction | $R_{C_xH_yO_z} = 2.7 \cdot 10^8 t_g^{0.5} \exp\left(\frac{-20131}{T_g}\right)$ |

Table 7.3: Chemical kinetic models for reactions of combustion

models chosen were first-order kinetic rate models.



University of Moratuwa, Sri Lanka.
Electronic Theses & Dissertations
www.lib.mru.ac.lk

7.1.1.3 Biomass properties for simulation

Biomass properties are varying in a huge range depending on the environmental conditions. Properties depicted in table 7.4 and 7.5 are only necessary as boundary conditions, initial conditions or as input parameters for the simulation. Therefore, depending on the type of biomass used; these conditions can be picked up by the users.

7.1.1.4 Boundary conditions

Figure 7.4 is an end elevation of the packed bed in figure 7.3. Fuel wood chip enters from the left hand side of the combustion chamber and gases enter through the grate. Due to the negative pressure created by the ID fan; gas will flow in the direction of the fan suction. That is rather than gas flowing upward direction it will flow in the BC direction. Boundaries and boundary conditions used for the simulation are shown in table 7.6.


| Property | Value | | | | | | | | | | | | | | | | | | | | | | | | |
|---|---|-------------------|------------|------------|-------|------|---|------|-------|-----------|--------|-------|---|-------|-------|-----------|-------------------|-------|-----------|----------------------|-----|---------|------|-----|-----------|
| Thermal properties of biomass(MJ/kg) | | | | | | | | | | | | | | | | | | | | | | | | | |
| Higher and Lower heating value of biomass | 21.54217, 11.2554108 | | | | | | | | | | | | | | | | | | | | | | | | |
| Overall devolatilization heat | 0 | | | | | | | | | | | | | | | | | | | | | | | | |
| Volatile combustion heat | 8.8002 ¹ | | | | | | | | | | | | | | | | | | | | | | | | |
| Combustion heat of $C_xH_yO_z$ | 47.88 | | | | | | | | | | | | | | | | | | | | | | | | |
| Enthalpy of formation(kJ/mol) | | | | | | | | | | | | | | | | | | | | | | | | | |
| H_2O (liquid/gas) | -285.83/ - 241.81 | | | | | | | | | | | | | | | | | | | | | | | | |
| CO | -110.53 | | | | | | | | | | | | | | | | | | | | | | | | |
| CO_2 | -393.5 | | | | | | | | | | | | | | | | | | | | | | | | |
| $H_2, N_2, O_2, \text{char}$ | 0 | | | | | | | | | | | | | | | | | | | | | | | | |
| CH_4 | -74.85 | | | | | | | | | | | | | | | | | | | | | | | | |
|  <p style="text-align: center;">University of Moratuwa, Sri Lanka. Electronic Theses & Dissertations www.lib.mrt.ac.lk</p> <p style="text-align: center;">Pyrolysis products[13]</p> | <table border="1"> <thead> <tr> <th>Pyrolysis product</th> <th>Fraction</th> <th>LHV(MJ/kg)</th> </tr> </thead> <tbody> <tr> <td>H_2</td> <td>0.25</td> <td>0</td> </tr> <tr> <td>CO</td> <td>0.183</td> <td>10.102427</td> </tr> <tr> <td>CO_2</td> <td>0.115</td> <td>0</td> </tr> <tr> <td>H_2</td> <td>0.005</td> <td>11.995258</td> </tr> <tr> <td>light hydrocarbon</td> <td>0.047</td> <td>50.009163</td> </tr> <tr> <td>Tar($C_6H_{6.2}O$)</td> <td>0.2</td> <td>35.2406</td> </tr> <tr> <td>Char</td> <td>0.2</td> <td>32.762454</td> </tr> </tbody> </table> | Pyrolysis product | Fraction | LHV(MJ/kg) | H_2 | 0.25 | 0 | CO | 0.183 | 10.102427 | CO_2 | 0.115 | 0 | H_2 | 0.005 | 11.995258 | light hydrocarbon | 0.047 | 50.009163 | Tar($C_6H_{6.2}O$) | 0.2 | 35.2406 | Char | 0.2 | 32.762454 |
| | Pyrolysis product | Fraction | LHV(MJ/kg) | | | | | | | | | | | | | | | | | | | | | | |
| | H_2 | 0.25 | 0 | | | | | | | | | | | | | | | | | | | | | | |
| | CO | 0.183 | 10.102427 | | | | | | | | | | | | | | | | | | | | | | |
| | CO_2 | 0.115 | 0 | | | | | | | | | | | | | | | | | | | | | | |
| | H_2 | 0.005 | 11.995258 | | | | | | | | | | | | | | | | | | | | | | |
| | light hydrocarbon | 0.047 | 50.009163 | | | | | | | | | | | | | | | | | | | | | | |
| | Tar($C_6H_{6.2}O$) | 0.2 | 35.2406 | | | | | | | | | | | | | | | | | | | | | | |
| Char | 0.2 | 32.762454 | | | | | | | | | | | | | | | | | | | | | | | |
| <p style="text-align: center;">Volatile reactions[56]</p> $H_2 + O_2 \rightarrow 2H_2O$ $CH_4 + \frac{3}{2}O_2 \rightarrow CO + 2H_2O$ $2CO + O_2 \rightarrow 2CO_2$ $C_6H_{6.202}O + 4.0505O_2 \rightarrow 6CO + 3.101H_2O$ | | | | | | | | | | | | | | | | | | | | | | | | | |

Table 7.4: Properties of biomass for simulation

| Analysis | Value | |
|--|---------------------|----------------------|
| Proximate analysis [13] | Component | Weight percentage(%) |
| | moisture | 20 |
| | volatile components | 67.848 |
| | fixed carbon | 9.992 |
| Ultimate analysis(assuming the wood used for combustion as soft wood)[13, 9] | ash | 0.216 |
| | Element | Weight percentage(%) |
| | C | 52.7 |
| | H | 6.3 |
| | O | 40.8 |
| | N | 0.2 |
| S | 0 | |

Table 7.5: Ultimate and Proximate analysis of biomass



University of Moratuwa, Sri Lanka.
Electronic Theses & Dissertations
www.lib.mrt.ac.lk

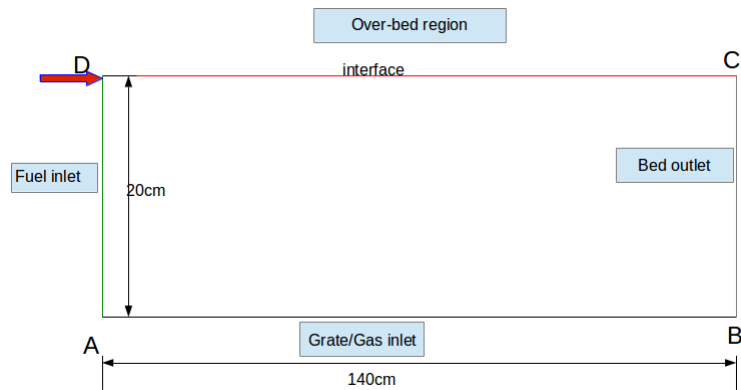


Figure 7.4: Packed bed with dimensions and boundaries


| Property | gasInlet | fuelInlet | outlet | interface |
|-----------------------------|---|----------------------------------|---|---------------------------------------|
| Pressure(p) | fixedValue 76000 | zeroGradient | fixedValue nonUniform (76000-75010) | zeroGradient |
| Velocity(U) | fixedValue uniform (0 0.25 0) | fixedValue uniform (0 0 0) | inletOutlet inletValue- (0 0 0) | inletOutlet inletValue- (0 0 0) |
| Gas temperature(tg) | fixedValue uniform 298.15 | zeroGradient | zeroGradient | zeroGradient |
| Solid temperature(ts) | zeroGradient | fixedValue uniform 298.15 | zeroGradient | groovyBC ² |
| Gas compositions(Y_i) |  $O_2 - 0.2314 N_2 - 0.768065$ $C_6H_6.202 O - 0$ other gases > 0 (trace amounts) | zeroGradient | zeroGradient | zeroGradient |
| solid compositions(Y_i) | zeroGradient | Refer Table 7.5 | zeroGradient | zeroGradient |
| Porosity(epsilon) | zeroGradient | zeroGradient | zeroGradient | zeroGradient |
| Solid density(rhos) | zeroGradient | fixedValue uniform 700 | zeroGradient | zeroGradient |

Table 7.6: packed bed boundary conditions

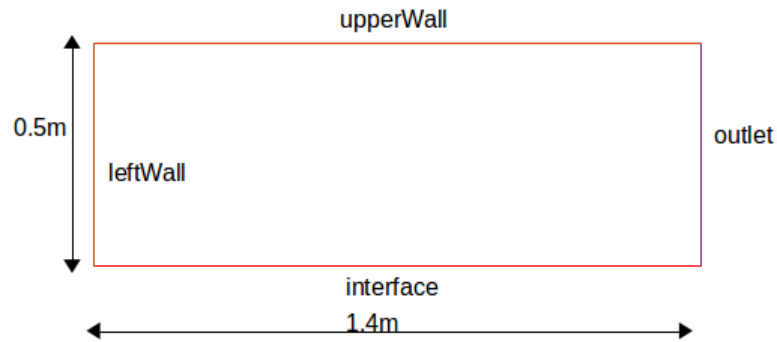


Figure 7.5: Free board with dimensions and boundaries

7.2 Free board simulation

Free board of the combustion chamber involves turbulence with chemical reactions as well. Therefore, modeling free board is complex. Turbulence-chemistry interaction has been achieved via *PaSR* (Partially Stirred Reactor) model in OpenFOAM, which is more suitable than other models such as Eddy Break Up, Eddy Dissipation concept, laminar flamelet model. *PaSR* model is more flexible, which is primarily developed for diesel spray combustion.

7.2.1 Turbulence simulation

Turbulence is simulated using Launder-Sharma Low Reynolds number $k - \epsilon$ model (*lauderSharmaKE* in OpenFOAM). Turbulence properties like k , ϵ , μ_t , α_t and other property boundary conditions and initial conditions are summarized in the Section 7.7.

7.2.2 Radiation

Radiation heat transfer is modeled by finite volume discrete ordinates method. This model solves Radiation Transfer Equation (RTE) for n , number of directions in participating media and scattering is neglected. For a two-dimensional case polar angle will be considered as zero. In this model number of azimuthal angles in $\frac{\pi}{2}$, is considered as 4. For absorption and emission modeling *greyMeanAbsorptionEmission* model in OpenFOAM have been used out of *greyMeanAbsorptionEmission* model, *constantAbsorptionEmission* model and *wideBandAbsorptionEmission* model. This model is called

| Property | inlet | outlet | leftWall | upperWall | Initial conditions |
|----------------------|---|--------------|-----------------|-----------------|-------------------------------------|
| k | $k = \frac{2}{3}(U_{ref}T_i)^2$ $T_i = 30\%$ | zeroGradient | $0(10^{-25})^3$ | $0(10^{-25})^4$ | 0 |
| ϵ | $\epsilon = \frac{k^{\frac{3}{2}}C_{\mu}^{0.75}}{\ell}$ where ℓ -assumed as 10% of bed length | zeroGradient | $0(10^{-25})$ | $0(10^{-25})$ | 0 |
| U | 'interface' boundary values from packed bed- nonuniform fixedValue | zeroGradient | 0 | 0 | 0 |
| T | 'interface' boundary values from packed bed- nonuniform fixedValue | zeroGradient | zeroGradient | zeroGradient | 1200 |
| p | 'interface' boundary values from packed bed- nonuniform fixedValue | 75000 | zeroGradient | zeroGradient | zeroGradient |
| Gas compositions | 'interface' boundary values from packed bed- nonuniform fixedValue | zeroGradient | zeroGradient | zeroGradient | $N_2 - 0.768065$ $O_2 - 0.23195$ |
| mut(μ_t) | automatically corrected by the model | | | | |
| alphan(α_t) | automatically corrected by the model | | | | |

Table 7.7: Free board boundary conditions

weighted- sum-of-grey-gases (WSGG) model in general context.

Three major Green House Gases(GHGs) are involved in this combustion model; CO_2 , CH_4 and H_2O which absorption and emissions of radiation have to be considered.WSGG model parameters have used for those gases from the *fireFoam* case files in OpenFOAM tutorials.

7.2.3 Transport properties

Dynamic viscosity of gas is modeled using the sutherland transport which calculates from the formula shown in Equation 7.1.

$$\mu = \mu_0 \left(\frac{a}{b}\right) \left(\frac{T}{T_0}\right)^{\frac{3}{2}} \quad (7.1)$$

where; $a = 0.0555T_0 + c$, $b = 0.555T + c$, T-input temperature in degrees Rankine, μ – viscosity in centipoise at input temperature T.

Rearranging the formula as values have to be provided in OpenFOAM;

$$\mu = \frac{A_s \sqrt{T}}{1 + T_s/T} \quad (7.2)$$

using 7.1, $A_s = \mu_0 \left(\frac{0.555T_0}{0.555T_0}\right)$ and $T_s = 0.555T_0$.

7.2.4 Thermo-physical properties

Heat capacity at constant pressure is calculated using the Equation 7.3.The equation is valid across temperature range; between lower temperature(T_l) and upper temperature(T_h). Two sets of parameters specified(two sets of a_0, a_1, a_2, a_3, a_4) for lower temperature range ($T_c - T_l$) and higher temperature range ($T_h - T_c$).

$$c_p = R((((a_4T + a_3)T + a_2)T + a_1)T + a_0) \quad (7.3)$$

The parameters of the equations are obtained from janaf thermo chemical tables.This method of heat capacity calculation is used in *janafThermo* class in OpenFOAM.

Turbulent diffusivity will be calculated from Section 2.23 and all the boundary conditions will be recalculated.Therefore,wrong boundary conditions would not be a matter for the accuracy of simulation.

7.2.5 Combustion properties

PaSR model is used for turbulence-combustion interaction in free board model. In the PaSR model; to determine the 'k' value (equation 2.42) chemical time scale and mixing time scale is necessary. Chemical time scale depends on the reaction rates but mixing time scale has to be decided prior to the simulation. Different approaches have been used for mixing time calculations; for instance in OpenFOAM it is calculated according to Equation 7.4;

$$\tau_{mix} = C_{mix} \sqrt{\frac{\mu_{eff}}{\rho \epsilon}} \quad (7.4)$$

It has found that results are independent of C_{mix} value as much as it is less than 1 [57]. Typical values for C_{mix} is 0.001-0.3 [33]. Then in this work C_{mix} is assumed as 0.14.

7.2.6 Chemistry properties

In a system having number of species and number of reactions; the specie concentrations have to be calculated by using reaction rates which are changed due to reactions as well as reaction changes due to changes in overall system as well. When calculating the changes due to chemistry it creates linear differential equations and then OpenFOAM have different ordinary differential equation solvers to select. This model have used "ode" solvers and out of KRR4, SIBS and RK; KRR4 is chosen. Latest version of OpenFOAM(2.3.0) is having large number of ODE solvers than which is used in this work(2.2.2).

CHAPTER VIII

RESULTS AND DISCUSSION

8.1 Simulation results of packed bed-free board

Free board inlet conditions and packed bed outlet conditions should be same. In steady state conditions free board boundary conditions are not known. Therefore, initially the temperature incident on packed bed from free board region is guessed. Using that value sequentially packed bed simulation and free board simulation have carried out. Simulation stopped when packed bed outlet temperature and radiation temperature from free board region are converging. Initial radiation temperature have assumed as 1125K. Using the final iteration results from both models; parameters at the inlet to the heat exchangers have been predicted (refer Figure 7.3).

Figure 8.1 and Figure 8.2 depicts the results of iterations.

Final iteration (3rd iteration) results are the packed bed outlet conditions, which enter the free board region from biomass combustion. Velocity and gas compositions at packed bed outlet are presented in Figure 8.5 and 8.6 respectively.

Further to the graphical representation of inlet parameters to the free board; packed bed model simulation results of each property at steady state can be extracted from paraFoam which is the post-processing tool provided with OpenFOAM.

8.1.1 Mesh Refinement

Mesh refinement have been tested with four mesh refinements for 2D geometry ; 100×100 , 200×200 , 300×300 and 400×400 number of meshes. The temperature of gas phase at packed bed outlet plotted against distance along the grate. Results are shown in Figure 8.3.

Results converging at 300×300 mesh refinement. Therefore, simulation has carried out using 300×300 mesh for the packed bed. Residual plot for 300×300 mesh in first iteration for the packed bed is shown in Figure 8.2. It shows the convergence of the

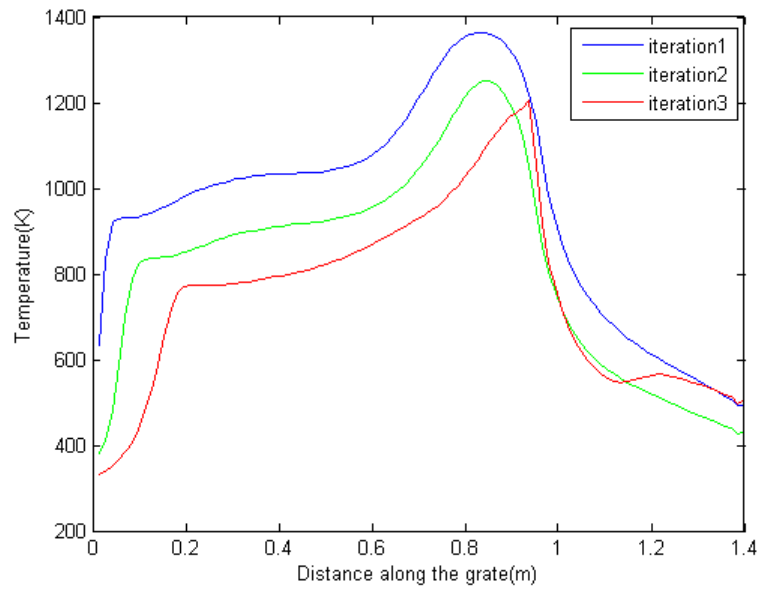


Figure 8.1: Packed bed gas outlet(interface) temperature with iterations

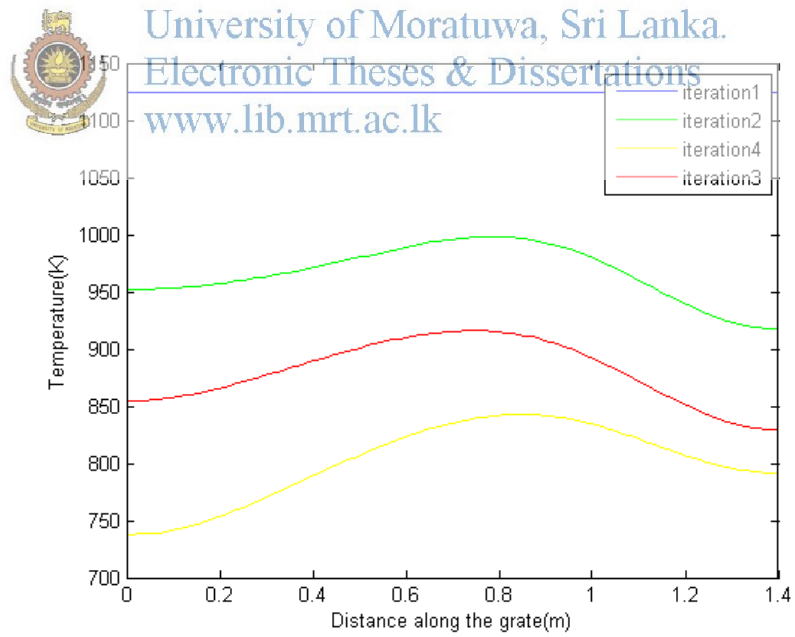


Figure 8.2: Radiation temperature incident on packed bed

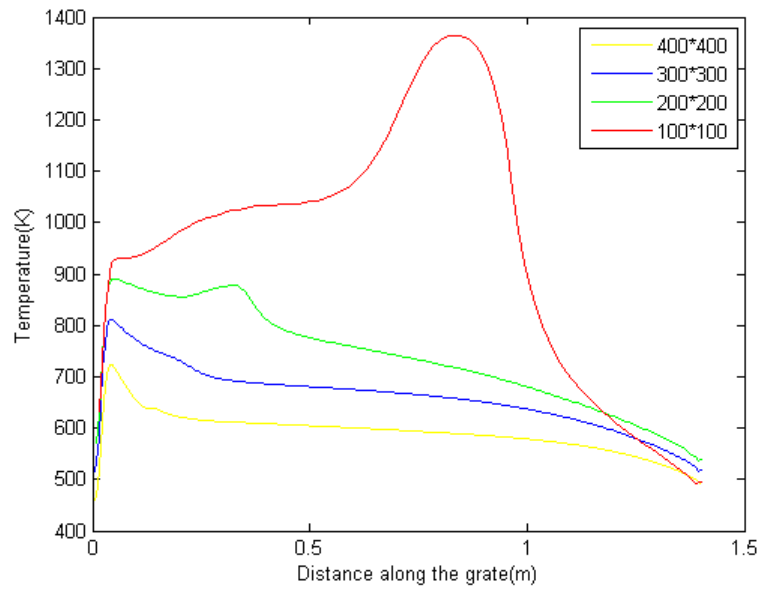


Figure 8.3: Mesh refinement results(Temperature at packed bed outlet)

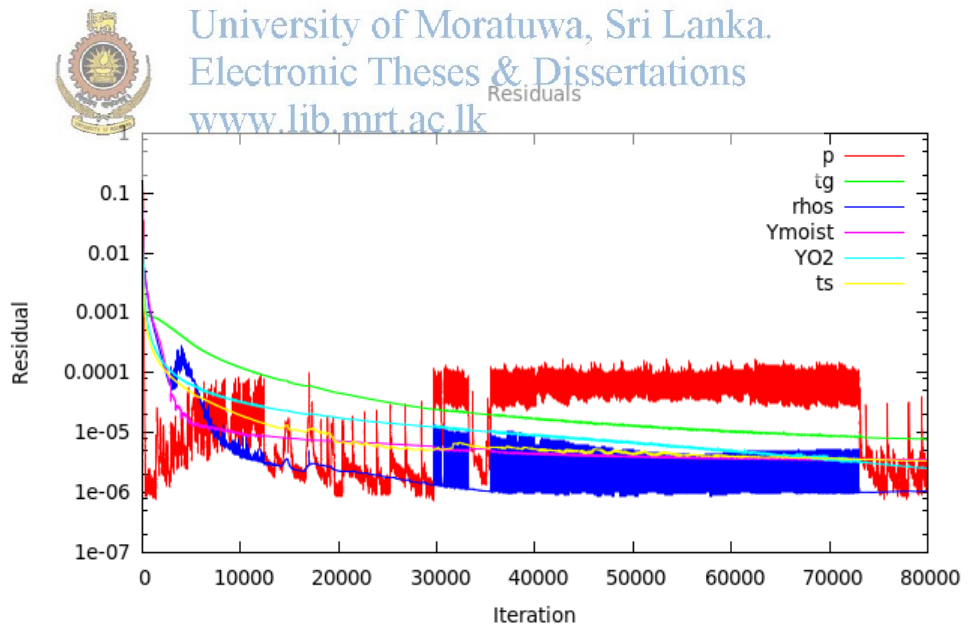


Figure 8.4: Residual mapping of packed bed simulation with 300*300 mesh

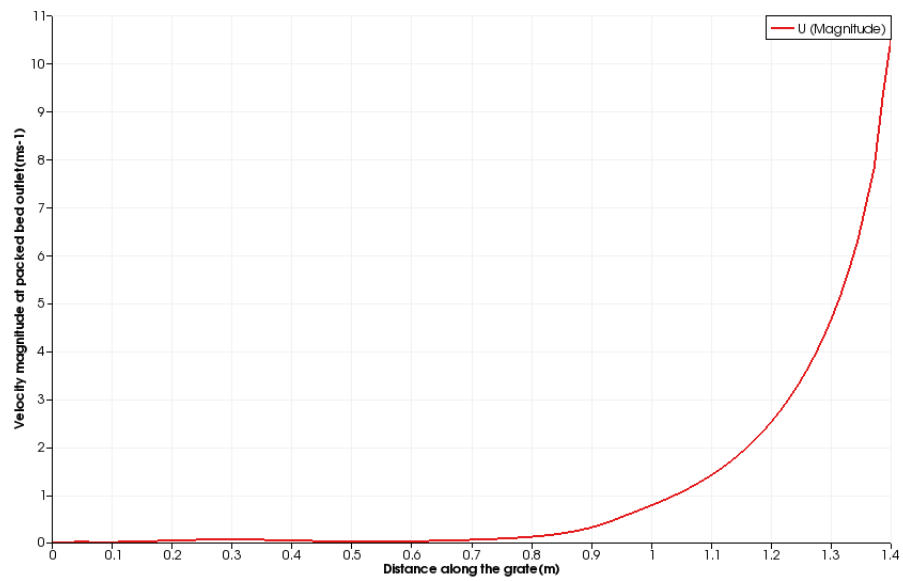


Figure 8.5: Velocity at packed bed outlet along the grate

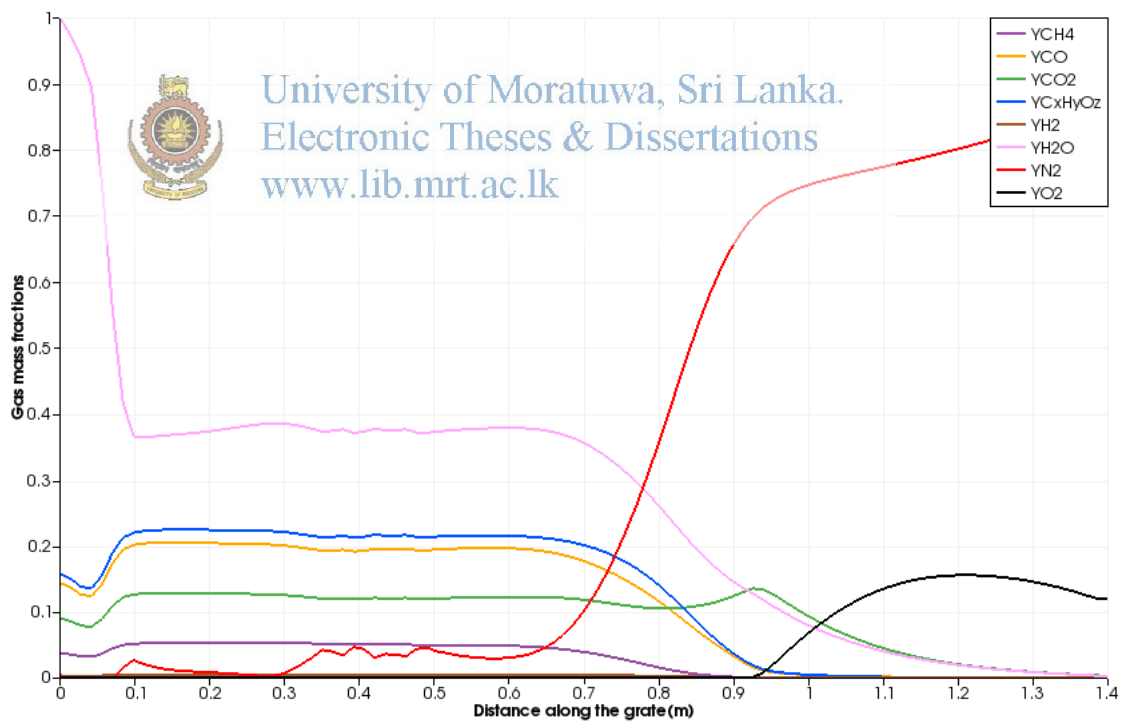
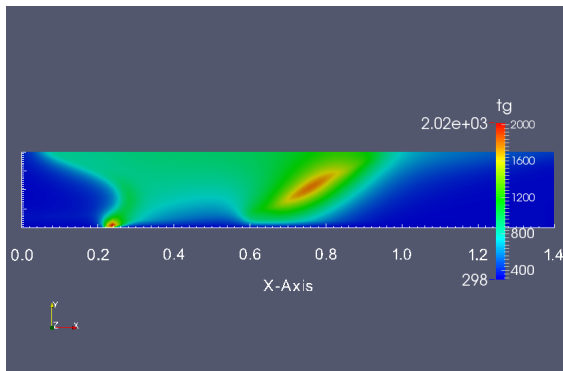
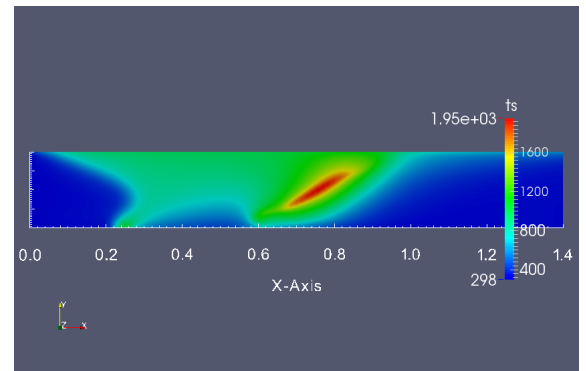


Figure 8.6: Mass fractions of CO , CO_2 , H_2O and O_2 at packed bed outlet



(a) Temperature of gas phase (K)



(b) Temperature of solid phase (K)

Figure 8.7: Gas phase and solid phase temperature of packed bed at steady state



University of Moratuwa, Sri Lanka.
Electronic Theses & Dissertations
www.lib.mrt.ac.lk

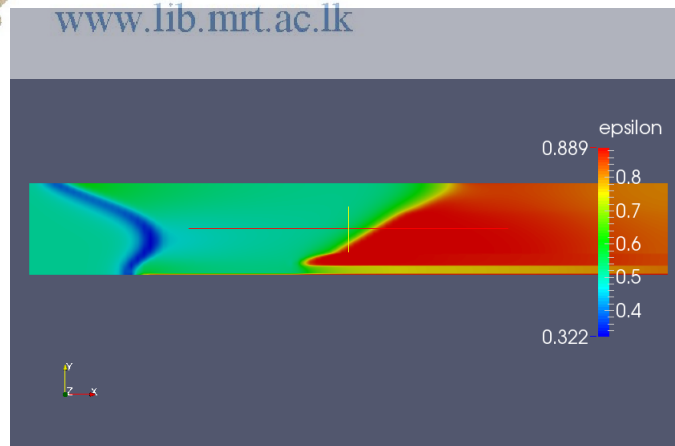
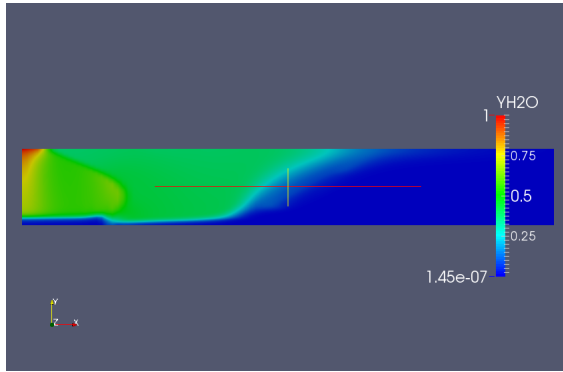
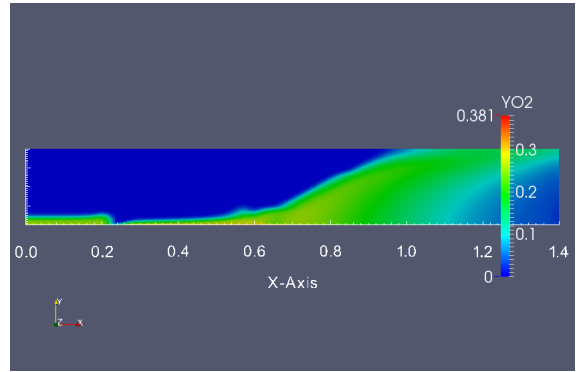


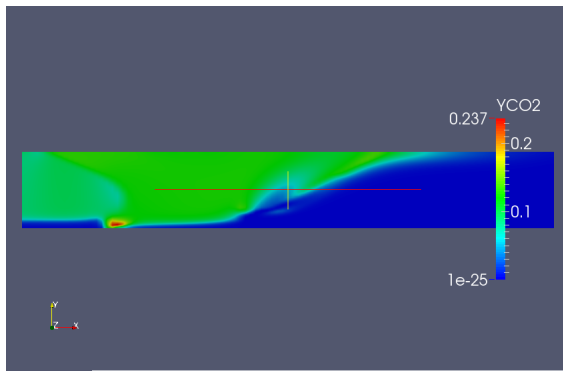
Figure 8.8: Packed bed porosity at steady state



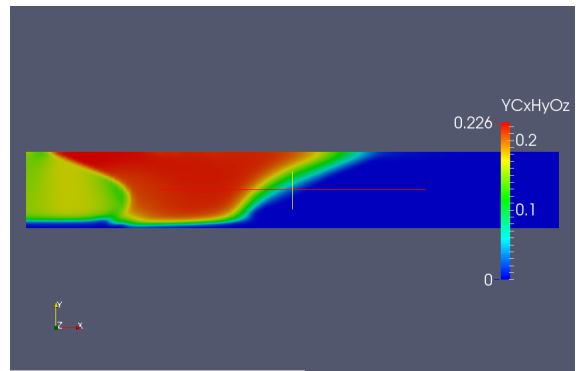
(a) H_2O mass fractions



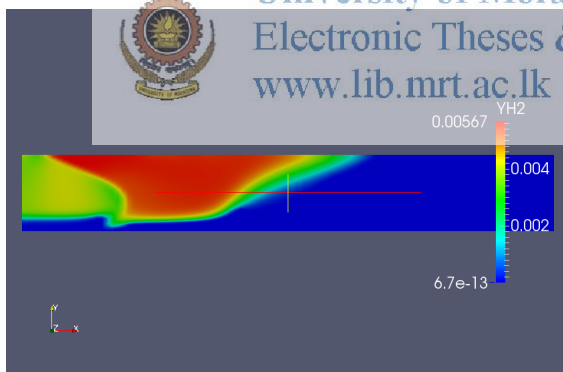
(b) Oxygen(O_2) mass fractions



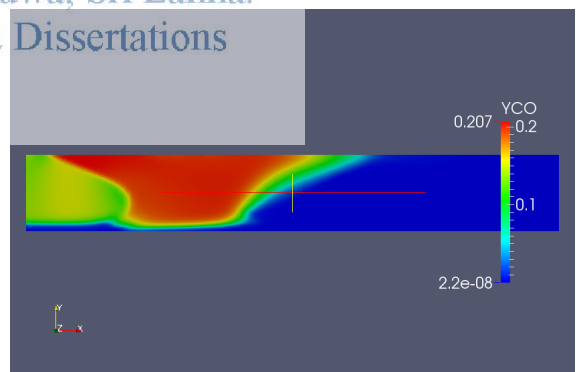
(c) Carbon dioxide(CO_2) mass fractions



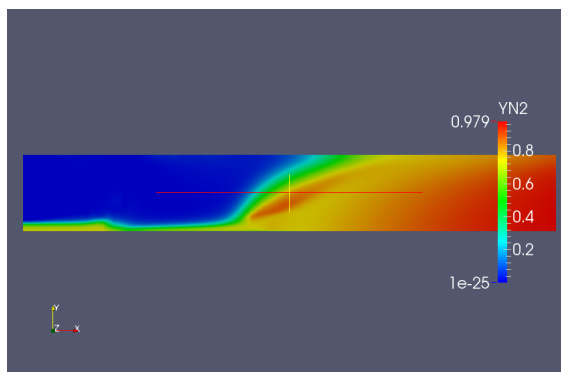
(d) $C_xH_yO_z$ mass fractions



(e) Hydrogen(H_2) mass fractions



(f) Carbon monoxide(CO) mass fractions

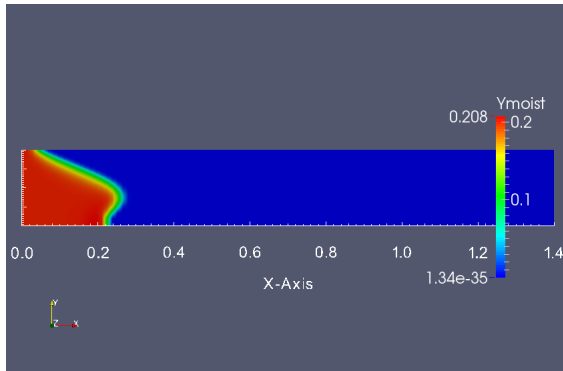


(g) Nitrogen(N_2) mass fractions

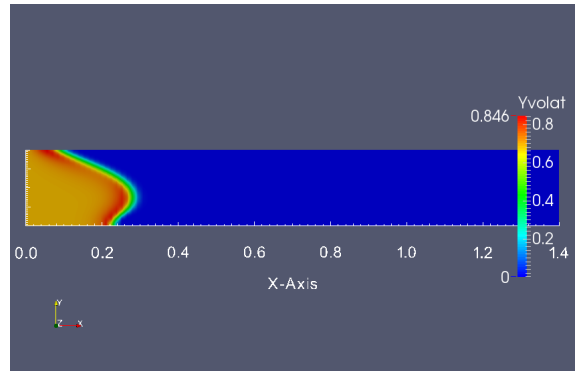
Figure 8.9: Gas component mass fraction at steady state



University of Moratuwa, Sri Lanka.
Electronic Theses & Dissertations
www.lib.mrt.ac.lk



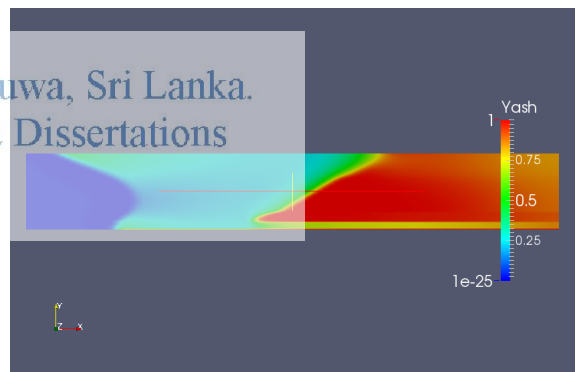
(a) Moisture fraction in solid phase



(b) Volatile mass fraction in solid phase



(c) Char mass fraction at solid phase



(d) Ash mass fractions at solid phase

Figure 8.10: Moisture,volatile,char and ash mass fractions in solid phase at steady state

residuals with iterations of the SIMPLE algorithm. Simulation carried until the temperature residuals reach the range of 10^{-6} .

8.1.2 Evaluation of simulation results

The main purpose of this research work is to develop a packed bed CFD model for wood chip combustion. Modeling and simulation of free board region is a matter of selection of proper models for turbulence, chemistry, radiation, etc although it took about half of the research period for simulation work. Therefore, evaluation of simulation results mainly focused on packed bed.

One very important result in this simulation is; inlet air flow comes through the grate does not enter more than half of the packed bed volume. This can be proved by the Nitrogen (N_2) mass fractions in the bed which is almost zero in a region within the packed bed (See Subfigure 8.9g). Oxygen seems to flow in to the packed bed about 25cm only. It can be further explained by velocity diagram in Figure 8.5; gas phase velocity is almost zero at outlet of the packed bed. The inlet gas might be resisted by the gas flow generated during combustion or due to the boundary conditions assumed for pressure (Pressure at boundary conditions could not measure due to the lack of facilities and available data). However, at the other end of the fuel bed there is a high velocity region which seems to have an unusual cooling effect to the combustion process. The effect of the regional air flow to the combustion process can be evaluated in optimization section.

The fuel bed starts to heat at the bed top by the radiation effect from the free board region. When temperature increases the bed starts to dry out and the drying reaction zone is thin showing a rapid reaction (See the Subfigure 8.10a). As soon the drying starts, the devolatilization reaction is occurring and the reaction zone is thinner than drying zone (See the Subfigure 8.10b).

A complete dry out region appears at the bottom of the packed bed after drying and devolatilization (See Subfigure 8.7a). At the same point a high Carbon Dioxide (CO_2) generation is evident (See Subfigure 8.9c) and there is no reduction of char mass fractions according to the Figures (Subfigure 8.10d). Therefore the ignition should be created from volatile combustion. This ignition region shows a move down due to lack of oxygen in the upper regions of packed bed. So, this is an ignition in the gas phase with a very high temperature in the gas phase and comparatively low temperature in solid

phase of the same region. There is another high temperature region in both gas and solid phase with a cocurrent reduction of char mass fraction. Therefore, this region should have been created due to char combustion. Some char is remaining at the bottom of the packed bed with out combustion even at the end of the grate. This might be due to the cooling effect of high velocity air flow at the end of the grtae.

As per the simulation results obtained following decisions can be made;

1. Air flow rate is too high at ash pit end of the moving grate creating an unnecesary cooling effect.
2. Packed bed outlet conditions of the combustion regions show no excess air in the gas flow.
3. Drying and devolatilization shows rapid reactions with thin reaction zones.
4. Two distinct ignition regions appear from gas phase volatile combustion and solid phase char combustion reactions.

8.1.3 Validation of Results

The dimensions used for the hot air generator simulations are from New Hopewell Tea factory, Balangoda, Sri Lanka; which is in the Figure 7.1 and 7.2. Although the dimensions used, due to the difficulty of obtaining air flow rates and pressure differences from ID fan, those values have been assumed comparing with literature. Therefore, validation using the measurements from that system would not very well suggest that the model is fitting for simulating similar hot air generator systems.

Figure 8.11 depicts the temperature at 'outlet' boundary of free board region, which is inlet to the heat exchangers of the hot air generator. Despite the fact that there are few measured points, the measured values are corresponding well with model results. Measured temperature shows a maximum of 108K temperature deviation of the three points.

Figure 8.12 is showing temperature measured at the edge of the flame which was 1083K and at the same point model results showing 1017K temperature.

Therefore, when comparing with the temperature the model results are validatable.

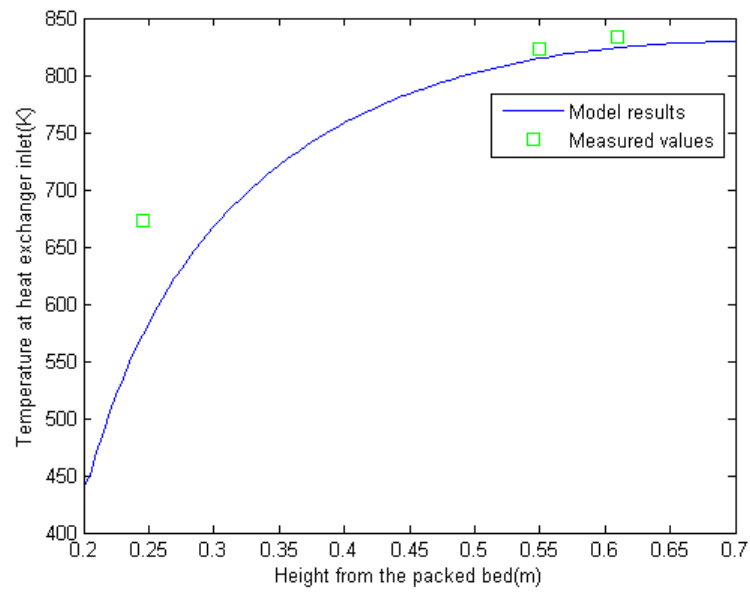


Figure 8.11: Temperature of the gas at inlet to the heat exchangers with the height from the packed bed

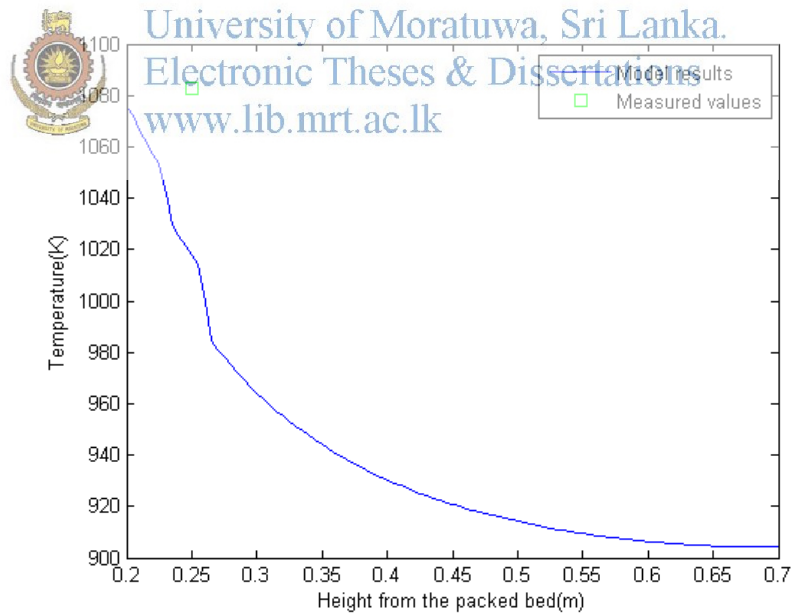


Figure 8.12: Temperature along a vertical line starting from edge of the flame at packed bed -free board interface

8.2 Comments on the model

8.2.1 Ash density

This model considers that the ash density is negligible (please refer 3.8) compared to the components in solid phase (moisture, char and volatile). This is clear when looking at equation 3.8 where always reduces the density of solid phase with the combustion reactions occurring in solid phase. In the meantime this can be used to calculate the bed shrinkage using the simulation results, although assumption might be affected to the model as a whole and therefore; important to test the sensitivity of the parameter for model results in further developments.

8.2.2 Interface between packed bed-free board

The simulation work carried out in this work involves basically two models; packed bed and free board. Then it was a vital thing to determine the boundary (interface) between the two. In most practical cases this would be a challenging task with the spatial variation of interface with the combustion progress. But, in this model according to the assumption made that the bed volume does not shrink; interface is placed just above the packed bed which is a horizontal plane.

8.2.3 Radiation heat flux

Referring to the thermal conductivity model described in section 3.4.2; an effective thermal conductivity model have been used integrating radiation and conductivity for the packed bed modeling instead of accounting radiation heat transfer as a different aspect. This effective thermal conductivity is for the whole bed; which accounts as common for both solid phase and gas phase. Therefore, the radiation incident on the packed bed which has a significant impact on combustion of the bed have considered as a heat flux boundary condition on the interface boundary of the bed. Repeating the equation 3.12 here;

$$(\nabla T_s)_{boundary} = \left(\frac{\epsilon_{rad} \sigma (T_{env}^4 - T_{top}^4)}{(1 - \epsilon_b) \lambda_s} \right)_{boundary}$$

which can be simplified as;

$$\frac{T_{top} - T_{cell}}{\Delta y/2} = \left(\frac{\epsilon_{rad} \sigma (T_{env}^4 - T_{top}^4)}{(1 - \epsilon_b) \lambda_s} \right) \quad (8.1)$$

where T_{cell} —temperature of the interface cell and Δy -height of the interface cell of the bed and T_{env} -radiation temperature.

The equation 8.1 is making a complex boundary condition which was overcome using “groovyBC”. The radiation temperature is assumed as the ‘upperWall’ (refer Table 7.1) temperature from the results of the free board region simulation, assuming the gases are only a participating medium for radiation heat transfer; although absorption and emission considered for free board model.

8.2.4 Simulation time

This model requires more time and computational requirements due to the number of iterative runs which has to be carried out to obtain the radiation temperature incident on packed bed and thereby to predict the packed bed combustion results which enter in to the free board region. Despite that the packed bed model is for steady state as the free board model is a transient one; the iterative runs took more time as it had to run until the steady state is reached.

Simulation of a transient packed bed model will not involve iterative runs as the initial and boundary conditions are known in advance unlike in a steady state situation. Therefore, it is suggested either to develop a transient packed bed model to predict the radiation temperature or a steady state solver for free board region; else high performance computers are essential for the running of the simulations.

For a single complete run for the whole case took more than 60 hours, which made it was difficult to test with sensitivity of the mesh resolution for the models. The turbulence model used in the free-board region; Low-Reynolds $k - \epsilon$ model results are sensitive to mesh resolutions. Therefore, it is important to run the solvers with different grid levels.

8.3 Drawbacks of the model

The major drawbacks identified in the model of packed bed combustion.

- Model neglected packed bed spatial variation with the advancement of combustion and considered porosity variation only. Although this assumption is used as

an initiative to packed bed modeling;this is not practical for biomass combustion.But it is better to compare the values of this model with a model which accounts bed shrinkage and see whether this model provides satisfactory results as a simple model will be better in usage.

- Negligence of secondary air to the free board region;might deviate gas compositions of flue gas from the results of the model.
- Simulating a steady state solver pre-requisites a knowledge on the parameter values to stop iterations, except that the values should be converging with iterations.But in this work as the knowledge is having only about the final results; it does not make a comfort on where to stop the initial iterations.This leads to number of overall simulation of the model which took a longer time period.Technically this model costs lot of time.

8.4 Optimization of packed bed combustion

Optimization is tested considering the temperature as the optimizing parameter.Following instances have tested to find the optimum conditions for the packed outlet.

- Initial packed bed porosity
 - 0.5
 - 0.45
 - 0.55
- Inlet air flow rate to the packed bed
 - $0.25ms^{-1}$
 - $0.20ms^{-1}$
 - $0.30ms^{-1}$

To view the performance of combustion at different condittions the packed bed outlet temperature is plotted against distance from the grate to the fuel feeding side(See Figure 8.12).

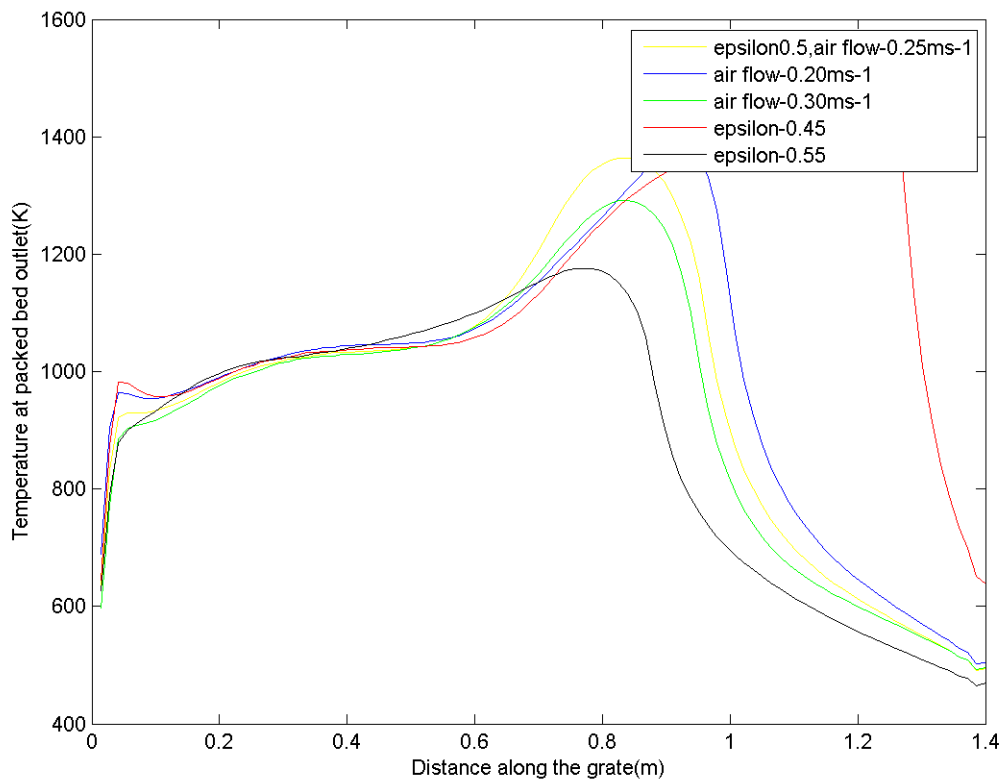



 Figure 8.13: Temperature at packed bed outlet with different input conditions
 University of Moratuwa, Sri Lanka.
 Electronic Theses & Dissertations
www.lib.mrt.ac.lk

As per the results; highest temperature can be achieved by increasing the bulk density of the fuel supplied through the grate. The results suggest that the packing density has higher improvement of the performance compared to decrease of air flow rate. Performance is lowest at lowest packing density (porosity-0.5).

CHAPTER IX

CONCLUSION AND FURTHER STUDIES

Major conclusions drawn from the results of the research work may be listed as follows;

- The packed bed model developed using CFD tool OpenFOAM can be used to predict the temperature of wood chip combustion at steady state of the similar size range hot air generators in the industry (Small scale horizontal moving bed type hot air generators).
- Gas compositions entering the heat exchangers could not be validated using the models. The result suggesting that the secondary air shall be considered for further models.
- Major improvements can be done by considering shrinkage effects to the packed bed.
- It is suggested to develop a transient model for packed bed combustion; to predict combustion progress which will assist in continuous monitoring and control of parameters at industrial level.
- It is suggested to deepen the study of oxy-fuel turbulent combustion modeling on the free board region.
- Instead of the euler-euler packed bed model developed; an euler-lagrange model would be ideal with the cost of computational requirements for large particle modeling (Thermally thick); specially to study single particle combustion.
- According to the optimization results, highest performance can be achieved by decreasing the porosity of the bed to around 0.45 (increasing bulk density of fuel).




University of Moratuwa, Sri Lanka.
Electronic Theses & Dissertations
www.lib.mrt.ac.lk

References


- [1] “Climate change 2007:synthesis report,” IPCC, IPCC, Geneva, Switzerland, Tech. Rep., 2007.
- [2] (2010) Sustainable Energy Authority. [Online]. Available: http://www.energy.gov.lk/sub_pgs/energy_managment.html
- [3] (2008, June) National energy policy & strategies of sri lanka. Ministry of Power and Energy. [Online]. Available: http://www.ceb.lk/download/db/national_energy_policy.pdf
- [4] W. E. Council. World energy resources -2013 survey. World Energy Council. [Online]. Available: http://www.worldenergy.org/wp-content/uploads/2013/09/Complete_WER_2013_Survey.pdf
- [5] (2012) Sri lanka energy balance. Sustainable Energy Authority, Sri Lanka. [Online]. Available: <http://www.info.energy.gov.lk/>
- [6] T. Jurena and J. Hajek, “Mathematical modelling of grate combustion: Bed and freeboard coupling issues,” in *Chemical engineering transactions*, P. Varbanov, J. Klemes, P. Seferlis, A. I. Papadopoulos, and S. Voutetakis, Eds., vol. 35, no. DOI:10.3303/CET1335164. The Italian Association of Chemical Engineering, 2013, pp. 985–990.
- [7] H. Thunman and B. Leckner, “Thermo chemical conversion of biomass and wastes,” Nordic graduate school BiofuelGS-2, Chalmers, Goteborg, November 2007.
- [8] C. D. Blasi, “Multi-phase moisture transfer in the high-temperature drying of wood particles,” *Chemical Engineering Science*, vol. 53, no. 2, pp. 353–366, 1998.

- [9] T. Jurena, “Numerical modelling of grate combustion.” Ph.D. dissertation, Brno University of Technology, Faculty of Mechanical Engineering, Institute of Process and ENvironmental Engineering, 2012.
- [10] Y.B. Yang, Y.R. Goh, R. Zakaria, R. Nasserzadeh, and J. Swithenbank, “Mathematical modelling of msw incineration on a travelling bed,” in *Waste Management*. Elsevier Science Limited, 2002, vol. 22, pp. 369–380.
- [11] Y. B. Yang, C. Ryu, J. Goodfellow, V. N. Sharifi, and J. Swithenbank, “Modelling waste combustion in grate furnaces,” in *Trans IChemE, Part B, Process Safety and Environmental Protection*, vol. 82, 2004, pp. 208–222.
- [12] Y.B. Yang, H. Yamauchi, V. Nasserzadeh, and J. Swithenbank, “Effects of fuel devolatilisation on the combustion of wood chips and incineration of simulated municipal solid wastes in a packed bed,” *Fuel*, vol. 82, no. 18, Dec 2003.
- [13] K. W. Ragland, D. J. Aerts, and A. J. Baker, “Properties of wood combustion for analysis,” in *Bioresource Technology*, vol. 37. Elsevier Science Ltd, 1991, pp. 161–168.
- [14] Y. B. Yang, V. N. Sharifi, and J. Swithenbank, “Numerical simulation of the burning characteristics of thermally thick biomass fuels in packed-beds,” in *Trans IChemE, Part B, Process Safety and Environmental Protection*, vol. 83, 2005, pp. 549–558.
- [15] R. Mehrabian, R. Scharler, A. Weissinger, I. Obernberger, and S. Stangl, “Cfd simulation of biomass grate furnaces with a comprehensive 3d packed bed model,” in *Proceedings of the 25th German Flame Day*, September 2011.
- [16] C. Ryu, Y. B. Yang, A. Khor, N. E. Yates, V. N. Sharifi, and J. Swithenbank, “Effect of fuel properties on biomass combustion - identification of the controlling factors (part two- modelling approach),” in *Fuel*, vol. 84. Elsevier Ltd., 2005, pp. 2116–2130.

- [17] D.Shin and S.Choi, “The combustion of simulated waste particles in a fixed bed,” in *Combustion and flame*, vol. 121, The Combustion Institute. Elsevier Science Inc., 2000, pp. 167–180.
- [18] Y. B. Yang, V. N. Sharifi, and J. Swithenbank, “Converting moving-grate incineration from combustion to gasification (numerical simulation of the burning characteristics),” 2006.
- [19] J.C.Wurzenberger, S.Wallner, H.Raupenstrauch, and J.G.Khinast, “Thermal conversion of biomass: Comprehensive reactor and particle modeling,” in *AIChE Journal*, vol. 48, no. 10, October 2002, pp. 2398–2411.
- [20] H.Sabelstrom, Tech. Rep.
- [21] M. van Blijderveen, “Ignition and combustion phenomena on a moving grate: with application to the thermal conversion of biomass and municipal solid waste,” Ph.D. dissertation, University of Twente, December 2011.
- [22] R. Mehrabian, R. Scharler, A. Weissinger, and I. Obernberger, “Optimisation of biomass grate furnaces with a new 3d packed bed combustion model -on example of a small-scale underfeed stoker furnace,” In *18th European Biomass Conference & Exhibition*. ETA-Renewable Energies (Ed.), Italy, May 2010.
- [23] W. Yang, C. Ryu, and S. Choi, “Unsteady one-dimensional model for a bed combustion of solid fuels,” *Proceedings of Institution of Mechanical Engineers*, vol. 218, 2004.
- [24] Y. B. Yang, V. N. Sharifi, J. Swithenbank, L. Lin Ma, I. Darvell, J. M. Jones, M. Pourkashanian, and A. Williams, “Combustion of a single particle of biomass,” in *Energy & Fuels*, vol. 22, no. 1. American Chemical Society, 2008, pp. 306–316.
- [25] C. Brucha, B. Petersb, and T. Nussbaumerc, “Modelling wood combustion under fixed bed conditions,” in *Fuel*, vol. 82. El, 2003, pp. 729–738.

- [26] S. R. Turns, *An introduction to combustion-Concepts and Applications*, 2nd ed. McGraw Hill, 2000.
- [27] A. Frassoldati, A. Cuoci, T. Faravelli, E. Ranzi, C. Candusso, and D. Tolazzi, "Simplified kinetic schemes for oxy fuel combustion," in *1st International Conference on Sustainable Fossil Fuels for Future Energy*, 2009, pp. 4–5.
- [28] H.K.Versteeg and W. Malalasekera, *An Introduction to Computational Fluid Dynamics*. Pearson Education Limited, 2007, no. 978-0-13-127498-3.
- [29] R. Bord, W. E.Stewart, and E. N.Lightfoot, *Transport Phenomena*, 2nd ed. Chemical Engineering Department,University of Wisconsin: John Wiley & Sons,Inc, 2002.
- [30] L. Davidson. (2011, February) An introduction to turbulence models. Department of Thermo and fluid dynamics. Chalmers University of Technology,Goteborg,Sweden. [Online]. Available: <http://www.tfd.chalmers.se/~lada>
- [31] J. Karlsson, "Modeling auto-ignition, flame propagation and combustion in non-stationary turbulent sprays," Ph.D. dissertation, Chalmers university of technology, (1995).
 University of Moratuwa, Sri Lanka.
 Electronic Theses & Dissertations
www.lib.mrt.ac.lk
- [32] F. P. Karrholm, *Numerical Modelling of Diesel Spray Injection and Turbulence Interaction*. Department of Applied Mechanics, Chalmers Univesity of Technology, 2006, ch. Appendix-Rhie-Chow interpolation in OpenFOAM.
- [33] P. Nordin, "Complex chemistry modeling of diesel spray combustion," Ph.D. dissertation, Chalmers University of Technology,Dept. of Thermo and Fluid Dynamics,Goteborg, 2001.
- [34] D. Joseph, P. Perez, M. E. Hafi, and B. Cuenot, "Discrete ordinates and monte carlo methods for radiative transfer simulation applied to cfd combustion modelling," Tech. Rep., February 2008. [Online]. Available: http://www.cerfacs.fr/~cfdbib/repository/TR_CFD_08_21.pdf

- [35] Y. B. Yang, C. N. Lim, J. Goodfellow, V. N. Sharifi, and J. Swithenbank, "A diffusion model for particle mixing in a packed bed of burning solids," in *Fuel*, vol. 84, 2005, pp. 213–225.
- [36] G. Borman and K. W. Ragland, *Combustion Engineering*, 1st ed. McGraw-Hill, 1998, no. 0-07-006567-5.
- [37] V. Francescato, E. Antonini, L. Z. Bergomi, C. Metschina, C. Schnedl, N. Krajnc, K. Kosciak, P. Gradziuk, G. Nocentini, and S. Stranieri. (2009, April) Wood fuels handbook. AIEL - Italian Agriforestry Energy Association. [Online]. Available: WWW.BIOMASSTRADECENTRES.EU
- [38] B. M. Jenkins, L. L. Baxter, and J. Koppejan, *Thermochemical Processing of Biomass: Conversion into Fuels, Chemicals and Power*, R. C. Brown, Ed. John Wiley & Sons, Ltd., 2011.
- [39] B. Jenkins, L. Baxter, T. M. Jr., and T. Miles, "Combustion properties of biomass," *Fuel processing technology*, vol. 54, pp. 17–46, 1998.
- [40] (2012, January) Lower and higher heating values of fuels. U.S. Department of Energy. Hydrogen analysis resource center. [Online]. Available: http://hydrogen.pnl.gov/cocoon/morf/hydrogen/site_specific/fuel_heating_calculator
- [41] R. H. Perry and D. W. Green, *Perry's Chemical Engineering Hand Book*, R. H. Perry, Ed. McGraw-Hill, 1999.
- [42] L. R. I., H. Sabelstrom, S. K. Kaer, H. Sorensen, M. Berry, R. Jensen, S. Heinesen, and K. B. Andersen, "Ps02002-4730 development of generalised model for grate combustion of biomass-final report," Aalborg University, Tech. Rep., February 2007.
- [43] Y. R. Goh, R. G. Siddall, V. Nasserzadeh, R. Zakaria, J. Swithenbank, D. Lawrence, N. Garrod, and B. Jones, "Mathematical modelling of the waste incinerator burning bed," *Journal of the Inst. Of Energy*, 1998.

- [44] Y.R.Goh, C.N.Lim, K.H.Chan, R.Zakaria, G.Reynolds, Y.B.Yang, R.G.Siddall, V.Nasserzadeh, and J.Swithenbank, "Mixing, modelling and measurements of incinerator bed combustion," in *2nd International Symposium on Incineration and Flue Gas Treatment Technology*, 1999.
- [45] A. Kimbrell, "Development and verification of a navier-stokes solver with vorticity confinement using openfoam," Master's thesis, University of Tennessee, 2012.
- [46] E.Kindler and I.Krivy, "Object-oriented simulation of systems with sophisticated control," in *International Journal of General Systems*, 2011, pp. 313–343.
- [47] L. John and L. William, *section 1.6"Object-Oriented Programming"*, 2008, no. ISBN 0-321-53205-8.
- [48] B. Wuthrich, "Simulation and validation of compressible flow in nozzle geometries and validation of openfoam for this application," Master's thesis, Institute of Fluid Dynamics,ETH Zurich, 2007.
- [49] *OpenFOAM Programmer's Guide v2.2.1*. OpenFOAM Foundation, 2013, June.
- [50]  *OpenFOAM User Guide v2.1.0*. OpenFOAM Foundation, 2011, December.
 Electronic Theses & Dissertations
 www.lib.mrt.ac.lk
- [51] <http://openfoamwiki.net/index.php/Contrib/swak4Foam>. (2014, April)
- [52] B. F. Gschaider, *README for swak4Foam*, 2012.
- [53] <http://openfoamwiki.net/index.php/Contrib/groovyBC>. (2014, April)
- [54] <http://openfoamwiki.net/index.php/Contrib/PyFoam>.
- [55] N.Wakao and S.Kaguei, *Heat and Mass Transfer in Packed Beds*. Gordon & Breach Science Publishers & Breach Science Publishers, 1982.
- [56] T. Lang, K. D. Johansen, E. Garrijo, P. Glarborg, T. Grotkjaer, A. D. Jensen, P. A. Jensen, J. E. Johnsson, A. Kavalauskas, J. N. Knudsen, K. B. Pedersen, and H. Zhou, "Straw combustion on a grate physical, chemical and reaction kinetic

data for grate modeling(the joint project),” Department of Chemical Engineering, Technical University of Denmark and Department of Mechanical Engineering, Technical University of Denmark, Tech. Rep., May 2005.

- [57] F. P. Karrholm, “Numerical modelling of diesel spray injection, turbulence interaction and combustion,” Ph.D. dissertation, Chalmers University of Technology, Department of Applied Mechanics, Chalmers University of Technology, Goteborg, Sweden, 2008.



University of Moratuwa, Sri Lanka.
Electronic Theses & Dissertations
www.lib.mrt.ac.lk